

Geological Field Trips and Maps

2019
Vol. 11 (1.2)



ISSN: 2038-4947



The city of Napoli and its active volcanoes

IAVCEI Meeting - Naples, 2018

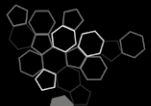
<https://doi.org/10.3301/GFT.2019.02>



*Società Geologica
Italiana*



ISPRA
Dipartimento per il
SERVIZIO GEOLOGICO D'ITALIA
Organo Cartografico dello Stato (legge n°68 del 2-2-1960)



**Sistema Nazionale
per la Protezione
dell'Ambiente**

GFT&M - Geological Field Trips and Maps

Periodico semestrale del Servizio Geologico d'Italia - ISPRA e della Società Geologica Italiana
 Geol. F. Trips Maps, Vol. **11** No.1.2 (2019), 107 pp., 63 Figs. (<https://doi.org/10.3301/GFT.2019.02>)

The city of Napoli and its active volcanoes**Pre-Conference Field Trip of Cities on Volcanoes 10, Napoli/Italy September, 2018****Raffaello Cioni¹, Roberto Isaia¹, Roberto Sulpizio³**

With contributions of:

Sandro de Vita², Mauro A. Di Vito², Marco Pistolesi⁴, Victoria Smith⁵, Mike Stock⁶, Pierfrancesco Talamo²¹ Dip.to Scienze della Terra, Università di Firenze (Italy)² INGV, Osservatorio Vesuviano, Napoli (Italy)³ Dip.to Scienze della Terra e Geoambientali, Università di Bari (Italy)⁴ Dip.to Scienze della Terra, Università di Pisa (Italy)⁵ Research Laboratory for Archaeology and the History of Art, University of Oxford (UK)⁶ Dept. Earth Sciences, University of Cambridge (UK)Corresponding Author e-mail address: roberto.sulpizio@uniba.it

Responsible Director

Claudio Campobasso (ISPRA-Roma)

Editor in Chief

Andrea Zanchi (Università di Milano-Bicocca)

Editorial Manager

Mauro Roma (ISPRA-Roma) - corresponding manager*Silvana Falcetti* (ISPRA-Roma), *Fabio Massimo Petti* (Società Geologica Italiana - Roma),*Maria Luisa Vatovec* (ISPRA-Roma), *Alessandro Zuccari* (Società Geologica Italiana - Roma)

Associate Editors

M. Berti (Università di Bologna), *M. Della Seta* (Sapienza Università di Roma),*P. Gianolla* (Università di Ferrara), *G. Giordano* (Università Roma Tre), *M. Massironi*(Università di Padova), *M.L. Pampaloni* (ISPRA-Roma), *M. Pantaloni* (ISPRA-Roma),*M. Scambelluri* (Università di Genova), *S. Tavani* (Università di Napoli Federico II)

Editorial Advisory Board

*D. Bernoulli, F. Calamita, W. Cavazza,
 F.L. Chiocci, R. Compagnoni,
 D. Cosentino, S. Critelli, G.V. Dal Piaz,
 P. Di Stefano, C. Doglioni, E. Erba,
 R. Fantoni, M. Marino, M. Mellini,
 S. Milli, E. Chiarini, V. Pascucci,
 L. Passeri, A. Peccerillo, L. Pomar,
 P. Ronchi, B.C. Schreiber, L. Simone,
 I. Spalla, L.H. Tanner, C. Venturini,
 G. Zuffa.*

ISSN: 2038-4947 [online]

<http://gftm.socgeol.it/>

The Geological Survey of Italy, the Società Geologica Italiana and the Editorial group are not responsible for the ideas, opinions and contents of the guides published; the Authors of each paper are responsible for the ideas, opinions and contents published.

Il Servizio Geologico d'Italia, la Società Geologica Italiana e il Gruppo editoriale non sono responsabili delle opinioni espresse e delle affermazioni pubblicate nella guida; l'Autore/i è/sono il/i solo/i responsabile/i.

INDEX

Information

Abstract	4
Hospitals and First Aid.....	5
Itinerary and daily schedule	5

Excursion notes

Days 1 and 2 - Campi Flegrei volcanoes.....	8
Days 3 and 4 - Somma-Vesuvius	55

Itinerary

Campi Flegrei – Itinerary	17
Day 1	17
Stop 1.1: The Campi Flegrei caldera from the Camaldoli hill	17
Stop 1.2: Verdolino quarry and Campanian Ignimbrite.....	20
Stop 1.3: The Astroni volcano	25
Stop 1.4: The Agnano Monte Spina Plinian eruption.....	29
Stop 1.5: INGV - Osservatorio Vesuviano and its surveillance center.....	32

Day 2.....	34
Stop 2.1: Baia-Fondi di Baia eruptive sequence	34
Stop 2.2: The Averno 2 crater	39
Stop 2.3: The Monte Nuovo volcano	43
Stop 2.4: The volcanic and hydrothermal activity in the volcano Solfatara.....	46
Stop 2.5: The Serapeum and the bradyseism	51
Stop 2.6: Rione Terra	54

Itinerary – Days 3 and 4..... 75

Day 3.....	75
Stop 3.1: Caldera wall and Vesuvius Crater	75
Stop 3.2: The 1944 lava flow	77
Stop 3.3: The Royal Observatory of Vesuvius.....	79
Stop 3.4: San Vito Quarry	85
Stop 3.5: Pollena Quarry	86
Day 4	88
Stop 4.1: Pozzelle Quarry	88
Stop 4.2: Villa di Poppea archaeological excavations - Oplontis	89
Stop 4.3: Herculaneum archaeological excavations.....	91

Reference	96
------------------------	-----------

Abstract

Somma-Vesuvius and Campi Flegrei are among the most famous active volcanoes in the world and are part of the Neapolitan landscape. The activity of the volcanoes punctuated the human history since Bronze Age, as testified by archaeological finds recognised in the plain and relieves surrounding the volcanic area. The world-famous eruption of AD 79 consigned the Somma-Vesuvius to the history, because of the burying of some important roman towns like Pompeii and Herculaneum. The field trip dedicated to Somma-Vesuvius illustrates the volcanology of main historical eruptions, with special emphasis to the activity of the last 4000 years. The visit to the summit cone provides a panoramic view of the inner caldera wall. Deposits of the Plinian and subplinian eruptions can be observed in old quarries around the volcano. The AD 79 deposits are exposed in both quarries and archaeological excavations such as Herculaneum and Oplontis, in which the interaction of the pyroclastic deposits with an inhabited area will be the argument for discussion about the present day volcanic hazard and risk in the Neapolitan area. A visit to the historical site of the Osservatorio Vesuviano will be the occasion to illustrate the birth and the history of volcanic surveillance. The itinerary in the Campi Flegrei caldera, provides an overview of i) the deposits of the Campanian Ignimbrite and Neapolitan Yellow Tuff caldera forming eruptions, ii) the pyroclastic density currents and fallout deposits of the post caldera volcanism, iii) different preserved volcano edifices and volcano tectonic structures, along with fumarolic and hydrothermal active field are hosted. A visit to the remnants of the Serapeum Roman market and the Pozzuoli harbour, are the best examples to discuss of caldera unrest at Campi Flegrei. The several diverse monitoring stations site at Solfatara and a visit to the Monitoring Centre of the Osservatorio Vesuviano provide an opportunity to illustrate the surveillance network of the INGV-OV for the Neapolitan volcanoes and discuss on the future eruption scenario and the related risk.

Key words: Somma- Vesuvius, Campi Flegrei, active volcanoes, volcanic deposits, caldera, volcanic edifice, volcanic stratigraphy, volcanic hazards.

Emergency contact telephone numbers:

112 Carabinieri

113 Police

115 Fire Fighters

118 First Aid

Hospitals and First Aid

Campi Flegrei Area

Ospedale S. Maria delle Grazie

Via Domitiana, La Schiana

Phone number: +39 (0)818552111

Pozzuoli (Napoli)

Vesuvius Area

Presidio Ospedaliero Maresca di Torre del Greco

Via Montedoro

Phone number: +39 (0)818824033

Torre del Greco (Napoli)

Itinerary and daily schedule

First day

Campi Flegrei (general introduction to the CF caldera, caldera-forming eruptions, and the activity of different intracaldera vents)

Stop 1.1 - View from the Camaldoli Hill; Stop 1.2 - The Campanian Ignimbrite and Tufo Giallo Napoletano at Verdolino Quarry; Stop 1.3 - The Astroni hydromagmatic activity; Stop 1.4 - The Agnano Monte spina volcano; Stop 1.5 - Visit to the monitoring centre of Osservatorio Vesuviano

Second Day

Campi Flegrei (the activity of the western sector and the Solfatara-Pozzuoli area)

Stop 2.1 - The Baia tuff ring (with visit to the archaeological area); Stop 2.2 - The Averno tuff ring; Stop 2.3 - The last activity of CF: the Mt. Nuovo volcano; Stop 2.4 - The Solfatara crater; Stop 2.5 - Visit to the Serapeo and Rione Terra archaeological excavations

Third Day

Somma-Vesuvius (general introduction to the SV activity, the Somma caldera and the deposit of the north flank of the volcano)

Stop 3.1 - Visit to the Vesuvius Crater and view of the Somma caldera; Stop 3.2 - The lava flow of the 1944 last Vesuvius eruption; Stop 3.3 - Visit to the historical Museum of the Osservatorio Vesuviano; Stop 3.4 - The San Vito quarry (the deposits of the Bronze Age Plinian eruption of the Avellino Pumice); Stop 3.5 - The Pollena quarry (the pyroclastic density currents deposits of the north flank of the volcano, and the parasitic cones of the ancient activity); Stop 3.6 - Visit to the Vesuvio National Park in the historical Palazzo Mediceo at Ottaviano

Fourth Day

Somma-Vesuvius (the AD 79 Pompeii eruption)

Stop 4.1 - The Pozzelle quarry (overview of the entire pyroclastic record of the last 22 ka of SV activity; focus on the AD 79 Pompeii eruption); Stop 4.2 - Oplontis archaeological excavations (the deposits of the AD 79 eruption and the effects on the villa of Poppea); Stop 4.3 - Herculaneum archaeological excavations (the effects of a large explosive eruption on a town; visit to the excavated area)

Fifth Day (morning)

The deposits of CF and SV in the city of Naples

Stop 5.1 - Maschio Angioino (distal tephra beds from CF and Vesuvius); Stop 5.2 - Visit to the historical centre: the building stones; Stop 5.3 - MANN museum: visit to the Pompeii exposition



Satellite image of the city of Napoli and its surrounding active volcanoes.

Days 1 and 2 - Campi Flegrei volcanoes

Campi Flegrei (CF) is a ~14 km wide volcanic caldera located in Southern Italy, a very urbanized area including the western part of the city of Naples. The northern and western parts of the caldera are above sea level and characterized by the presence of many dispersed cones and craters, whereas the southern part is principally submarine and extends into Gulf of Pozzuoli. The oldest rocks date back till ~80 ka and are represented by pyroclastic deposits cropping out outside and on the borders of the caldera (Pappalardo et al., 1999; Scarpati et al., 2012). The generation of the large caldera-collapse occurred during Campanian Ignimbrite (CI) eruption, (~40 ky BP; Giaccio et al., 2017) and the second major caldera-collapse followed the eruption of the Neapolitan Yellow Tuff (NYT, ~15 ky BP; Orsi et al., 1992; Deino et al., 2004). Pre caldera volcanism mainly generated monogenetic tuff cones and subordinate lava domes widespread also within the city of Naples (e.g., Rosi and Sbrana, 1987; Scarpati et al., 2012). The Campi Flegrei volcanic field (Fig. 1), includes small volcanic apparatus and several monogenetic tuff rings, tuff cones and rarely cinder cones and lava domes. These volcanoes are exposed outside, on

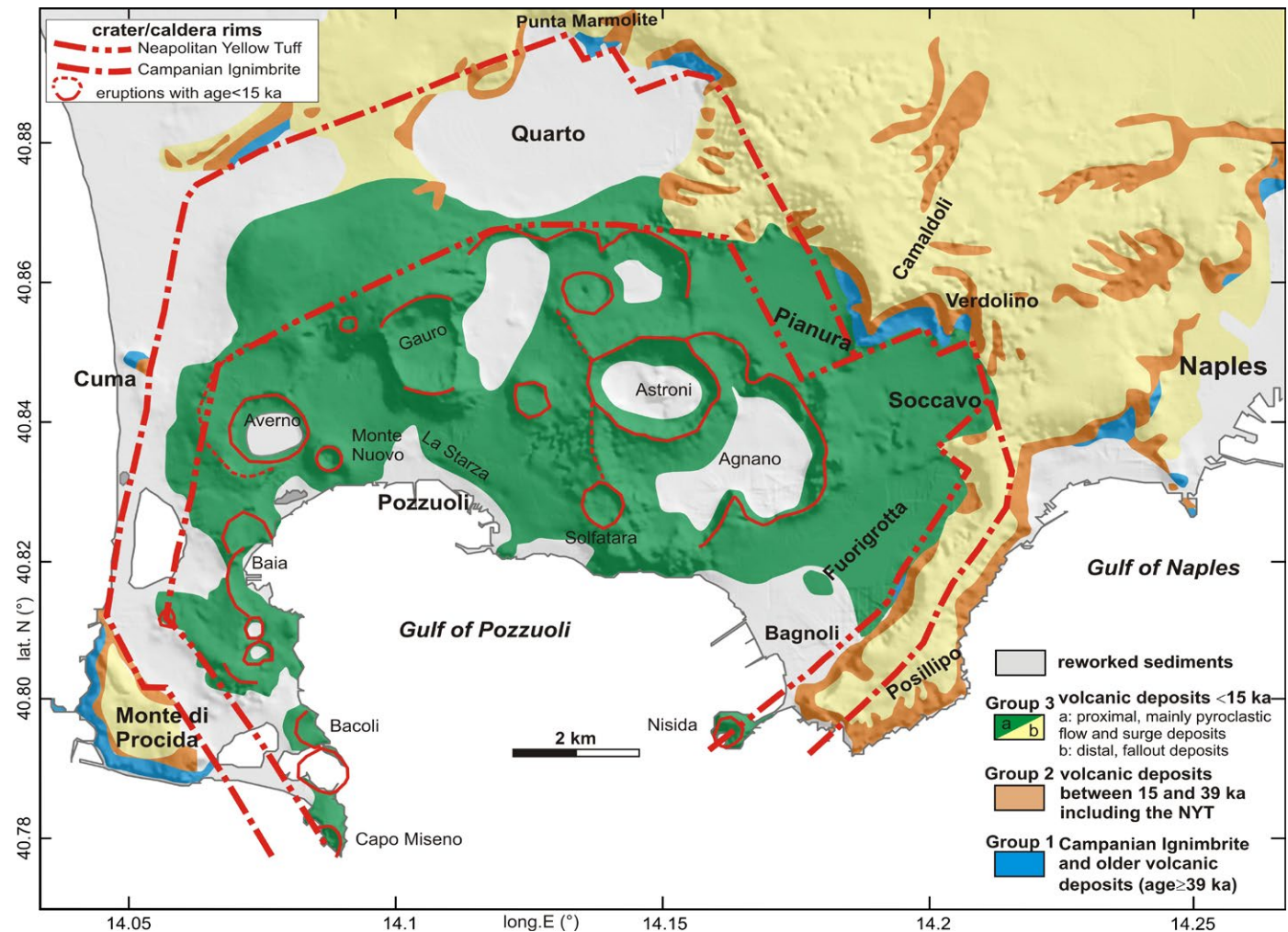


Fig. 1 - Geological sketch map of the Campi Flegrei (from Vitale and Isaia, 2014)

the borders, and within a large polygenetic caldera formed by the eruptions of the Campanian Ignimbrite (CI) and the Neapolitan Yellow Tuff (NYT) (e.g., Armienti et al., 1983; Di Girolamo et al., 1984; Rosi & Sbrana, 1987; Orsi et al., 1992, 1995, 1996, 1999; Cole & Scarpati, 1993; Rosi et al., 1996, 1999; Di Vito et al., 1999; De Vivo et al., 2001; Ort et al., 2003).

Thick pyroclastic sequences generated from at least 60 ky ago also occur (Orsi et al., 1996; Pappalardo et al., 1999). The caldera forming large volume CI (Fisher et al., 1993; Rosi et al., 1996) erupted $\sim 300 \text{ km}^3$ of trachytic dense rock equivalent magma (D.R.E.). The CI eruption was the largest magnitude eruption to occur in the Mediterranean region during the late Quaternary, and resulted in the formation of a 14-km wide caldera (Rosi and Sbrana, 1987). The eruption began with a Plinian phase, during which a SE-distributed pumice fallout was emplaced. This was followed by a succession of pyroclastic density currents (PDC) that deposited ash and pumice flows and densely-welded ignimbrites that covered the Campanian Plain and surrounding hills (Barberi et al., 1978). Proximal deposits (e.g., Breccia Museo, Piperno) cropping out at the top of the eruption deposits along the caldera margins are interpreted as proximal facies related to the final caldera-forming phase (Rosi and Sbrana, 1987; Rosi et al., 1996). On these deposits, several age data were produced ($\sim 37 \text{ ka}$, Deino et al., 2004; $\sim 39 \text{ ka}$, De Vivo et al., 2001; $\sim 38 \text{ ka}$, Fedele et al., 2008). A very recent and high precision ^{14}C and $^{39}\text{Ar}/^{40}\text{Ar}$ age determination of the CI yielded an age of $39.85 \pm 0.14 \text{ ka}$ (Giaccio et al., 2017).

After the CI caldera forming eruption volcanic activity occurred almost exclusively through the formation of pyroclastic deposits from several volcanic centers located within or along the border of the caldera. This period of activity culminated with the second large eruption at CF dates back at 15 ka (Deino et al., 2004) named Neapolitan Yellow Tuff (NYT; Cole & Scarpati, 1993; Wohletz et al., 1995), whose volume has been estimated larger than 20 km D.R.E of latitic to trachytic magma (Orsi et al., 1992, 1995; Scarpati et al., 1993). The eruption was mainly preatomagmatic producing pyroclastic density currents and subordinate thin fallout layers. The PDC deposits close to CF caldera were largely zeolitized and forms the substrate on which lie the city of Naples. Ashes were mainly dispersed toward North-Northeast from the vent area.

The eruptions of the post-NYT period were confined within the structural boundaries of the caldera and comprised at least 70 known events, dominated by low- to medium-magnitude phreatomagmatic-magmatic eruptions with volumes of $< 0.1 \text{ km}^3$ (Di Renzo et al., 2011; Smith et al., 2011). The Monte Nuovo tuff cone formed as consequence of the most recent eruption at AD 1538 (e.g., D'Oriano et al., 2005; Di Vito et al., 2016). After the NYT eruption, the caldera suffered significant ground deformation phenomena, especially in its central sector, where the uplift is still ongoing.

Campi Flegrei magma compositions

The generation of melt beneath the Campanian region is related to the northwest subduction of the Ionian oceanic plate beneath the Eurasia plate (e.g., Faccenna et al., 2007), with the slab (Wadati–Benioff zone) located at a depth of around 350 km (Giardini and Velonà, 1991). The primary magmas produced have a mid-ocean ridge basalt (MORB)-like asthenospheric mantle wedge composition, and these are modified by aqueous fluids, oceanic sediment, and continental crust (Tonarini et al., 2004; D’Antonio et al., 2007). Trench roll-back has resulted in a region of back-arc extension in the Campanian region and it is in this thinner and fractured crust that the magmas ascend and erupt (e.g., Patacca and Scandone, 1989).

The mafic melts that make it into the crust (upper 25 km) at Campi Flegrei are K-basalts (e.g., Webster et al., 2003). These mafic compositions are preserved as melt inclusions in antecrystic Mg-rich olivines and clinopyroxenes in some eruption deposits (e.g., Cannatelli et al., 2007). The composition of the erupted melts range from shoshonitic through to phonolitic and trachytic, with the most differentiated compositions dominating (e.g., Mangiacapra et al., 2008; Smith et al., 2011; Tomlinson et al., 2012). The phenocrysts in these Campi Flegrei magmas are predominantly plagioclase + K-feldspar + clinopyroxene ± biotite. Magnetite and apatite occur as accessory phases and eruptions occasionally contain olivine or rare feldspathoids.

The SiO_2 and Na_2O contents of the magmas increase with differentiation, whereas CaO , FeO , MgO , and P_2O_5 contents decrease (e.g., Civetta et al., 1991b). There is a noticeable inflection in K_2O melt compositions, denoting K-feldspar-in, at ~60 wt% SiO_2 (Fowler et al., 2007; Smith et al., 2011; Tomlinson et al., 2012). The Sr, Ba, and Eu contents behave compatibly, and reflect the significant amount of feldspar fractionation. Other REE (excluding Eu), Y, Nb, Zr, Rb, Th, and Ta are all incompatible (e.g., Civetta et al. 1997; Bohrsen et al. 2006, Arienzo et al., 2010; Tomlinson et al., 2012). These major and trace element compositions follow an evolutionary trend that could be generated through fractional crystallization of a single parental melt (e.g., Civetta et al., 1991; D’Antonio et al., 1999; Fourmentraux et al., 2012) but isotopic variations indicate that the melt that erupt are derived from different batches of magma (Pappalardo et al., 1999, 2002; D’Antonio et al., 2007; Di Renzo et al., 2011).

Samples from Campi Flegrei eruption deposits suggest that only evolved magmas were erupted in the early history (Pappalardo et al., 1999) and it was only after the last caldera-forming NYT eruption (~15 ka) that more compositionally diverse melts were erupted (e.g., D’Antonio et al., 1999; Smith et al., 2011). The isotope (Nd, Pb and Sr) and occasionally the major and trace element glass compositions of the magmas indicate that the



eruptions tap distinct batches of melt, and some have interacted at depth (e.g., Di Renzo et al., 2011). This has been well documented for the large caldera-forming events (e.g., Forni et al., 2018) and for eruptions in the last 15 ka (e.g., Tonarini et al., 2009; Fourmentraux et al., 2012). The general trend between 60 and 10 ka is that Nd and Pb isotopic compositions the erupted magmas became progressively less radiogenic ($^{143}\text{Nd}/^{144}\text{Nd}$ - 0.51252 to 0.51236 and $^{206}\text{Pb}/^{204}\text{Pb}$ - 19.2 to 18.9) while the Sr-isotope composition became more enriched (0.70700 to 0.70864) over time (Pabst et al., 2008; Di Renzo et al., 2011). These changes in the isotopic compositions are consistent with an increase in crustal contamination. However, the Campi Flegrei liquid line of descent and extent of Sr and Pb isotopic heterogeneity is compatible only with very minor assimilation (D'Antonio et al., 2007; Fowler et al., 2007).

Constraints on the architecture of the magma storage at Campi Flegrei

The architecture of the crustal magma plumbing system at Campi Flegrei has recently been constructed based on the integration of all existing petrological and geophysical datasets (Fig. 2; Stock et al., 2018).

Seismic tomography data show that there are currently two main zones of magma storage at Campi Flegrei: a major magma storage region at 7-8 km and small melt pockets at approximately 2 and 4 km (Zollo et al., 2008; De Siena et al., 2010). The shallower magma storage region correlates with the depth of sill emplacement during recent seismic crises (e.g. Woo & Kilburn, 2010). Phase equilibrium models indicate that most of magma crystallisation and phenocryst formation before past eruptions of Campi Flegrei occurs between 150 and 300 MPa (i.e. 6.6–13.3 km; Bohron et al., 2006; Fowler et al., 2007; Cannatelli, 2012; Arienzo et al., 2016), which correlates with the deeper magma storage region. Crystallisation within these two zones of magma storage has recently been further corroborated by clinopyroxene-melt geobarometry (Astbury et al., in review).

Apatite inclusions and microphenocrysts have been used to provide a long-term history of volatile behaviour in the Campi Flegrei system, utilising the fact that the volatile contents of apatite inclusions cannot be reset post-entrapment. These data indicate that magmas in the deep Campi Flegrei storage region experience protracted volatile-undersaturated crystallization until late in magmatic evolution (Stock et al., 2016; Stock et al., 2018). Rhyolite-MELTS fractional crystallisation models (Gualda et al., 2012) support the fact that the system only becomes volatile saturated after biotite starts to crystallise approximately $\sim 910^\circ\text{C}$ (at 150-200 MPa; Stock et al., 2016). Once the melts become H_2O saturated, only a small amount of crystallisation would result in a substantial increase in the amount of gas, which could easily generate overpressures that exceed the fracture

criterion and result in eruption (Stock et al., 2016). It is likely that many of the eruptions from Campi Flegrei are triggered through this 'internal' mechanism, with diffusion timescales indicating these processes can occur within years of the eruption (Stock et al., 2016).

The volatile compositions of the Campi Flegrei melt inclusions range from 1 to 4 wt % H_2O , and CO_2 concentrations are typically low with <250 ppm (e.g., Marianelli et al., 2006; Arienzo et al., 2016; Stock et al., 2016, 2018). Phonolite and trachyte solubility data from CO_2 -free melts at 850–950 °C (e.g. Carroll & Blank, 1997; Webster et al., 2014) indicate that melt inclusions typically became saturated at pressures of 25–75 MPa, which equates to a depth of around 1–3.5 km (Stock et al., 2018). These depths are much shallower than the main zone of magma storage determined using geophysical and petrological techniques. Furthermore, there is no relationship between H_2O and MgO concentrations in many clinopyroxene-hosted melt inclusions (Arienzo et al., 2016), which would be anticipated during volatile-undersaturated crystallisation. This implies that the H_2O contents of the melt inclusions may have been diffusively reset post-

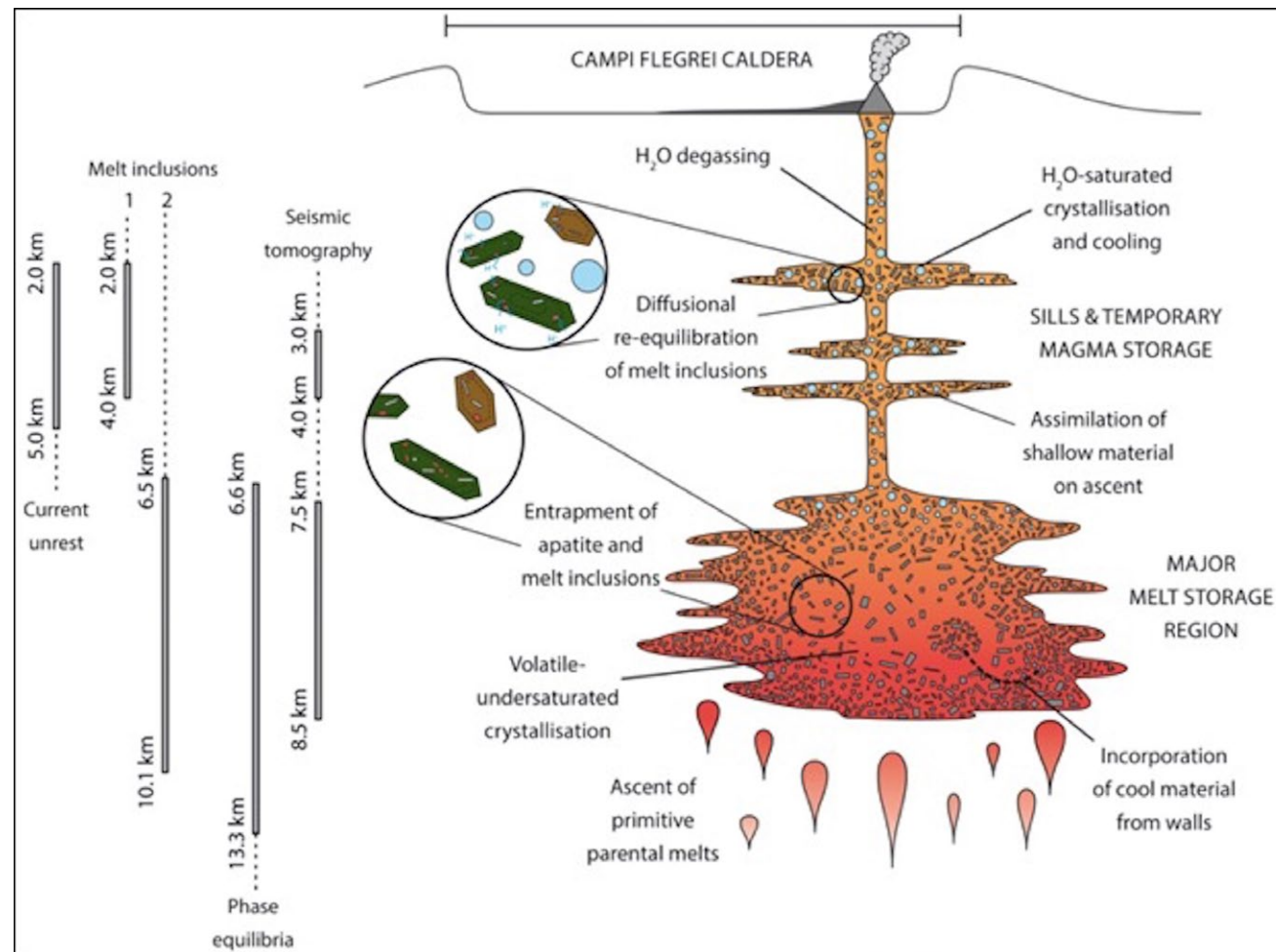


Fig. 2 - Schematic diagram of magmatic storage at Campi Flegrei, modified from Stock et al., (2018). The grey bars on the left show the estimates of magma storage depths, which have been derived from: recent ground deformation ('current unrest'; e.g., Woo & Kilburn, 2010; Amoroso et al., 2014); melt inclusions (e.g., 1-Fourmentraux et al., 2012, 2-Arienzo et al., 2016); phase equilibria constraints (Fowler et al., 2007, Bohrsen et al., 2006; Cannatelli, 2012); and seismic tomography data (Zollo et al., 2008; De Siena et al., 2010).



entrapment, consistent with the short experimental timescales of H^+ diffusion (e.g., Reubi et al., 2013). The melt inclusion data therefore only provide information on the last phase of magma storage and crystallisation at Campi Flegrei, where the magmas ascending from depth interact and mix with small, volatile-saturated magma bodies.

The Campanian Ignimbrite sequence

The CI sequence is composed of a proximal to medial fall deposits indicate the first phase of the eruption which generated a Plinian column widespread deposits directly eastward from the vent (Rosi et al., 1999). PDC deposits associated with the CI eruption occur on top of the fallout deposits and are commonly found on land up to about 80 km from the vent, covering an area of about 30,000 km² (Barberi et al., 1978; Fisher et al., 1993, Fig.3). These PDC deposits include different units identified in the CI deposits by Fisher et al. (1993), Rosi et al. (1996), Fedele et al. (2008) and Scarpati and Perrotta (2012). Five main PDC units are observed on top of the Plinian fallout in proximal area while in medial to distal locations, e.g., Lago Grande

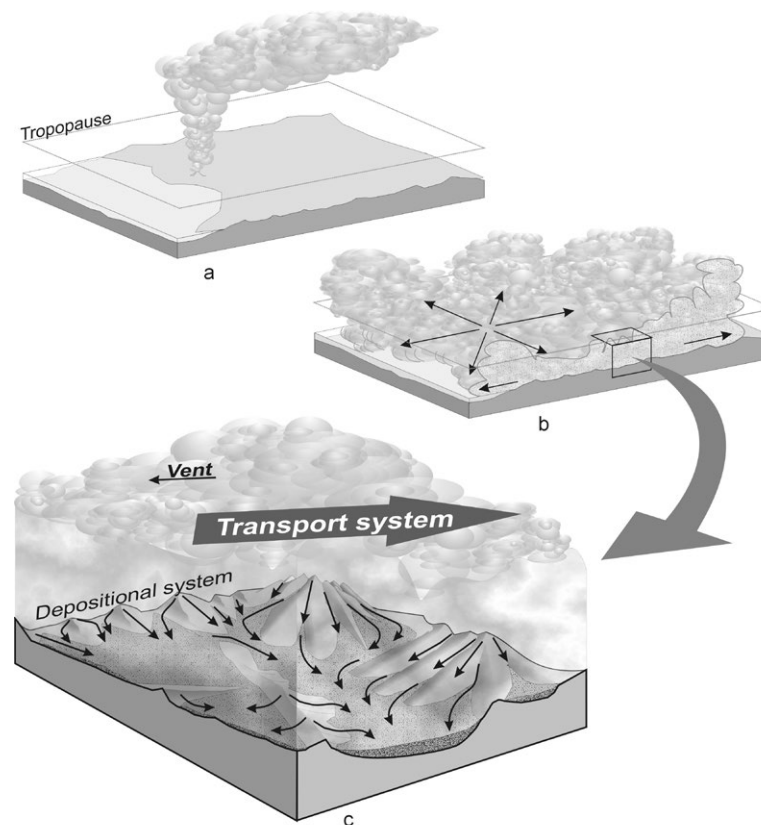


Fig. 3 - Left: CI eruption phases (a, b) and model of the transport and depositional system of the PDCs (c). a) sustained plinian eruption column; b) expanding PDCs; c) block diagram showing the movement of the PDCs over the topography (after Fedele et al., 2003). Right: grey welded tuff facies (Piperno) of Campanian Ignimbrite, from Avanzinelli et al., 2017.

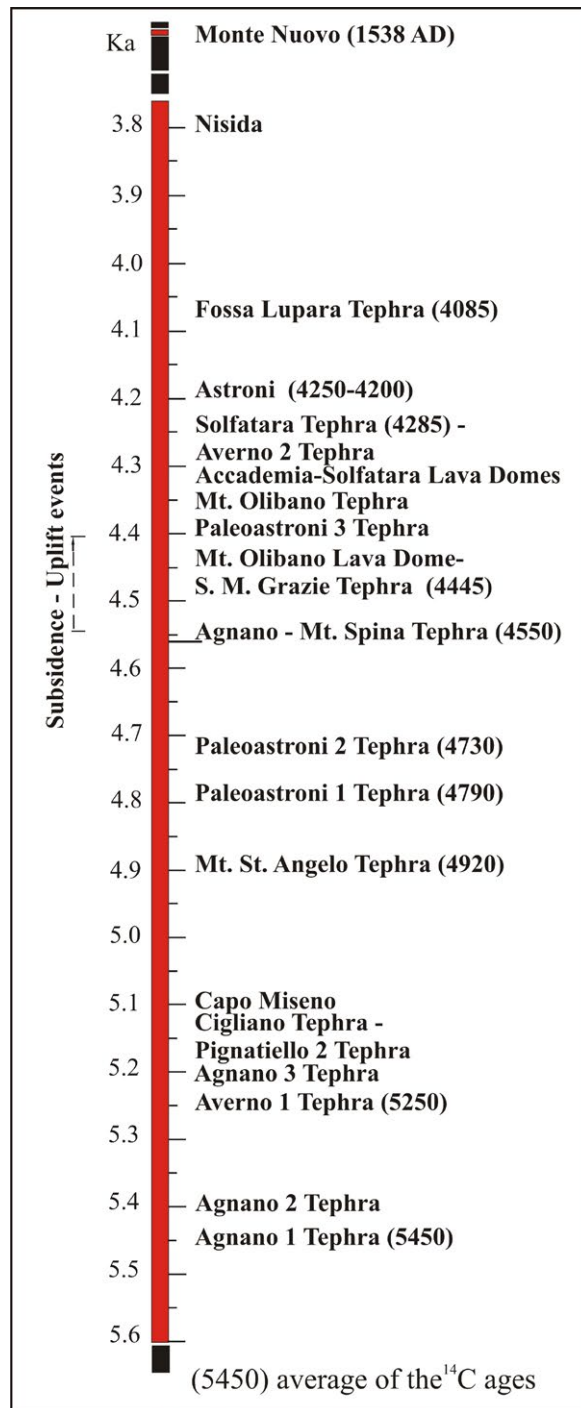
di Monticchio (LGdM), the Plinian fallout is overlain by fine ash that is interpreted to be co-ignimbrite deposits from these 5 PDCs. PDC units, which in very proximal areas contain the typical "Piperno" facies composed by a densely welded ignimbrite (Piperno; Fig. 3) and the "Museum Breccia" lithic-rich breccia units related to the final caldera-forming phase. During this eruption, more than 300 km³ of magma and volcanic ash were emitted, with ashes related to both phases dispersed eastward up to Russia (Fig. 8; Giaccio et al., 2008; Costa et al., 2012; Smith et al., 2016). The CI show a slightly compositional variability of pyroclastics from trachytic to trachytic-phonolitic (eg. Melluso et al., 1995; Civetta et al., 1997; Signorelli et al., 1999; Pappalardo et al., 2002; Marianelli et al., 2006; Giaccio et al., 2008).

Civetta et al. (1997), described three main composition groups, in terms of major element composition; the difference among these groups mainly concerns the K₂O/Na₂O ratio and the relative abundance of CaO, Fe₂O₃, MgO and Cl. Glasses and melt inclusions of the CI fallout and breccia deposits (Signorelli et al., 1999; Marianelli et al., 2006) indicates a similar compositional variability also for these eruptive units. The chemical composition variability in the CI rock indicates that the CI eruption was fed by a trachytic magma chamber which included a more evolved upper magma layer, and a less evolved lower layer (e.g. Civetta et al., 1997).

Marianelli et al., 2006 studying melt inclusions within CI rocks estimated a 6 and 8 km depth for the magma chamber that fed the eruption. The caldera formation linked to the CI eruption and particularly its eastern margins have been the subject of various interpretations in recent literature (e.g., Rosi and Sbrana 1987; Orsi et al., 1996; Acocella 2008). An alternative interpretation by other authors (Lirer et al., 1987; Rolandi et al., 2003) identifying the CF caldera formation at around 15 ka and linked to the NYT eruption.

The Neapolitan Yellow Tuff succession

The NYT deposits are generally zeolitized within the City of Naples and surroundings and is commonly used as building material. The NYT has been produced by the second largest eruption of the CF caldera at about 15 ka (Deino et al., 2004). The eruption of about 40 km³ of magma (Orsi et al., 1992; Scarpato et al., 1993) led to a second major caldera collapse, affecting mainly the central sector of the previous CF caldera. The NYT caldera margin is probably today exposed only along the eastern edge of the Bagnoli plain. Phreatoplinian and phreatomagmatic events laid down the NYT sequence, which was divided into a Lower Member (LM) and an Upper Member (UM), on the basis of textural characteristics, dispersal and occurrence of an angular unconformity which separates the two units. LM is the product of the largest known trachytic phreato-Plinian



eruption and covered an area of about 1,000 km², varying in thickness from 11 m in the most proximal exposures, to 85 cm at 35 km from the vent area. UM are typical of a phreatomagmatic eruption with its thickness varying from about 100 m in proximal exposures, to 7 m in the Caserta Plain. Compositional variation of products from latite to alkali trachyte and eruption dynamics suggested that the magma chamber was composed of three discrete layers: an upper alkali trachyte, an intermediate trachyte and a lower alkali trachyte to latite magmas separated by compositional gaps (Orsi et al., 1995).

Post-NYT activity

Following the eruption of the NYT, activity within the caldera generated at least 70 volcanic eruptions mainly concentrated in discrete periods alternating with periods of quiescence of variable length (Di Vito et al., 1999; Isaia et al., 2009; Fig. 4).

The 70 post-NYT eruptions are grouped into three eruptive epochs, separated by periods of quiescence: Epoch 1 (15.0–10.6 ky BP), Epoch 2 (9.6–9.1 ky BP), and Epoch 3 (5.5–3.5 ky BP) (Di Vito et al., 1999; Isaia et al., 2009; Smith et al., 2011). After a repose period of more than 3000 years occurred the only historical eruption of the caldera of Monte Nuovo in 1538 AD. This period of volcanic activity at Campi Flegrei was characterized mainly by explosive eruptions with less frequent effusive events. The last 15,000 years of volcanism was characterised by predominant small and medium scale eruptive events, and only two high-scale eruptions characterized by Plinian phases occurred at about 12 ky BP (Agnano Pomici-Principali) and 4.5 ky BP (Agnano-Monte Spina), respectively (Di Vito et al., 1999; De Vita et al., 1999). The variability of the events is evidenced by the different areal distributions of

Fig. 4 - Chronostratigraphic scheme of the volcanism younger than 15 ka at the Campi Flegrei caldera (after Isaia and Smith, 2013).



deposits and by different volumes of magma erupted, which only for the largest scale events exceeded 1 km^3 (Orsi et al., 2004; Di Renzo et al., 2011). Indeed, volume estimates of magma erupted during many post-NYT events represents generally an underestimation due to the lack of proximal deposits for many of the recognized eruptions. The largest post-15 ka events erupted $>>0.1 \text{ km}^3$ DRE of magma, and dispersed ash over wide areas. The most intense phases of these eruptions formed Plinian and subplinian columns with height up to about 30 km. Deposits generated by these phases were generally widespread toward east-northeast, while low height column laid down fallout deposits in variable directions according with the wind directions.

The central-eastern part of the caldera was the prevailing sector of the caldera where eruptive vents opened (Isaia et al., 2009; Vilardo et al., 2010; Bevilacqua et al., 2015). During Epoch 1, vents were mainly aligned along the structural boundaries of the NYT caldera, but Epoch 2 was mainly characterized by eruptions from the NE sector of the caldera, with the exception of the Baia-Fondi di Baia eruption. It occurred at the onset of Epoch 2 and was located in the western sector of the NYT caldera. Finally, Epoch 3 vents were hosted mainly in the central-eastern sector of the caldera, at the western margin of the Agnano collapsed area (Isaia et al., 2009, Bevilacqua et al., 2015). The sector encompassing the area Agnano-Astroni-Solfatara is considered as the calderas sector with the higher probability of vent opening in case of renewal of volcanism at CF (e.g. Bevilacqua et al., 2015 and reference therein)

Simultaneous eruptions in the two different sectors of the caldera were also highlighted at 4.3 ky BP, when Solfatara and Averno volcanoes erupted simultaneously (Isaia et al., 2009; Pistolesi et al., 2016).

Epochs of volcanism have been generally preceded by significant caldera ground uplift, which reached its maximum in the central sector (Di Vito et al., 1999; Isaia et al., 2009). The doming of the caldera floor, leading to $\sim 90 \text{ m}$ of structural uplift, occurred mainly through two primary episodes of uplift, began soon after the collapse. It was related to the persistent displacement correlated with magma volumes intruded and accompanied the contemporaneous volcanic activity (e.g. Marturano et al., 2018). Period of rest are associated to subsidence of the cladera floor. Even several decades before the Monte Nuovo eruption ground uplift attained several meters (e.g., Dvorak and Gasparini, 1991; Morhange et al., 2006; Guidoboni et al., 2011), and lately concentrated close to the vent area of Monte Nuovo (Di Vito et al., 2016).



Campi Flegrei – Itinerary

The itinerary in the Campi Flegrei caldera allows us to observe some of the main volcanic structures of the area as well as tephra deposits of representative eruptions. This will give us the opportunity to illustrate and discuss about the volcanic history of the Campi Flegrei, the ground deformation dynamics, and to focus on the possible future scenario and the risk related to a possible resumption of the eruptive activity at Campi Flegrei. Fig. 5 shows the location of the stops.

Day 1

Stop 1.1: The Campi Flegrei caldera from the Camaldoli hill (40°51'23.69"N - 14°11'26.78"E)

Significance. - A general view of the Campi Flegrei caldera structure and surroundings, including Somma-Vesuvius and Gulf of Naples and Pozzuoli.

The CF caldera. - From left to right: the Somma-Vesuvius, the city of Naples, the Campi Flegrei caldera, the islands of Procida and Ischia (Fig. 6).

A very good view of the Somma-Vesuvius and its relationships with the city of Naples and surrounding towns can be appreciated. Well visible is also the town of San Sebastiano and the 1944 lava flow which destroyed it. About CF caldera, the Vomero-Arenella saddle was a preferential pathway for PDC erupted in the present day Soccavo plain, where many vents were active during the I epoch (9.5-15 ka) of volcanism following the NYT eruption (15 ka; Deino et al., 2004). The largest part of the morphological boundaries of both CI and NYT calderas, are visible. To the east, the horizontally laying CI deposits are cut by a southward dipping high-angle surface, which is part of the CI caldera margin overlain by the NYT. The St. Martino hill is one of the tuff rings and tuff cones generated before the CI eruptions.

The scarp bordering the Posillipo hill towards the northwest is the only exposed part of the NYT caldera margin. The densely urbanized Fuorigrotta-Bagnoli and Soccavo plains, have been the site of eruption vents during the I epoch (15 - 9.5 ka).

Looking to the south-west, an almost complete view of the caldera is visible, along with the islands of Procida and Ischia. Looking to the inner part of the caldera, the articulated morphology of the landscape can be

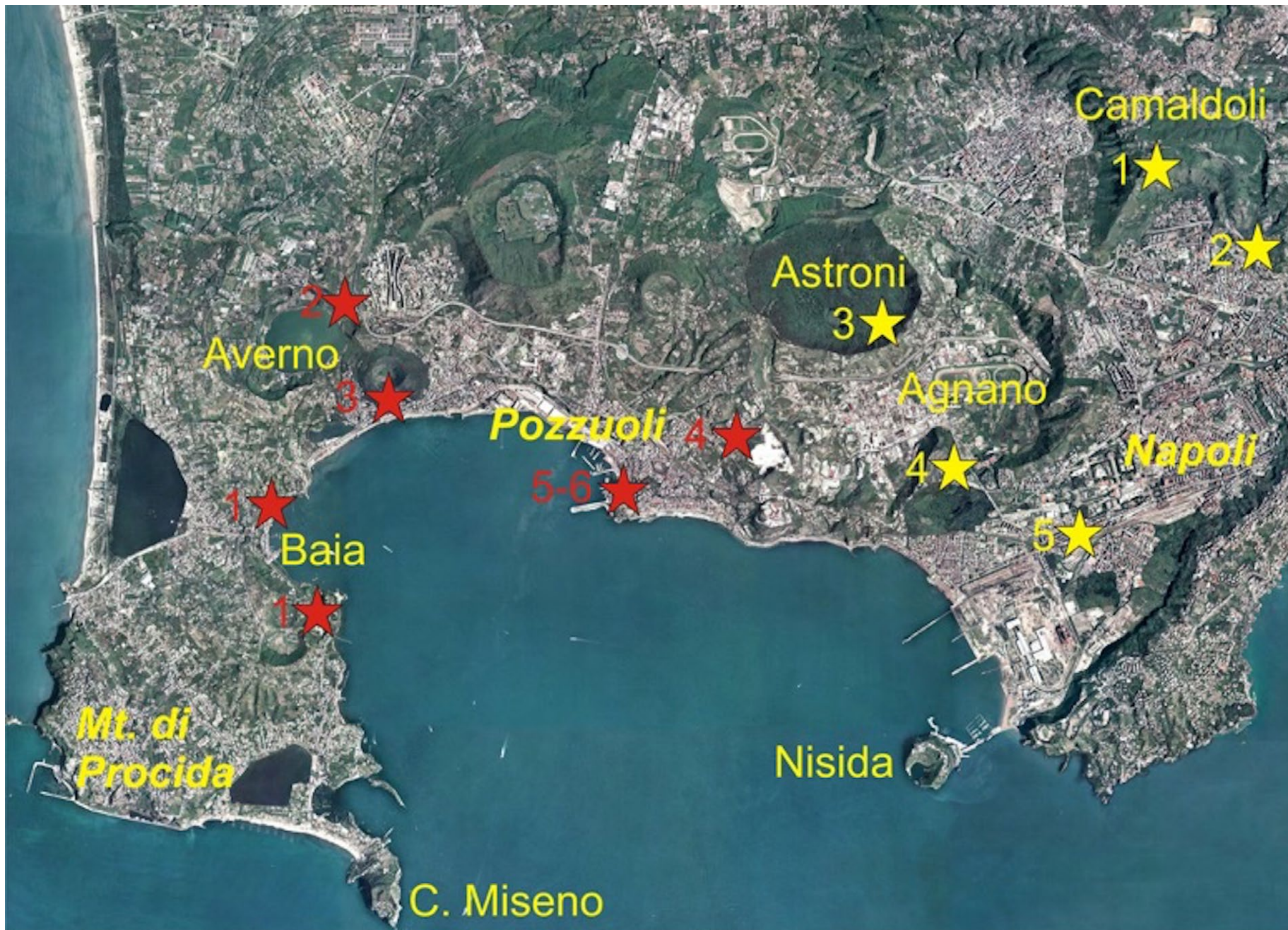


Fig. 5 - Aerial view of the central part of the Campi Flegrei caldera with the field trip stops

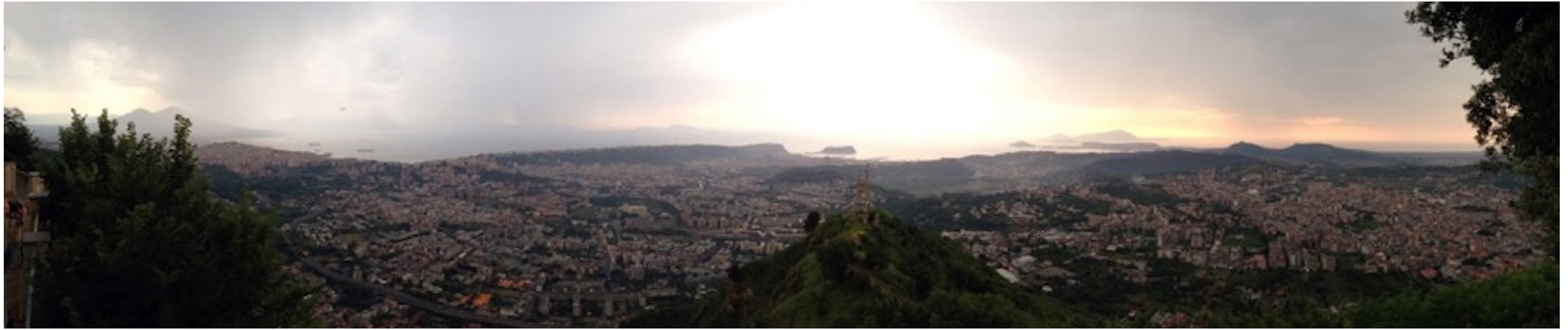


Fig. 6 - View from Camaldoli towards the south-southeast

observed, mainly due to presence of several overlapping volcanic edifices. In many cases, these edifices are only partially preserved due to both subsequent explosive activity and erosion process mainly by the sea. In the foreground the Agnano plain and the Astroni tuff ring are visible. The former results from a volcano-tectonic collapse occurred during the Agnano-Monte Spina eruption (about 4.5 ka). Behind the Astroni and Gauro volcanoes, is the Averno-Capo Miseno alignment of tuff cones and tuff rings, which marks the western margin of the NYT caldera. All these volcanoes but Fondi di Baia (9.6 ka) and likely Capo Miseno, formed during the I epoch (15-9.5 ka).

Close by view toward southwest is the Astroni volcano (Fig. 7) (about 4.2 ka), a well preserved elliptical edifice with axes of about 2 and 1 km, formed during the III epoch of activity (4.8-3.8 ka) of the Campi Flegrei caldera (Di Vito et al., 1999).

Camaldoli Hill

This site is the highest point of the Campi Flegrei caldera, and allows to observe at the main structure of the caldera as well as to the very dense urbanisation of the area, providing an immediate idea of the associated volcanic risk. From this point of view it is also interesting highlight the differences of the volcanoes surrounding Naples and how this different morphology is perceived by the local population.



Fig. 7 - The Astroni crater from Camaldoli hill.

Stop 1.2: Verdolino quarry and Campanian Ignimbrite ($40^{\circ}51'18.51''\text{N}$ - $14^{\circ}12'27.77''\text{E}$)

Significance – The CI caldera forming eruption, and its stratigraphical and geometrical relationships with the NYT and interposed deposits.

The Campanian Ignimbrite deposits

Proximal to medial fall deposits indicate the first phase of the eruption generated a Plinian column and dispersed pumice and ash directly east of the vent. This Plinian fallout unit reaches ~ 1.4 m at ~ 40 km from the caldera,



and thins to ~ 15 cm at 120 km from the vent. Two subunits are observed within the fall deposits for an estimated total volume of the Plinian fallout unit to be ~ 15 km³ and the maximum column height to be ~ 44 km (Rosi et al., 1999). Outcrops of PDCs associated with the CI eruption are commonly found on land up to 70 km from the vent (Fig. 8). Various different flow units have been identified in the CI deposits by Fisher et al. (1993), Rosi et al. (1996), Cappelletti et al. (2003), Fedele et al. (2008) and Scarpati and Perrotta (2012). These previous studies observe five main flow units on top of the Plinian fallout, many of which can still be identified up to 60 km from the vent (Cappelletti et al., 2003; Scarpati and Perrotta, 2012). The first flow unit is an unconsolidated

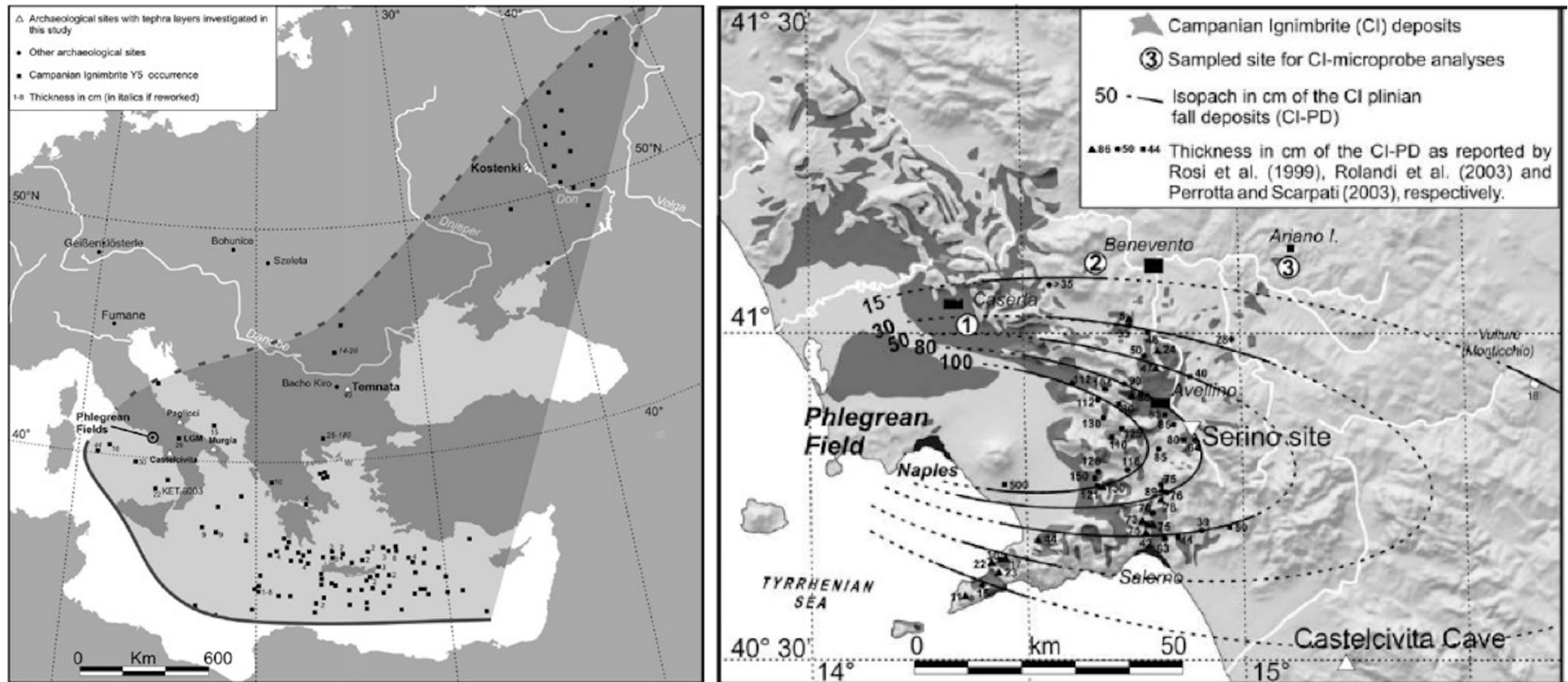


Fig. 8 - Distribution of the Campanian Ignimbrite distal tephra (left) and its intermediate-proximal deposits (right); modified from Giaccio et al. (2008).



stratified ash flow (SAF), grading from a white color at the base to slightly red at the top, and is less than 0.5 m thick close to the vent. The second unit is a welded grey ignimbrite (WGI) that is subdivided into 2 subunits; the first is a monolithologic grey welded ignimbrite which has characteristic fiamme (flattened scoria) and grey lava fragments, and is often referred to as the Piperno facies (Rosi et al., 1996 and references therein; Fedele et al., 2008). This Piperno subunit can reach up to 20 m in thickness in proximal locations. The second WGI subunit is a reversely graded welded ignimbrite with a black scoria in an ashy matrix, which reaches up to 45 m, and is suggested to be the main flow unit preserved at medial sites in the Apennine Mountains by Scarpato and Perrotta (2012). The thickest flow unit in proximal sections, is the Lower Pumice Flow Unit (LPF). It is mostly lithified and zeolitized yellow flow unit with blocks of pumice and some scoria clasts. The fourth flow unit is a distinct lithic-rich breccia, which appears to relate to the Breccia Museo (BM). The unit displays some crude stratification, has some juvenile pumice and obsidian clasts, and up to 3 distinct spatter agglutinate units within it (Fedele et al., 2008). The large volume of lithics and their variety, along with the opening of new vents depositing the spatter, indicates that this BM deposit was associated with the major caldera-forming phase of the eruption (Rosi et al., 1996). The uppermost flow unit (UPF) is a poorly sorted, unlithified flow with pumice and lithic clasts and has abundant degassing pipes.

The CI tephra is found all across the central and eastern Mediterranean (Fig. 8), on land to the east of Italy and in an area including northern Libya in the south and River Don river valley, Russia in the northeast.

Costa et al. (2012) estimated that the eruption column was ~37-40 km and the total volume of fallout material, associated with both the Plinian column and the co-ignimbrite plume, to be 250-300 km³, corresponding to 104-125 km³ of magma (dense rock equivalent, DRE). Once the volume of the PDC (Pyle et al., 2006) is considered, the total bulk volume for the CI eruption is estimated in 430-680 km³, which is equivalent to 180-280 km³ DRE (Costa et al., 2012).

Using the glass compositional data, Smith et al. (2016) clearly indicates that most of the ultra-distal dispersal during the CI eruption was associated with the late co-ignimbrite plume that was generated during caldera collapse. Authors highlight that the dominance of the co-ignimbrite component is likely to be linked to the fact that the flows are the most voluminous component of the eruption, and estimated that the Plinian column dispersed approximately 17-20% of the volume erupted, with 45-67% that was dispersed by the co-ignimbrite plume, and 13-38% emplaced as flows. The area over which the ash was dispersed increased due to co-ignimbrite plume would have been transported by both tropospheric and stratospheric winds, which could have been in different directions (Smith et al., 2016).



The Neapolitan Yellow Tuff.

The NYT is the second largest pyroclastic deposit of the Campanian area. Conservative estimates of the area covered by the tuff and volume of erupted magma are 1,000 km² and about 20-40 km³ (DRE), respectively. The deposit, is zeolitised and yellow in the proximal Neapolitan-Phlegraean area (Fig. 9), from which the name, and generally grey and poorly lithified in distal areas. The Stratigraphic and chemo-stratigraphic sequence, the eruption mechanisms, the feeding magmatic system, and the relationships among eruption dynamics, magma withdrawal, and timing of caldera collapse, have been reconstructed in details by different authors Orsi et al. (1992; 1995) Scarpati et al. (1993) and Wohletz et al. (1996).

The NYT sequence was divided into a Lower Member (LM) and an Upper Member (UM), on the basis of textural characteristics, dispersal and occurrence of an angular unconformity. LM is the product of the largest known



Fig. 9 - Neapolitan Yellow Tuff deposit (loc. Trentaremi, Napoli; Foto by R. Isaia).



trachytic phreato-Plinian eruption. Its thickness varies from 11 m in the most proximal exposures, to 85 cm at Sant'Angelo in Formis, at the foot of the Apennine mountains, 35 km from the vent area. In contrast, the characteristics of UM are typical of a phreatomagmatic eruption. Its thickness varies from about 100 m in the Quarto Plain, to 7 m at Scarafea, in the Caserta Plain.

A time break occurred after LM eruptions, and then activity resumed with very different characteristics in UM explosions. The time break is likely marked by initiation of a caldera collapse and a change from central-vent to ring-fracture eruptions. Water/magma interaction during UM eruptive phases was not as efficient as during LM phases. Explosions fed mainly pyroclastic flows and surges widely dispersed in the city of Naples.

The Verdolino quarry. – Along the wall of an old quarry dug at the mouth of the Verdolino valley, in the Soccavo plain (Fig. 5), the Piperno and Breccia Museo deposits of the CI are exposed (Fig. 10). They are overlain by younger pyroclastic deposits up to the deeply zeolitized sequence of the NYT. In between the CI and NYT thick sequences are exposed a sequence containing at least 5 pyroclastic units generated mainly by phreatomagmatic explosions with minor magmatic events from vents located not far from the outcrop area.



Fig. 10 - View of the Verdolino valley from the north-west showing the unconformity between Campanian Ignimbrite proximal facies (on the left) and the sequence of younger tuffs with the Neapolitan Yellow Tuff forming the top part of the sequence (on the right).



The sequence of Piperno and Breccia Museo, whose top is at about 200 m a.s.l., dips of about 6° towards the north and is intersected by an erosional surface dipping about 35° southward. Units between CI and NYT unconformably mantle this surface and die out toward its upper part. Also, these units are cut by an erosional surface, whose dip increases southward. This surface is mantled by the NYT, whose thickness of about 100 m increases towards the Soccavo plain and whose base, at about 240 m a.s.l. at the top of the surface, is 170 m a.s.l. at its foot.

Stop 1.3: The Astroni volcano (40°50'23.24"N - 14°09'23.21"E)

Significance. – The succession of 7 eruptions closely spaced in time in the same area during a period of very intense volcanism

The Astroni volcano is one of the well-preserved edifices within the caldera hosting a forest and two small lakes. The tuff ring, characterized by axes of about 2 and 1 km and a maximum elevation of 253 m a.s.l., (Fig. 11) formed at about 4.2 ka during the most recent epoch of activity (5.5-3.8 ka) of the CF caldera (Di Vito et al., 1999; Isaia et al., 2009; Smith et al., 2011).

The activity of the volcano was dominated by explosive, mostly phreatomagmatic eruptions, with only subordinate lava effusions. Isaia et al. (2004) identified 7 depositional units, their internal stratigraphy and areal distribution, and their relationships with the other volcanic units of the Campi flegrei caldera. The entire Astroni sequence is found between the deposits of Solfatara and Averno 2 Tephra (Isaia et al., 2009; Pistolesi et al., 2016) and Fossa Lupara tephra (Fig. 12).

The recognized Units have been named 1 through 7 from base upwards and are delimited by either thin paleosols or erosional unconformities. They are composed of pyroclastic deposits mainly generated by phreatomagmatic with subordinate magmatic explosions. Only two (Units 5 and 7) include products of late low-energy explosions and lava extrusion. All phreatomagmatic explosions have generated large amount of ash widely dispersed in the Campanian Plain (Fig.13).

The texture of the deposits of such explosions varies according to distance from the vent, from coarse and wavy to plane-parallel, to fine and plane-parallel to massive. The magmatic explosions produced strombolian fallout layer intercalated to the surge bed. In some cases, the particle fallout was contemporaneous to the surge flowage. The base of Unit 6 is the only Plinian fallout deposit of the entire Astroni sequence, deposited by a column which



Fig. 11 - View of the Astroni crater (G. Vilardo, Lab. Geomatica e Cartografia, Osservatorio Vesuviano)

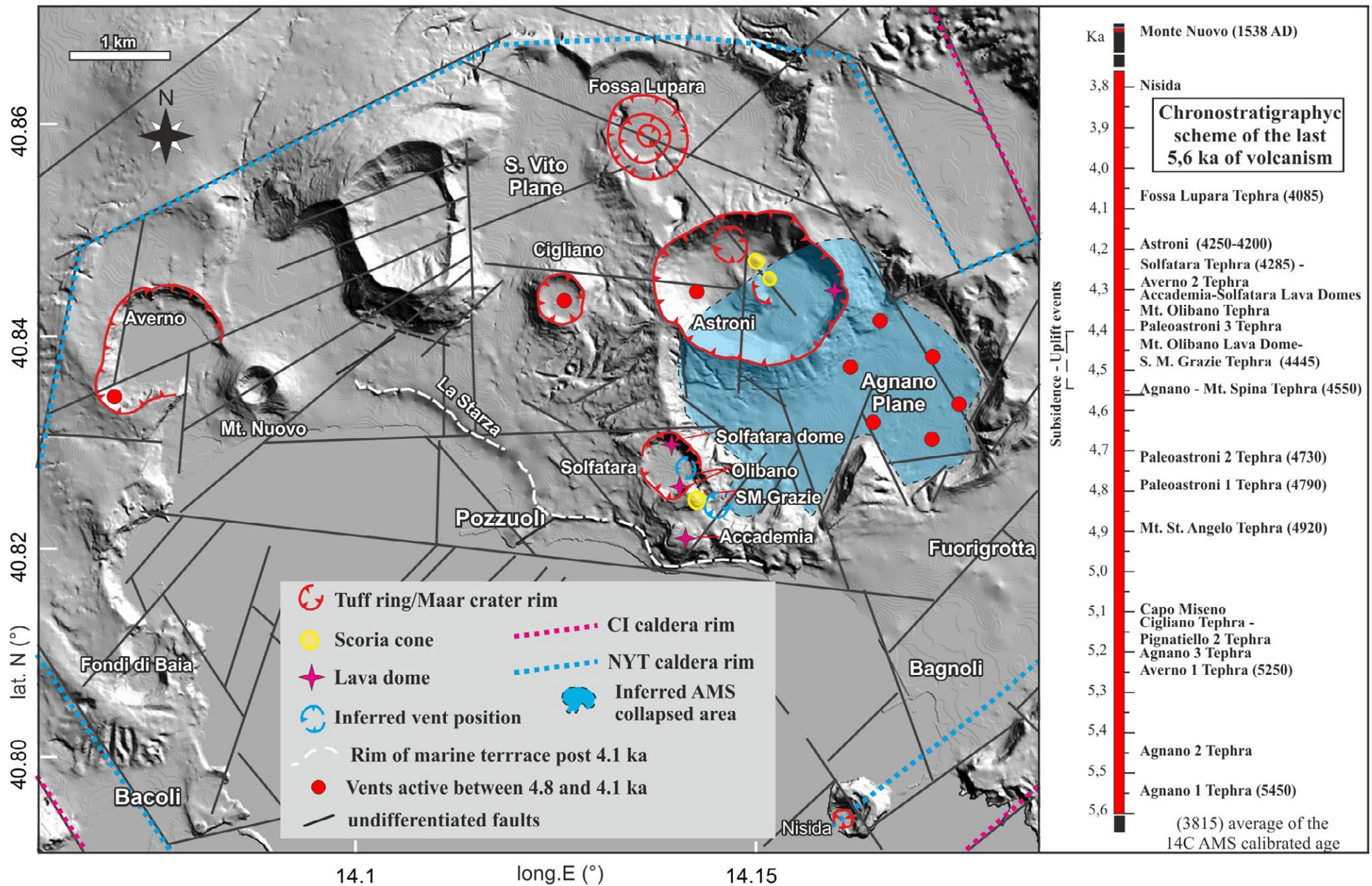


Fig. 12 - Vent location within the central sector of the Campi Flegrei caldera and chronostratigraphy between 5.6 ka and 1538 AD (from Isaia et al., 2015).

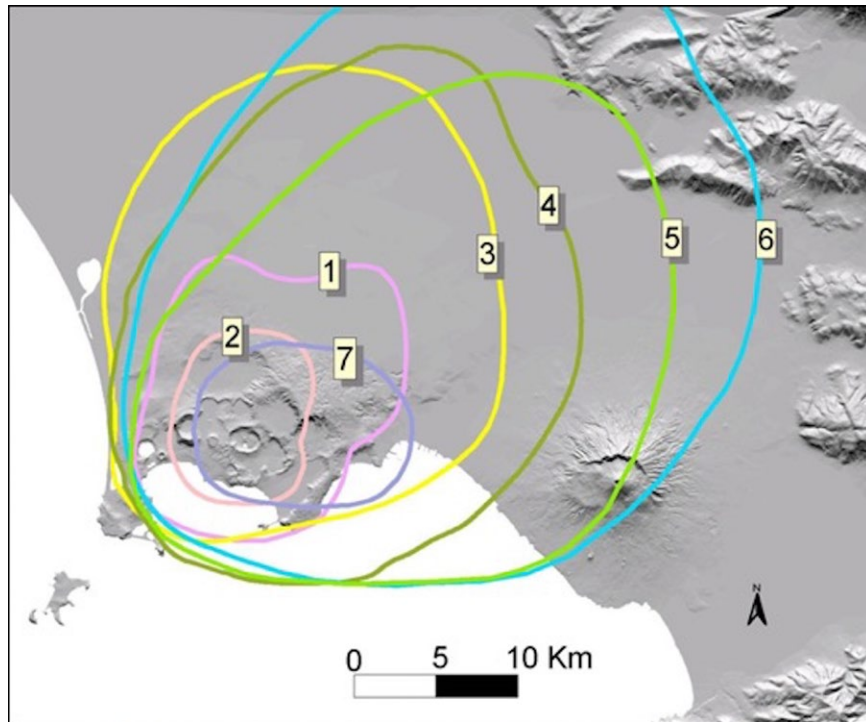


Fig. 13 - Isopachs maps of 10 cm thick tephra layers of the 7 Astroni units (from Isaia et al., 2004).

extruded alkali-trachytic and a less evolved trachytic magma.

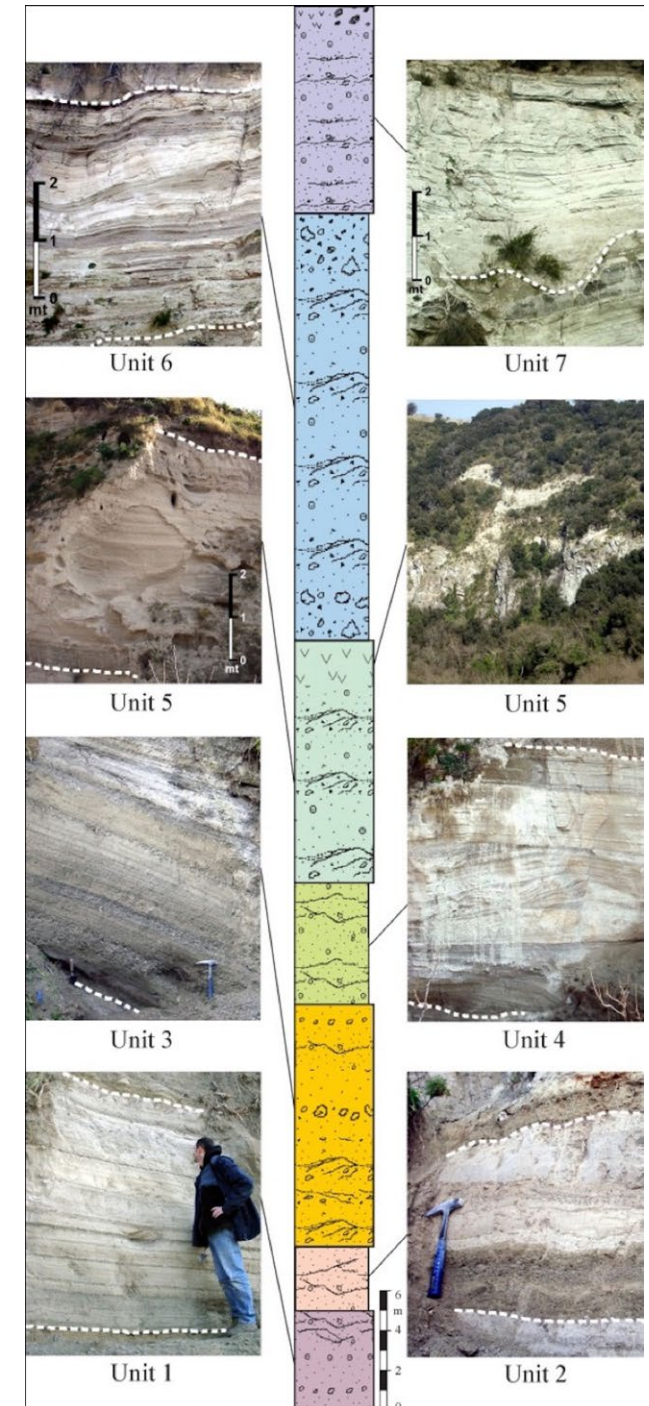
The volcano grew at the northwestern edge of the polygonal volcano-tectonic collapse, NW-SE elongated, which accompanied the Agnano-Monte Spina eruption (4.5 ka), the largest of the III epoch. Stratigraphical data and calibrated radiometric dates constrain the age of the volcano between 4.25 and 4.2 ka. This implies that the 7 eruptions followed each other at very short time intervals, soon after the eruptive activity of Solfatara maar system and slightly before the formation of the Fossa Lupara volcano. The sequence of 7 close eruptions in the same area during a period of very intense volcanism,

Fig. 14 - Reconstructed type sequence of the Astroni Units (from Isaia et al., 2004).

reach a maximum height of 20 km (Fig. 14).

Facies and thickness variation of the deposits indicate that the eruption vents, although confined in the present crater, migrated from NW to SE during the course of the eruption.

The total volume of erupted magma is 0.45 km^3 (DRE), while the total mass is $1.12 \cdot 10^{12} \text{ kg}$. The magma feeding the first 5 eruptions was alkali-trachytic and slightly zoned, while the last two eruptions tapped a magma batch resulting from mixing of the previously





makes the Astroni volcano peculiar in the recent history of the CFc, and provide also very important clue to understand the eruptive scenarios of the caldera, as relevant elements to forecast its behavior.

The Crater of Astroni

A viewpoint close to entrance of the Natural reserve of Astroni allows us to look at the well-preserved crater of the tuff ring generated after 7 distinct eruptive events. Along the internal flanks of the volcano, pyroclastic sequences crop out showing very interesting structures of proximal PDC deposits. The north-eastern sector of the edifice exposed the remnant of the lava dome (La Caprara) ending the eruptive event 5 of the sequence. The floor of the crater hosts different small scoria cone and a tuff cone, and among them small lakes.

The Crater of Astroni is presently a WWF Natural Reserve of 247 hectare near Napoli city centre. Most of the crater is covered in forest. At the bottom of the crater there are three lakes (Lago Grande, Cofaniello Piccolo e Cofaniello Grande) and a number of small hills (Colle dell'Imperatore and Colle della Rotondella) formed after the volcanic eruptions.

The whole area is an environmental mosaic of considerable complexity and the composition of the vegetation is the result of inverted plant zonation. This particular type of plant zonation, whereby high altitude species are found at lower altitudes and low altitude species grow at higher altitudes, is the result of the particular micro-climatic conditions of the crater.

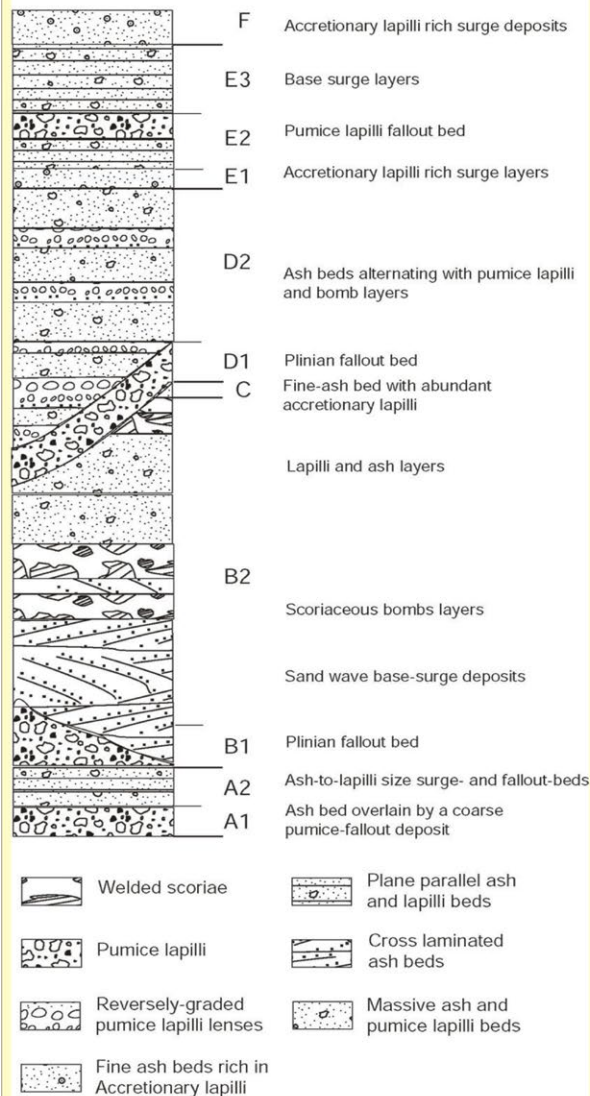
The remarkable biodiversity of the Reserve favoured the establishment of a very diverse animal community. Birds are the most interesting wildlife presence: there are approximately 130 different species that come to rest and/or nest during migration and the winter season.

Moreover, at the reserve Environment Education Centre (CEA) WWF staff organise educational activities both for schools and visitors, and specific labs during the Spring and Summer months for children and teenagers.

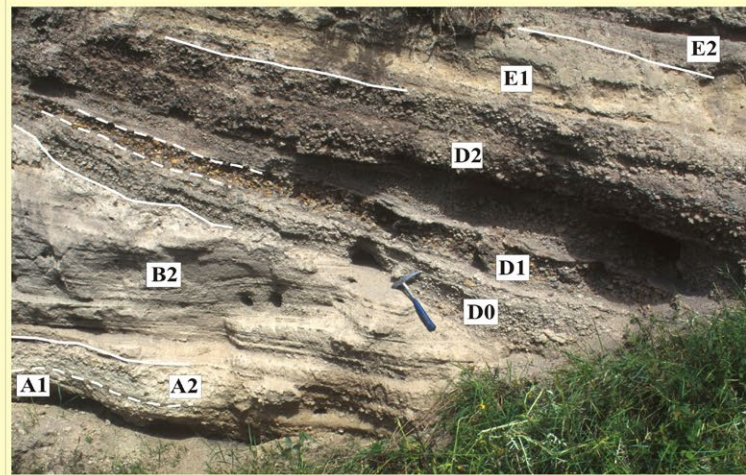
Stop 1.4: The Agnano Monte Spina Plinian eruption (40°49'32.91"N - 14°09'59.41"E)

Significance. - Agnano-Monte Spina eruption, the largest eruption in the Campi Flegrei caldera over the past 5.5 ka.

Agnano Monte Spina eruption (AMS) - The AMS is the highest-magnitude eruption that occurred over the past 5.5 ka within the CFc (de Vita et al., 1999; Di Vito et al., 1999; Dellino et al., 2001; Orsi et al., 2004; Costa



Agnano-Monte Spina schematic sequence



et al., 2009; Smith et al., 2011). de Vita et al. (1999) presented a detailed reconstruction of the pyroclastic sequence and obtained a radiocarbon age of the eruption to 4.1 ka, which successively has been calibrated and modelled by Smith et al. (2011) providing an age of about 4.5 ka. Authors subdivided the whole sequence into six members (A through F) mainly based on variation of lithological features (Fig. 15).

Members are further subdivided into sub-members upon sedimentological characteristics. Plinian/sub-Plinian fallout deposits generated by magmatic explosions frequently alternate with base-surge beds of phreatomagmatic origin (de Vita et al., 1999; Dellino et al., 2004). During some eruption phases the contrasting eruption dynamics were almost

Fig. 15 - Agnano Monte Spina composite stratigraphic succession; photos on the right refer to proximal deposits (below; Agnano area) and medial-proximal deposits (above; Pianura area).



contemporaneous (Dellino et al., 2004). Mele et al. (2015) studied the PDC generated during the AMS eruption with the aim of assessing the potential impact of similar events in the future. Laboratory analyses on samples from the main layers of deposits allowed obtaining the input data for the PYFLOW code, which was used for reconstructing the flow dynamic characteristics of the currents. In the large-scale even like AMS, the dynamic pressure ranges from 9.38 to 1.00 kPa (integrating the basal 10 m of the current) at distances of 1.5 and 4.0 km from the vent, respectively. These values are highly influenced by the local topography. provide

important information on the potential impact that similar PDCs could cause to buildings, infrastructures and population.

Only two of the six members of the AMS pyroclastic sequence comprise coarse fallout layers produced during Plinian phases. The stratigraphically lowest Plinian fallout deposit of the entire AMS sequence was recognized at the base of Member B (sub-Member B1). It is composed of a coarse pumice-fallout layer laid down by a pulsating column reaching a maximum height of about 23 km. Isopach maps indicate that B1 was dispersed towards the east up to 45 km from the vent area (Fig. 16). Another coarse pumice-fallout deposit (sub-Member D1) was recognized in the lower portion of the Member D. This fallout layer generated during magmatic explosions was deposited by a Plinian column that reached a maximum height of about 30 km. Layer D1 is a pumice-fallout deposit with a northeastward oriented dispersal axis. Isopachs are quite regular elliptical curves covering an area of at least 700 km² (Fig. 16). According to de Vita et al. (1999), thickness of AMS Tephra varies from a maximum estimated value of about 70 m in the Agnano plain, which is the inferred vent area, to a

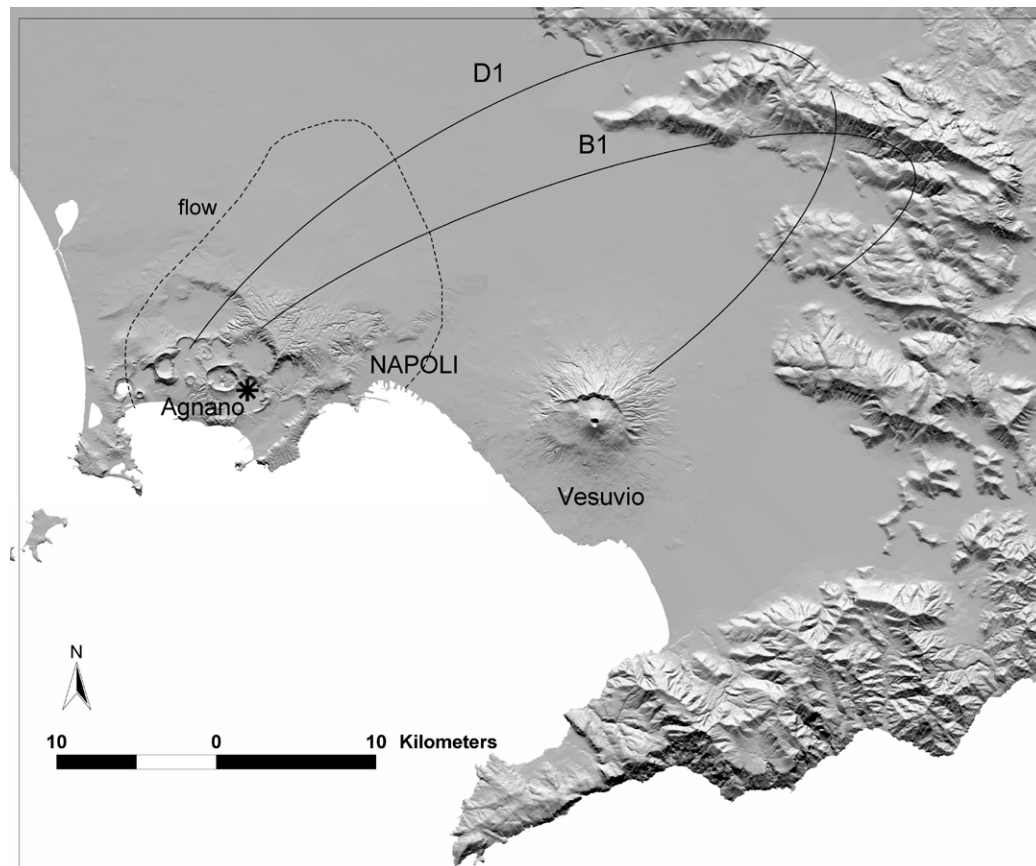


Fig. 16 - Areal distribution of Agnano Monte Spina deposits; the dashed line delimits the area of the PDC dispersion, the solid lines encompass the isopachs of 10 cm for the main fallout deposits, the asterisk indicates the vent area. After de Vita et al. (1999).



few centimetres over a distance of about 50 km (Fig. 16). The total volume of the erupted magma was 1.2 km³ (DRE), while a volume of 0.11 and 0.10 km³ (DRE) was here estimated for B1 and D1 fallout deposits, respectively.

The Agnano-Monte Spina Tephra range in composition from trachyte to alkali-trachyte. Pumice and scoria fragments are porphyritic, with phenocrysts of feldspar, clinopyroxene, black mica, apatite and opaques in order of decreasing abundance. Olivine is present only in few samples. Arienzo et al. (2010) on the base of chemical and isotopic data on whole rocks and glasses suggest that at least two magma batches mixed during the course of the eruption, whereas melt inclusion data highlight the pre-eruption storage conditions of two magmatic end-members. The H₂O and CO₂ contents in pyroxene-hosted melt inclusions yield entrapment pressures between 107 and 211 MPa, corresponding to depths between 4 and 8 km.

Glass chemistry data and information on the eruptions have been used to correlate eruption units in a proximal and distal locations (Smith et al., 2011). The chemical and physical characteristics of the uppermost Lago di Monticchio layers with a Campi Flegrei chemical affinity indicate that they are from the AMS eruption, and reveal that AMS comprised two separate plinian eruptions separated by 40 years (based on varve counts). This detailed information on volcanism enables also to use this data for hazard assessments of the Campi Flegrei active caldera.

The San Germano exposure

A very proximal sequence of the Agnano Monte Spina Tephra is exposed in an old quarry cut along the flank of the Monte Spina hill, in the Southern part of the Agnano Plain (Fig. 5). The exposure is a typical sequence of this tephra at proximal distance from the vent area supposed very close to the site, which show diverse deposits facies including a breccia and an unconformity separating the different members.

Stop 1.5: INGV - Osservatorio Vesuviano and its surveillance center (40°49'10.63"N - 4°10'58.54"E)

The Vesuvius Observatory, a section of the Istituto Nazionale di Geofisica e Vulcanologia, carries out research in various fields of geophysics, geochemistry and volcanology. The main objectives are to develop an increasingly detailed understanding of the processes which generate volcanic eruptions, and a definition of the mechanisms governing the evolution of such phenomena. Research activity covers the monitoring of active volcanoes, the physics of volcanism, geochemistry of fluids, geodetics, seismology, seismotectonics, volcanology and petrology.



To these ends, the Vesuvius Observatory collaborates with various Italian and foreign scientific institutes. Staff members are always on duty at the Vesuvius Observatory. The operators are responsible for checking seismic developments of the Campania volcanic areas (Vesuvius, Campi Flegrei and Ischia) and for communicating to the authorities any significant phenomena observed by the seismic monitoring system, under permanent observation. The Civil Protection Body are immediately informed of the location and the Magnitude (Md) of any potentially perceptible earthquake. In the Vesuvius area, this means information concerning earthquake with a Md of 2.5 and above, and in the Phlegrean area, with a Md of 2 or higher. The seismic monitoring system used for the shift system is based on a permanent seismic network (Italian only), consisting of several stations throughout the area which continually transmit data to the surveillance center (Fig. 17), via radio or via dedicated telephone lines. In the Vesuvius Observatory monitoring room the signals appear on monitors (rather than the traditional mode, on paper,) thanks to an innovative processing system, called SISMI, and hence the traces appear on the web. This system, which has been developed by our staff, has an automatic alarm system which sends messages to mobile phones in case of seismic event or malfunction of any component(s).



Fig. 17 - The surveillance center at the Osservatorio Vesuviano – INGV in Napoli.



Day 2

Stop 2.1: Baia-Fondi di Baia eruptive sequence (40°48'37.74"N - 14°04'48.10"E; 40°49'18.15"N - 14°04'19.69"E)

Significance. – Short time migration of the eruptive vents for small eruptions occurred closely to the sea level.

The Baia–Fondi di Baia eruption is one of the sporadic events that have occurred in the western sector of the Campi Flegrei caldera. It dates back to 9525–9696 BP and opened Epoch 2 of the caldera activity after a 1000-year-long period of quiescence. Although relatively small in terms of erupted volume with respect to most of the events of the past 15 ka, the Baia–Fondi di Baia eruption was characterized by a complex series of events. The stratigraphic succession has been related to two distinct eruptive episodes (Baia and Fondi di Baia). These were separated by a short time interval, and each was characterized by different eruptive phases (Pistolesi et al., 2017). The Baia eruptive episode started in a shallow-water environment with an explosive vent-opening phase that formed a breccia deposit (Unit I), rapidly followed by alternating fallout activity and dense, PDC deposits generation (Unit II).

Sedimentological features and pumice textural analyses suggest that deposition of Unit II coincided with the intensity peak of the eruption, with the fallout deposit being identified up to 20 km north of the Baia crater. This peak phase waned to turbulent, surge-like activity possibly associated with Vulcanian explosions and characterized by progressively lower intensity (Unit III). This first eruptive episode was followed by a short quiescence, interrupted by the onset of a second eruptive episode (Fondi di Baia) whose vent opening deposited a breccia bed (Unit IV) which at some key outcrops directly overlies the fallout deposit of Unit II. The final phase of the Fondi di Baia episode strongly resembles Unit II, although sedimentological and textural features, together with a more limited dispersal, suggest that this phase of the eruption had a lower intensity (Fig. 18). From the Baia Castle, on the southern side of the vent area, we have a complete overview of the inferred source location of the Baia-Fondi di Baia eruption. The Baia vent can be placed within the Baia harbor, today partially invaded by the sea. During the eruption, the source area migrated southward, and the inferred vent of the Fondi di Baia event coincides with the southernmost crater (Fig. 19).



Fig. 18 - Left: composite stratigraphic succession of Baia and Fondi di Baia eruptions. Right: pictures of the Baia succession. (a) Opening breccia (Unit I) which overlies the basal paleosol. (b) Fallout and PDC deposits of Unit II. (c) Detail of a pumice layer shown in (b). (d) PDC layers of the upper part of Unit II. (e) Detail of a breadcrust bomb shown in (d). (f) Cross-bedding of surge deposits of Unit III. (g) Pumice fallout deposit of Unit II overlying a paleosol 20 km north of the vent. On the left, idealized composite stratigraphy of the different phases of the eruption. Modified after Pistolesi et al. (2017).

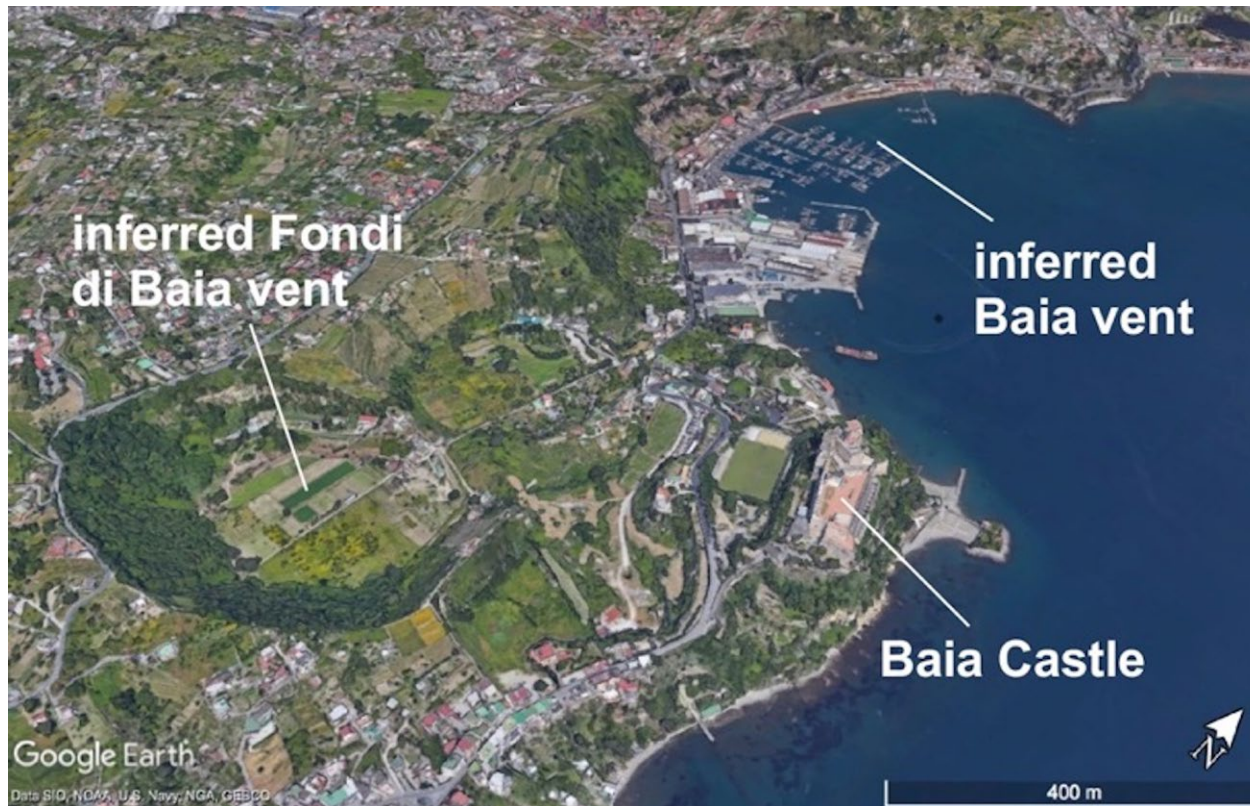


Fig. 19 - General overview of the source area, characterized by the presence of three circular depressions. The Baia harbor, vent of the Baia event today partially invaded by the sea, and the southernmost crater, vent of the Fondi di Baia eruptive episode. The central depression was unlikely the FdB eruptive center because its floor is covered by the soil over which Units II and III are emplaced and which form the crater walls. The depression possibly pre-dated the eruption or was formed by post-eruption collapse along the same N-S structure along which the vents are aligned.

The Baia Sequence

The key section of the Baia sequence is exposed on the western side of Baia's harbor. In this area, we have a complete overview of the >20-m thick tephra succession (Fig. 18). By walking on the internal rim of the Baia vent, we will

access all the stratigraphic sequence, from the altered, opening breccia, to the fallout-dominated deposits, to the PDC-dominated, surge-like deposits.

The Archaeological Museum of Baia

The Archaeological Museum of Campi Flegrei, which opened in 1993, is housed inside a fortress dating back to the Aragonese period, which has been specially restored and adapted to full its new role as an exhibition venue. It is located on the top of the high promontory southern closed to the gulf of Baia, and from which the entire bay of Pozzuoli and the islands of Capri, Ischia and Procida are visible.

In its splendid landscape setting, which can be admired from the Aragonese fortress, the museum reconstitutes dispersed contexts of Flegrean origin, thus reuniting objects found long ago that up until now have been kept



in storage at the Museo Archeologico Nazionale di Napoli, with objects discovered in recent excavations, following a logical exhibition layout organized by topography and by theme such as: Cuma, Puteoli, Baiae, Misenum e Liternum.

The tour begins with the Cuma Section on the second floor, housed in the former barrack- rooms used by the fortress soldiers: twenty-four rooms illustrate the history of the site from the 9th century BC Opican settlement to the 8th – 5th century BC Greek city, to the 4th century BC Samnite city, to the Roman city, to the final Byzantine period.

The Pozzuoli Section consists of twenty rooms on the first floor, illustrates the history of the site: the first urban expansion of the Augustan colony (theatre buildings, aqueduct, cosmopolitan city such as Grotta del Wady Minahy in the Egyptian desert), the Neronian colony and the new urban conformation imposed by the emperors, the late-ancient revival, the suburban villas and the necropolises.

The Rione Terra Section located in the Piazza d'Arme exhibits remains came from recent excavations related to the Capitolium architectural decoration and the sculpted decoration of other public buildings in the Augustan forum: ideal statues, including the head of Athena Lemnia, portraits of Julio-Claudian age and fragments of statues of caryatids and clipei, reminiscent of the attic in the forum of Augustus in Rome, which has been reconstructed as it might be looked.

The Baiae and Misenum reconstruct the Sacello degli Augustali da Misenum, the Ninfeo of Punta Epitaffio and the ancient plaster casts made from Greek originals of classical and Hellenistic age, presents the findings of the ancient Roman maritime villa late Republican, discovered under the Castle and the Knight Pavilion, with splendid mosaic floors and cocciopesto decorated, and frescoes fragments of late Pompeii style.

Liternum, a maritime colony founded in BC 194, shows finds (sculptures, inscriptions, tomb goods and various types of artefacts) recovered in old and new excavations performed by the Superintendency in urban areas, in the Forum area, in the amphitheater and in the necropolises.

Baia Roman Thermal Site

"No gulf in the world is as marvellous as Baia's". Wrote the poet Orazio at the end of the 1st century BC. In that period Baia was a residential centre with villas and thermal buildings built facing the little gulf, which was similar to a lake (*lacus Baianum*) connected by a canal to the open sea. The beauty of the panorama, the



Baia - Bath of Mercury

majestic dome of the thermal room, best known as "Truglio" or "Mercury Temple" or "Echo Temple" for the acoustic effect produced here. This dome, built at the end of the 1st century BC, was way ahead of its building techniques used a century later in the building of the Pantheon in Rome.

The imperial palace (*Palatium Baianum*) extended over all the mountain facing the gulf including the already existing villas and the thermal buildings. Its remains are identified by the big building known as Baia's thermal baths, because of the presence of many thermal rooms. These rooms extend on the longitudinal line of the hill, on different levels of terracing, but due to the bradisism, the lower level, which was at the mountainsides till the ancient coast

local springs of natural warm water and sulphurous steam coming from the volcanic subsoil, had attracted the Roman nobility here since the 2nd century BC. They loved to spend their *otia* (spare time) in these villas by the sea.

With the coming of the Empire, Baia became the imperial family's residence and in the next three centuries the building of structures for entertainment rose to such an importance that these buildings became models for Roman ones. One example is the



Baia - Nymphaeum - theatre



line, is today submerged. Long and steep flights of steps cut the buildings orthogonally to connect the various levels.

It is not a unitary monument but it's composed of five sectors that have not the same orientation, which is the sign of a different chronological construction. They are known as the Terrace complex, the Mercury thermal baths, the lower thermal baths, the Sosandra thermal baths and the Venus thermal baths.

Apart from the Terraces Complex which is the lonely nucleus appearing as a villa, all the other buildings are composed of thermal baths, nymphaeums, fountain tubs, lodges and residential buildings open onto gardens. In the Sosandra thermal baths there is also a hemicycle nymphaeum - theatre, used as a relaxing place and as *cavea* for performances.

The complex is dated between the 1st century BC and the 3rd AD. Later because of the bradisism, a quiet but progressive decaying of the area started but not the celebrity of the Baia thermal baths, whose structures survived until the age of the Spanish viceroy Pedro Antonio di Aragona in the 17th century.

Thanks to the recently concluded POR project, which dealt with the restoration and development, the entire monument has been restored, the Diana sector has been recovered and is now accessible also from the new lower entrance. In fact, thanks to the relocation of the old train station, in agreement with Bacoli town council, a new entrance from the lower side of the monument has been opened. The improvement of the monument has been completed thanks to the two other POR projects which have dealt with the institution of a route for disabled people and the link to the Monumental Park by a winding naturalistic path along the hill.

Stop 2.2: The Averno 2 crater (40°50'35.13"N - 14°04'49.02"E)

Significance. – The activity of a tuff ring generated contemporaneously to the Solfatara volcano (about 5 km far, on the eastern sector of the caldera).

The Averno 2 eruption was contemporaneous to the Solfatara one, which vent is located in the eastern sector of the Campi Flegrei caldera (Isaia et al., 2009).

The Averno 2 eruption history and dynamics have been reconstructed by Di Vito et al. (2011) using structural, stratigraphical and sedimentological data. The eruption was characterized by three explosive phases, with variable dynamics and dispersal of the pyroclastic products.



The first phase of the eruption began with dominant magmatic and minor phreatomagmatic explosions from a vent located SW of the present Averno lake (I in Fig. 20). These explosions generated a very low eruption column, and then turbulent PDC, that together formed the fall and surge deposits of the A0 sequence of Member A (Fig. 21). The eruption continued from a new vent opened in the southwestern concave sector of the Averno lake depression (II in Fig. 20) with generation of an 8-km high eruption column, fed mainly by magmatic explosions, that laid down the A1 sequence, composed of a fall deposit (Fig. 21) overlain by minor surge beds. At this stage the vent further shifted toward the center of the present lake (III in Fig. 20) and the eruption reached its climax, producing an oscillating eruption column that reached the maximum height of 10 km, with a mass discharge rate of 3.2×10^6 kg/s. Contemporaneous to this magmatic column, sporadic phreatomagmatic explosions also took place, probably through an unlocated but nearby secondary vent. This explosive activity produced the A2 sequence, the most widely distributed of the AV2 sequence (Fig. 21), including a fall deposit overlain by, and interbedded with minor surge beds. The eruption continued in the central part of the present lake depression with magmatic and a few phreatomagmatic explosions, generating an eruption column that reached a maximum height of about 9 km. This activity generated the subsequent A3, A4 and A5 sequences, composed of dominant fall deposits with minor surge beds.

During emplacement of the A4 sequence, fractures appear to have opened, as suggested by the increase in lithics content, allowing ground- and/or sea-water to enter the shallow feeding system. This change in structural conditions produced a change in eruption dynamics and triggered onset of the second phase of the Averno 2 eruption. This phase was dominated by explosions driven by a very efficient water/magma interaction, with only a few episodes of magmatic explosivity, which generated low, short-lived eruption columns during

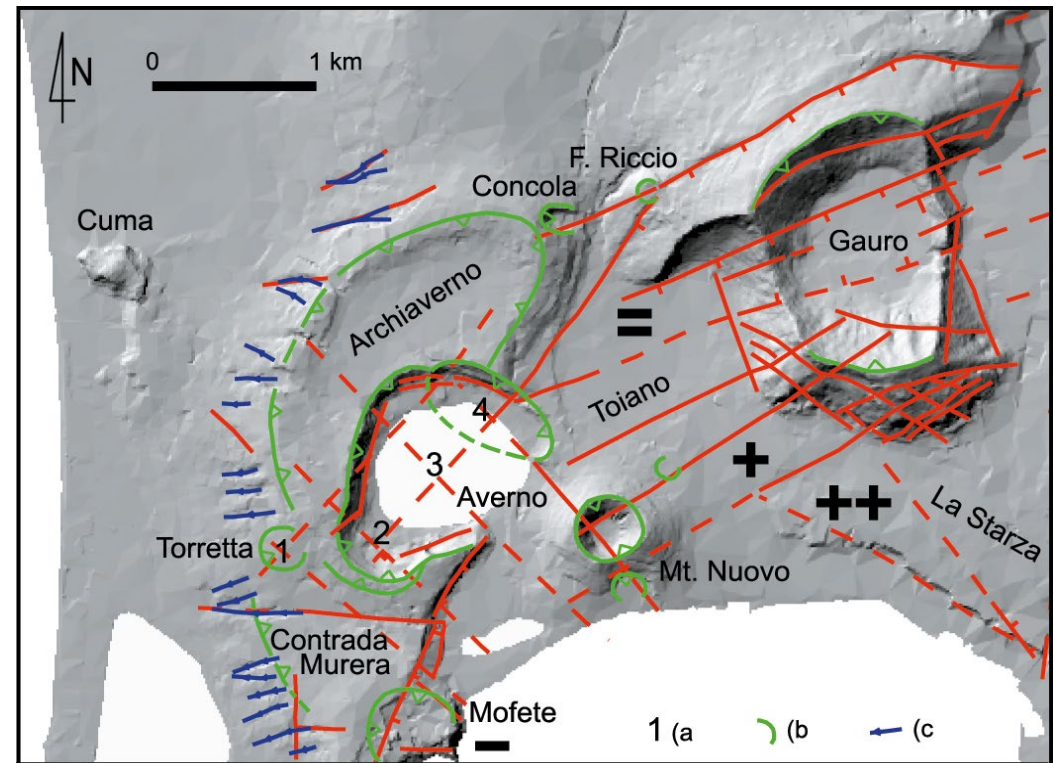
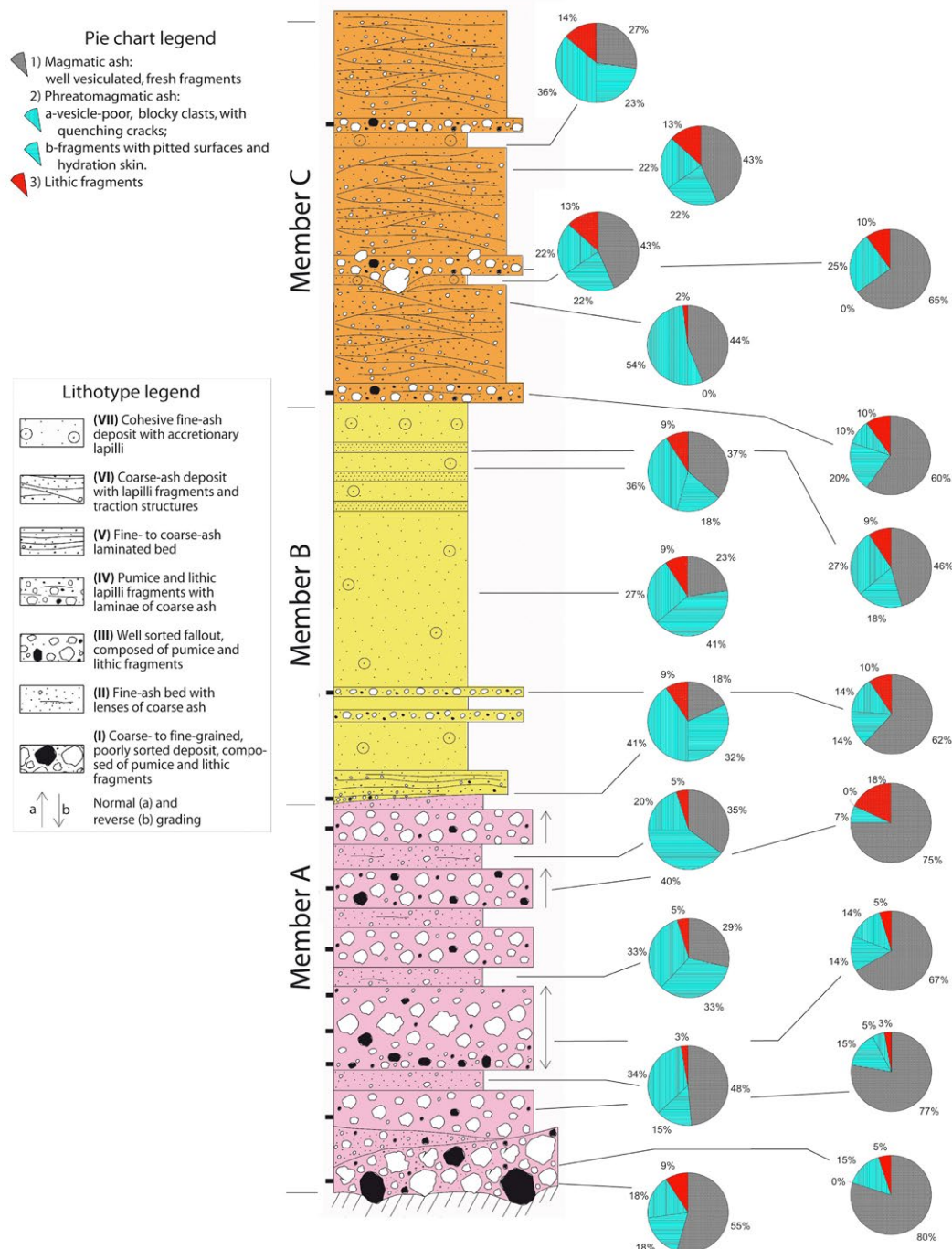


Fig. 20 - Morpho-structural sketch map of the Averno - Monte Nuovo area (after Di Vito et al., 2011).



the later stages of the activity. This second phase deposited Member B, a sequence dominated by wet surge beds, with minor fall deposits, dispersed preferentially northward from a vent still located in the center of the present lake (Fig. 20). The pre-existing Archiaverno tuff ring acted as a geomorphic barrier to the surge currents.

Another change in vent location and eruption characteristics marked the onset of the third phase of the eruption, which generated Member C. The eruption vent shifted towards the N-NE arched sector of the Averno lake depression (IV in Fig. 20), as suggested by distribution of the proximal facies of the pyroclastic deposits, distribution and geometry of impact sags by ballistic blocks and bombs, and Member C deposits draping the southern crater walls. This activity was dominated by phreatomagmatic explosions generated by efficient water-magma interaction, alternate with episodic magmatic explosions.

In summary, Member A was produced by three vents progressively active from SW toward the center

Fig. 21 - Stratigraphic type-section of the Averno 2 Tephra, with indication of the stratigraphic levels sampled for petrographic and geochemical studies in the left side of the section, as short dashes. Pie charts show the results of component analysis performed with SEM at the indicated levels; 1–3 are the types of fragments grouped according to their features (modified after Di Vito et al., 2011).



of the present lake. During emplacement of this Member the eruption, dominated by magmatic explosions, reached its climax (sub-member A2), although the total erupted volume (0.020 km^3 —DRE) was only about 1/3 of the total volume of the eruption. The eruption phases which produced Members B and C were dominated by phreatomagmatic explosions generating variably distributed pyroclastic surges from vents progressively shifting toward NE. These explosions were fed by more and more crystallized and degassed magma, which accounted for the remaining 2/3 of the total volume (Member B: 0.022 km^3 ; Member C: 0.025 km^3 —DRE). Notwithstanding the small volume of erupted magma (ca. 0.07 km^3 DRE), the products of this eruption show a slight variability of mineralogical, geochemical and Sr-isotopic characteristics, that sheds light on pre- and syn-eruption magmatic processes. The small range of composition, and the detected co-variations of major oxide and trace element concentrations, shown by the Averno 2 products (CaO from 2.4 to 1.8 wt.%), could result from a fractional crystallization process of a silica-rich magma, involving the mineral phases present in the rocks. This process is suggested by regular variation through the erupted sequence of major oxide and trace element contents with CaO as differentiation index. Sr-isotopic variations, however, indicate that open system processes, such as crustal contamination or magma mingling/mixing, operated in the magmatic system, rather than simple fractional crystallization.

Therefore, in order to explain all the detected geochemical and isotopical variations, Di Vito et al. (2011) proposed that two isotopically distinct magma batches were involved in the Averno 2 eruption. The first-erupted magma (A0 and A1 is the most evolved, least radiogenic batch ($^{87}\text{Sr}/^{86}\text{Sr}$ ca. 0.70751), while the second is slightly less evolved and more enriched in radiogenic Sr ($^{87}\text{Sr}/^{86}\text{Sr}$ ca. 0.70754). These two end-members mingled/mixed before and/or during extrusion of Member A. In fact, this member is slightly chemically zoned and characterized by the widest range of both chemical and Sr-isotopic composition of the whole sequence.

Belvedere di Averno, along the Domitiana road.

General view of the Averno crater filled by a perennial lake. The view is located near the vent IV, active at the end of the eruption. From the Belvedere it is possible to see the sequence of member A, dominated by coarse fallout beds, overlain by member B, dominated by ash surge deposits. This sequence is visible all around the crater walls. Looking towards the north the sequence of deposits continues with products of member C, composed by an alternation of laminated and undulated coarse and fine ash surge beds.



Stop 2.3: The Monte Nuovo volcano (40°49'58.32"N - 14°05'19.26"E)

Significance. – Precursor and eruptive phenomena associated to the only historic eruptions of Campi Flegrei.

The Monte Nuovo eruption, the most recent event of the Campi Flegrei caldera, has been reconstructed through both geological, volcanological and petrological investigations, and analyses of historical documents (Di Vito et al., 1987; and references therein; D'Orlando et al., 2005).

The eruption lasted one week and was fed by three vents (Fig. 20). The main vent (MV) was located in the present crater of the Monte Nuovo tuff cone, whereas two minor vents were along the southern (SouthV) and northeastern (NEV) slopes of the Monte Nuovo tuff cone. The eruption was characterized by three phases separated by pauses in the activity. The entire sequence of deposits has been subdivided in 5 members named A through E, from base upsection.

The eruption began on September 29th, 1538, at 7 p.m., and its first phase, which was the main phase of the entire event, lasted two days, until the night of September 30. This phase generated almost continuous phreatomagmatic with subordinate magmatic explosions, producing PDC and minor short-lived, low eruption columns, which deposited members A and B. Member A, composed of a sequence of plane-parallel to undulated fine- to coarse-ash beds forms the largest part of the Monte Nuovo tuff cone, and was erupted in about 12 hours through the MV. Phreatomagmatic explosions at the SV produced mainly PDC that deposited Member B. This member, composed of wavy fine-ash deposits containing coarse pumice and lithic fragments, is distributed only in the southern sector of Monte Nuovo and overlies unconformably member A. Strombolian explosions at the SouthV and NEV deposited the sequence of coarse scoria fallout deposits dispersed over narrow areas around the eruption vents, which form Member C. This activity marked the end of the first phase of the eruption and was followed by a pause that lasted two days.

The eruption resumed on October 3rd at 4 p.m. and lasted until the next night. This second phase of the eruption was characterized by a discontinuous sequence of low-energy phreatomagmatic and magmatic explosions at the MV, which deposited the sequence of Member D. The phreatomagmatic explosions produced laminated to massive ash surge deposits, while the magmatic events produced coarse pumice and scoria fallout deposits. Following a brief pause, the third phase of the eruption began at 4 p.m., October 6th, and lasted few hours. This last phase was characterized by low-energy magmatic explosions from the MV. This activity was likely characterized by the explosion of a small dome grown during the preceding pause, followed by minor, very low-



energy events at the crater of the MV, which produced Member E. This member includes fallout beds composed of dense to low-vesiculated, angular dark clasts. During this phase, 24 people died while climbing the slopes of the newly formed cone at the end of the second pause in the activity. The total emitted magma volume was 0.03 km^3 (DRE) and the maximum Mass Discharge Rate was $2.0 \cdot 10^6 \text{ kg/sec}$ (Orsi et al., 2009).

The juvenile products of the Monte Nuovo eruption are phenocryst-poor rocks containing alkali feldspars and subordinate clinopyroxene and Fe-Ti oxides. They are light-coloured pumice and dark scoria fragments, and represent the most evolved magma erupted over the past 15 ka at Campi Flegrei caldera. It extruded fairly homogeneous phonolitic magma ranging in Sr-isotope composition from 0.70741 to 0.70744, with $^{143}\text{Nd}/^{144}\text{Nd}=0.51247-49$ (Di Renzo et al., 2011).

For the volcanic hazards assessment of the Neapolitan area, the Monte Nuovo eruption is considered as the low-magnitude type event among those expected in case of renewal of volcanism.

Ground movements preceding the eruption

A detailed and quantitative reconstruction of the ground displacements predating the Mt. Nuovo eruption has been carried out by Di Vito et al. (2016). The authors integrated geomorphological, sedimentological, paleontological, archaeological and historical data of sites located along the entire coastline of the Pozzuoli Bay. The general results of their analysis are summarized in Figure 22, which shows the historical elevation changes, from 35 BC to Present, at the studied sites along the coastline of Pozzuoli Bay. These data show that in 35 BC the coastline extended outward into what is now the Pozzuoli Bay. However, since then all the area started to be affected by a quick subsidence, which resulted in progressive submersion of the coastline until 1251. The amount of subsidence in the investigated area varies from place to place. A subsequent progressive emersion of the area started during the 13th century, as suggested by historical and urban planning sources, archaeological evidence and geological data. The lower time limit for the caldera uplift is given by historical documents describing the Pozzuoli promontory of Rione Terra as an island in 1251, whereas at the end of the XIII and beginning of the XIV century the previously submerged area around the promontory is reported as the location of three new churches, testifying to the expansion of Pozzuoli on new land formed by the coastline regression, confirming the onset of a long-term uplift. The emersion of the area from the 13th to the 16th century was due to the ground uplift, with maximum values recorded in the Pozzuoli area.

The uplift rate was quite low (0.3 to 1 cm/yr; Fig. 22) from the middle of the 13th to the end of the 14th century, and increased to 2.9 to 9.1 cm/yr from 1400 to 1536. During this latter time-span, all the coastal strip emerged

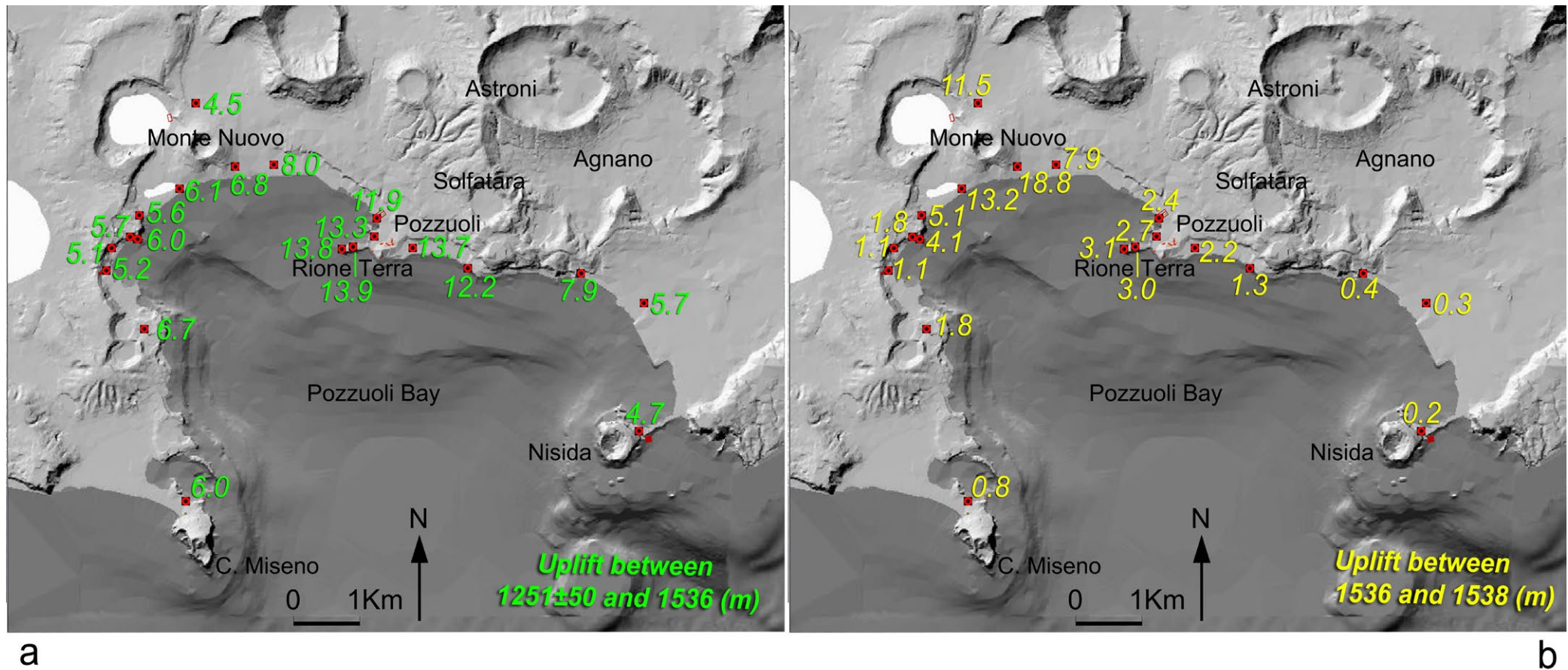


Fig. 22 - Distribution of the surface uplift preceding the Mt. Nuovo eruption. From 1251 to 1536 (a) the uplift affects the whole caldera, with a maximum in the Pozzuoli area. From 1536 to 1538 (b) the uplift is centred in the area of the future eruption (Monte Nuovo) (After Di Vito et al., 2016).

in response to the generalized uplift of the caldera floor, whose maximum of 12.3 m has been recorded again in the Pozzuoli area (Fig. 22).

Since the end of the 15th century this uplift was accompanied by strong seismicity (Guidoboni et al., 2010). A new and stronger uplift, with a rate of 10 to 940 cm/yr, followed the previous one between 1536–1538, reaching a maximum value of 18.8 m in the future vent-opening area (Mt. Nuovo; Fig. 22). This highest-rate uplift was accompanied by very intense seismicity, which affected all the Pozzuoli area and was felt also in the city of Naples (Guidoboni et al., 2010 and references therein). Furthermore, all the historical sources coeval to



the eruption report an evident uplift accompanied by continuous seismicity and opening of fractures in the vent area during the two days that preceded the eruption.

Monte Nuovo southern slope.

Along the road of the "Monte Nuovo Oasis" it is possible to observe the Member C, composed by very coarse scoriae fallout emitted by the SouthV and overlying unconformably Members B and A, emitted by the SouthV and MV respectively.

Monte Nuovo crater (MV).

The crater rim is asymmetrical in response to the syneruptive ground deformation of the vent area (Di Napoli et al., 2017). The crater walls show the products of the member A, composed almost exclusively by a sequence of plane-parallel to undulated fine- to coarse-ash beds forming the largest part of the Monte Nuovo tuff cone, overlain by scoriae and minor ash layers of the member D and E, both erupted by the MV.

Stop 2.4: The volcanic and hydrothermal activity in the volcano Solfatara (40°49'48.01"N - 14°08'11.07"E)

Significance. – Structural setting and intense fumarolic activities in a maar volcano.

The Solfatara volcano, is associated to a small scale eruptive events of the CF caldera with an age of about 4,300 years BP and is one of the most recent volcanic edifices located about 2 km east-northeast of Pozzuoli, Morphological, stratigraphic and structural analyses integrated with geo-electrical surveys suggest that the Solfatara volcano is a maar-diatreme with a sub-rectangular (0.5x0.6 km) crater (Fig. 23; Isaia et al., 2015). The shallow crater is cut in the pre-eruptive basement by prevailing NW-SE and SW-NE trending faults, and lie above a deep diatreme (down to 2-3 km) characterized by a lower sector where the gas-saturated conduit joins the root zone that is likely connected to a magmatic source (Isaia et al., 2015).

Solfatara grows after the effusive eruptions of Monte Olibano lava dome, Olibano phreatic eruption and Accademia lava dome-forming eruption. The eruptive activity of Solfatara was mainly characterized by initial phreatic explosions with scarce juvenile material which emplaced low-dispersed PDC. This initial activity was followed by magmatic phases, with generation of PDC and tephra fallout.

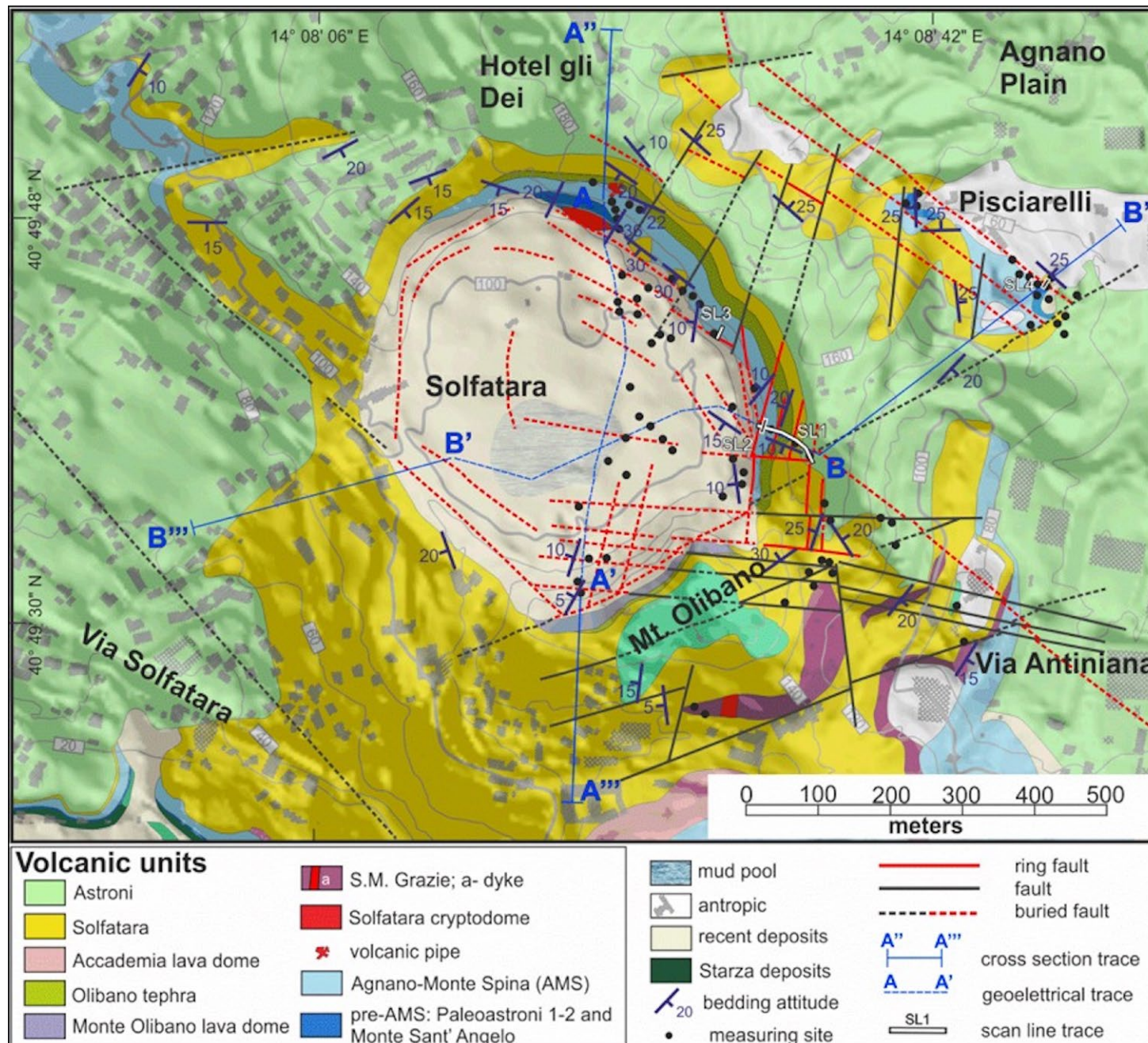


Fig. 23 - Geological map of the Solfatara area (from Isaia et al., 2015).

The deposits consist of prevailing massive coarse to fine ash beds in the lower part and alternating fine-to-coarse ash and pumice layers (Figs. 24, 25), with surge-like lenses rich pumice clasts and ballistics in proximal to medial areas. Thin fallout deposits dispersed to the NE up to around seven km from the eruptive center were associated with the Solfatara eruption.

At 4.3 ky BP, the Solfatara and Averno vents, 5.4 km apart, erupted simultaneously

A stratigraphic section, located at ~2 km northwest of Solfatara crater and 4 km northeast of Averno lake, shows a tephra succession 100 cm thick which consists of alternating greenish to light-gray ash beds containing accretionary lapilli (Fig. 25). Light-colored and white coarser ash beds with scattered pumice clasts are interlayered at various heights. The section has been subdivided into five main



Fig. 24 - Succession of volcanic rocks exposed along the inner wall of the eastern crater of Solfatara.



Fig. 25 - Pyroclastic deposits of the volcano Solfatara.

units (U1 to U5), mainly based on tephra sedimentological characteristics (color and grain-size variations), consisting of an alternation of accretionary lapilli-bearing ash layers with scattered pumice fragments. Based on geochemistry of matrix glasses, and through a comparison with source tephra chemical characteristics, the light parts were associated to the Averno eruption while the greenish material to the Solfatara event (Fig. 26). The crater of the Solfatara hosts an intense hydrothermal activity (Fig. 27) with the most impressive manifestation of the hydrothermal activity of the caldera, which includes both focused vents, with a maximum temperature of about 160°C (Bocca Grande fumarole), and large areas of hot steaming ground, mainly represented by H₂O

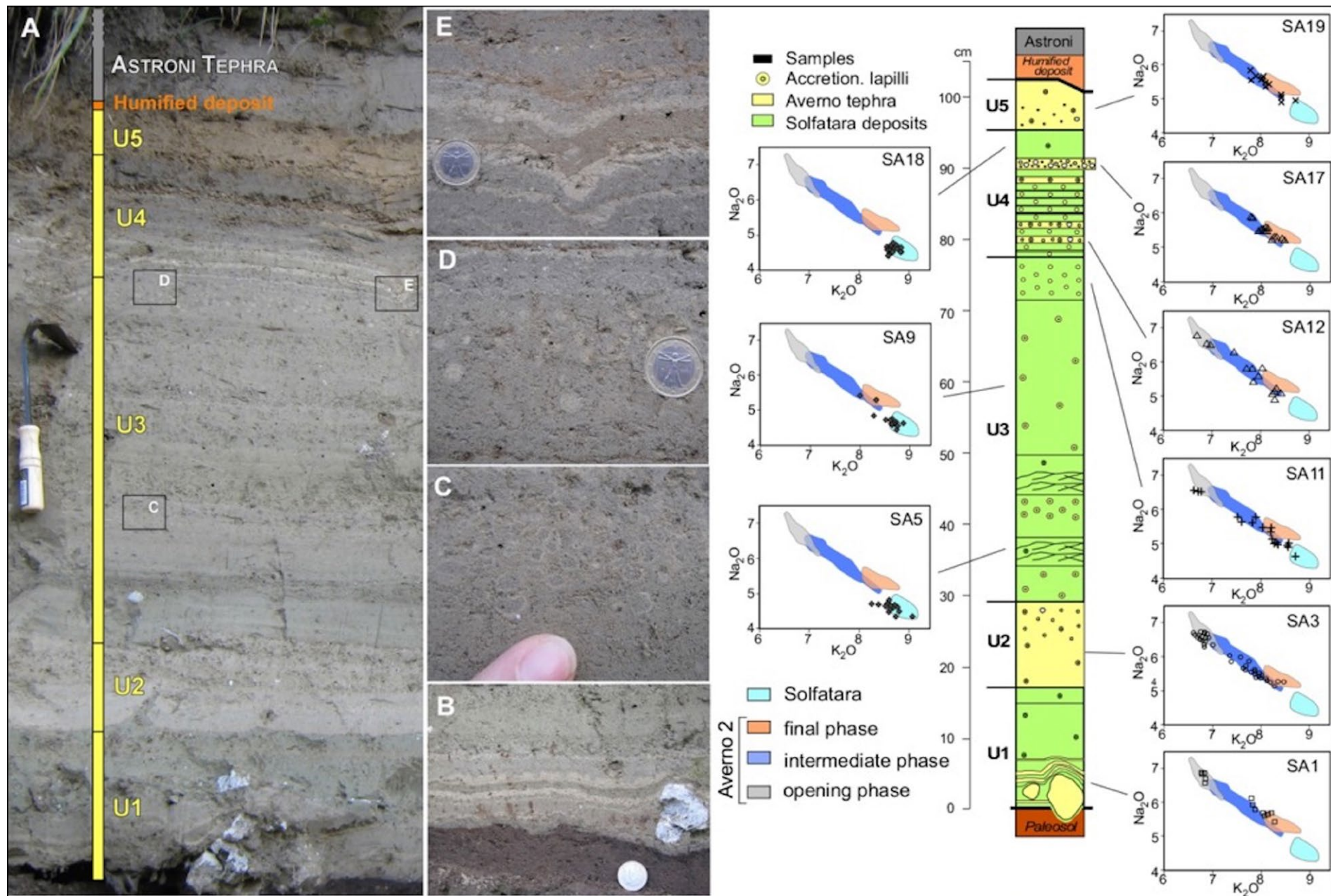


Fig. 26 - Stratigraphic section showing the interlayering among Solfatara and Averno products. Glass geochemistry fingerprinting the two sources. Modified after Pistolessi et al. (2016).



Fig. 27 - Fumarolic and hydrothermal vents in the crater of Solfatara.

about 82 wt. %, CO_2 17.5 wt.%, H_2S 0.13 wt.% and minor amounts of N_2 , H_2 , CH_4 and CO .

The isotopic compositions of H_2O , CO_2 and He suggest the involvement of magmatic gases in the feeding system of the fumaroles (Chiodini et al., 1997). Subsequently the original magmatic gases are condensed by an aquifer system. Boiling of this heated aquifer(s) generates the Solfatara fumaroles. At the present, the Solfatara together with the fumarolic field of Pisciarelli, located on the external flank of the volcano, are the main object of the geochemical surveillance of the caldera, including the continuous monitoring of the chemical compositions of the fumarolic fluids and CO_2 fluxes from the soil.

Solfatara Crater

The Solfatara volcano gives a peculiar example of the of low energy eruptions dynamics, and allows to understand the influence of tectonic structures in generating different volcano shapes. On the cratere floor, but also along the internal and external flanks of the Solfatara Maar we can also have a look at the intense fumarolic manifestations.



Stop 2.5: The Serapeum and the bradyseism ($40^{\circ}49'33.85''\text{N}$ - $14^{\circ}07'13.78''\text{E}$)

Significance. - Short-term deformation and ongoing ground deformation within an active caldera.

The ground deformation in the area of Campi Flegrei is a well-known phenomenon since Roman times. In the Baia area several Roman age buildings are now under the sea due to continuous subsidence of central-western sector of the caldera, while documentary sources reporting a consistent uplift of the ground in the area of the ancient Roman harbour of Averno before the 1538 AD eruption. Approximately 3-km northwest of Pozzuoli, coastal retreat and rapid uplift on the order of several meters are recorded by contemporary accounts near the eruptive site of the historical eruption of Monte Nuovo at least 30 years before the eruption and constantly increased with the approach of the eruptive event. The volcano-tectonic phase that culminated with the eruptive event, interrupted the secular trend of subsidence at the beginning of the fifteenth century, when the maximum degree of submersion was probably reached

An exceptional record of ground deformation from Roman times appears in the Serapis, which is a Roman market at Pozzuoli that was built in the second century BC. This site was buried by 9 m of sediments, and later excavated in 1750 during which two superimposed floors, located about 2 m apart, and the famous three columns unearthed. Each column, 13-m high, presents a zone, located 3 m above the base and with a vertical thickness of over 3 m, which is perforated by marine bivalves (*Litodomus litophagus*). The first scholar to analytically set the problem of how the columns of the Temple of Serapis were perforated by lithodomes was the abbot Scipione Breislak in the eighteen century. The construction of the two floors and the perforated columns suggests that Pozzuoli underwent episodes of subsidence and uplift between Roman times and the sixteenth century. After excavation, the columns showed lithodomes holes up to 7 m above the floor of the monument, testifying the maximum subsidence of the area.

Since then the Temple of Serapis became the object of several study aimed to quantify the ground movements occurred within the Campi Flegrei caldera. Measurements of benchmarks located within and nearby the Temple of Serapis since 1905 allow to estimate the ground deformation of the Pozzuoli area through the entire twentieth century and during the bradyseismic crisis of 1980-82 AD (Del Gaudio et al., 2010). Both Serapeum floor and topographic benchmark clearly show an elevation in meters with respect the sea level from 1905 AD, mainly due to a general slow uplift of the entire Pozzuoli area rather than an eustatic variation.



Ongoing unrest episodes lead to an uplift of more than 50 cm since 2005 and in particular 33.0 cm since January 2014 in the area close to Rione Terra at Pozzuoli. GPS data confirm a mean value of 0.7 cm/month for the uplift of the area since July 2017.

The Serapeum

Looking at the monument, constructed between the end of the I and the beginning of the II century, will be possible discuss of long- and short-term deformation in an active caldera and the evolution of these phenomena, as sign of unrest crises and also their relationships with eruptions, in quiescent volcano.



The two photos show the Serapeum invaded by water (left) and completely dry (right) respectively before and after the 1980-82 uplift crisis.

<http://www.ingv.ov.it/ov/it/campi-flegrei/storia-eruttiva.html>

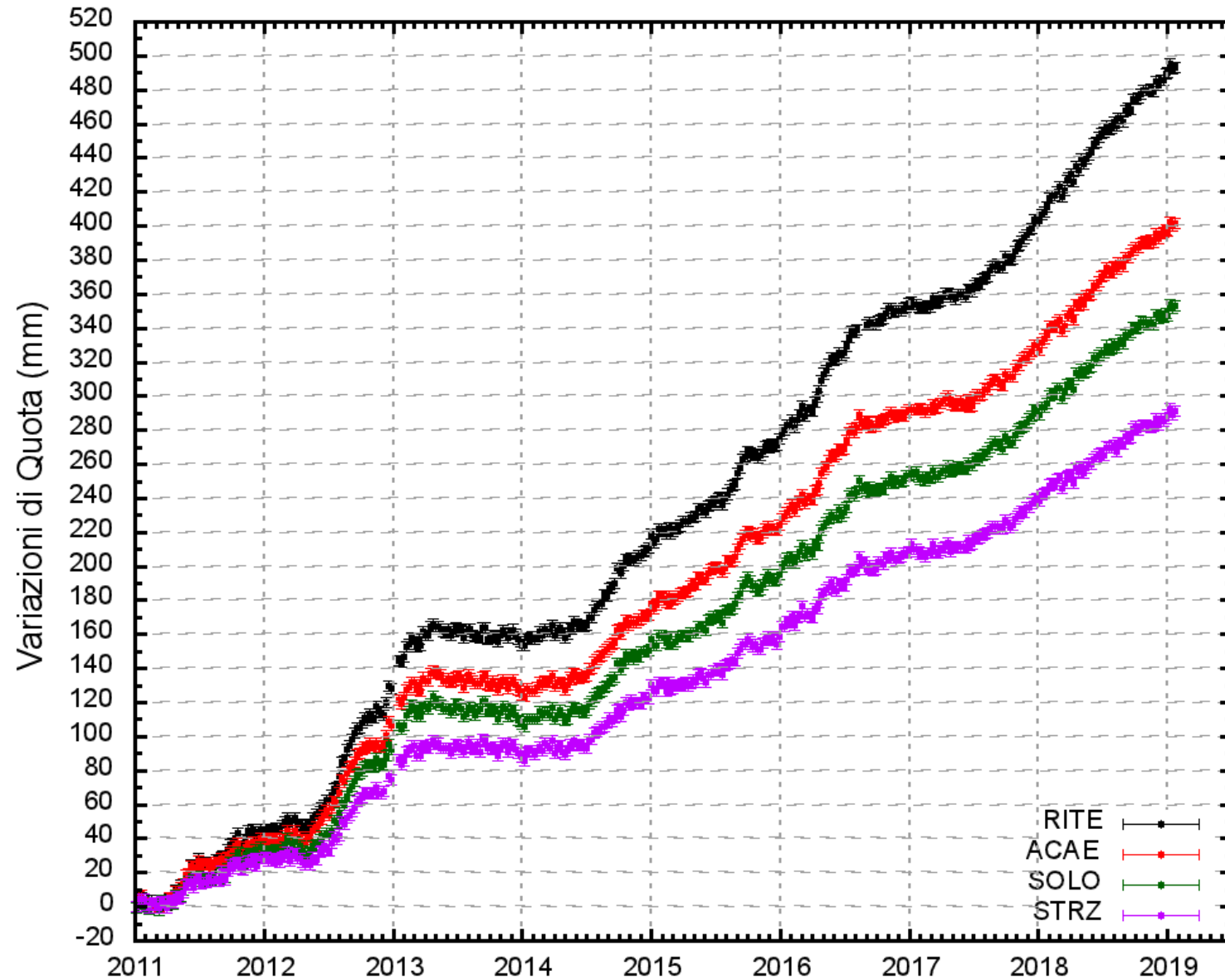


Fig. 28 - Time series of changes in elevation of the RITE stations (Pozzuoli - Rione Terra), ACAE (Accademia Aeronautica), SOLO (Solfatara) e STRZ (Pozzuoli - Cimitero) from January 1, 2011 to January 26, 2019 (Weekly Bulletin of Surveillance at Campi Flegrei; INGV - OV).



Stop 2.6: Rione Terra (40°49'17.46"N - 14°07'16.95"E)

The old part of the town of Pozzuoli (Fig. 29), deeply affected by the recent bradyseismic crises of 1969-1972 and 1982-84, host an interesting archaeological site of romans time.

The underground archaeological tour of Rione Terra is a journey in the ancient Roman colony, *Puteoli*, founded in 194 BC and soon become the commercial port of Rome. The course is located below the tuff rock overlooking the Gulf of Pozzuoli, between Nisida and Baia, and runs along the principal axes of the Roman city, hinges and decumani. The visitor, strolling along the streets of *Puteoli*, will be fascinated by the architecture of many buildings, the granaries, the oven for processing and baking bread (pistrinum) with millstones almost intact, from cryptoporticos, the workshops and warehouses. The archaeological itinerary is enriched by multimedia installations that guide the audience to discover the activities that took place in ancient *Puteoli*.



Fig. 29 - Rione Terra, Pozzuoli.



Fig. 30 - View from the archaeological tour of Rione Terra, Pozzuoli.



Days 3 and 4 - Somma-Vesuvius

The Somma-Vesuvius volcanic complex consists of an older volcano dissected by a summit caldera, Monte Somma, and a recent cone, Vesuvius, built within the caldera after the AD 79 “Pompeii” eruption (Cioni et al., 1999). The original Roman name Vesuvius (or Vesbuis) was first applied to the old volcano. Starting from the fifth century, chroniclers make mention of Mt. Somma, as the highest (“summa”) peak of the mountain. The new cone grew discontinuously during periods of semi-persistent, low-intensity activity (from strombolian to violent strombolian, accompanied by important effusive activity). These periods possibly occurred in the first to third centuries, in the fifth to eighth centuries (after the AD 472 “Pollena” eruption), in the tenth to twelfth centuries, and in 1631–1944 (Andronico et al., 1995; Cioni et al., 2008).

Until relatively recent times, the formation of Somma-Vesuvius (SV) caldera was ascribed to the Pompeii eruption. Roman paintings from Pompeii and Herculaneum prompted Stothers and Rampino (1983) to conclude that, prior to AD 79, the top of the volcano was asymmetrically shaped, indicating that a Somma-type caldera was already present. The volcanological interpretation of the Roman fresco from Pompeii “Mars and Venus”, now at Naples National Archaeological Museum, made by Nazzaro (1997) leaves few doubts about the presence of a pre-existing caldera (Fig. 2 in Cioni et al., 1999).

The SV caldera has a lobate, quasi-elliptical shape with a 5-km-long, east–west major axis (Fig. 31). The northern rim of the caldera is a well-defined steep wall, with an average elevation of approximately 1000 m. The drainage pattern of the highest portions of the volcano, unaffected by conspicuous deposition of recent products, is clearly radial, suggesting a symmetrical original cone. In this assumption, the shape and size of the ancient Mt. Somma can be constrained, placing the apex of the old volcano around 1900 m elevation and approximately 500 m north of the present Vesuvius crater. Another lobe of the caldera structure runs from the Cognoli di Levante, at the southern tip of the Somma caldera wall, to the southeastern tip of Piano delle Ginestre. This lobe is well identified by the presence of a sharp change in the slope of the mountain below a mean elevation of around 600 m. This rim of the caldera is nearly completely covered by a pile of recent lava flows and pyroclastic deposits that, after filling the caldera, overtopped its lowest rim possibly around AD 1000, when thick lava flows flooded the southwestern and southeastern sectors of the plain. The semielliptical arc delimiting the flat morphology of Piano delle Ginestre lava field completes the multilobate shape of the SV caldera. This structure forms an acute angle with the southern rim of the caldera and is clearly related to the crescent-shaped relief of the Observatory Hill. The outer slopes of this structure consist mostly of

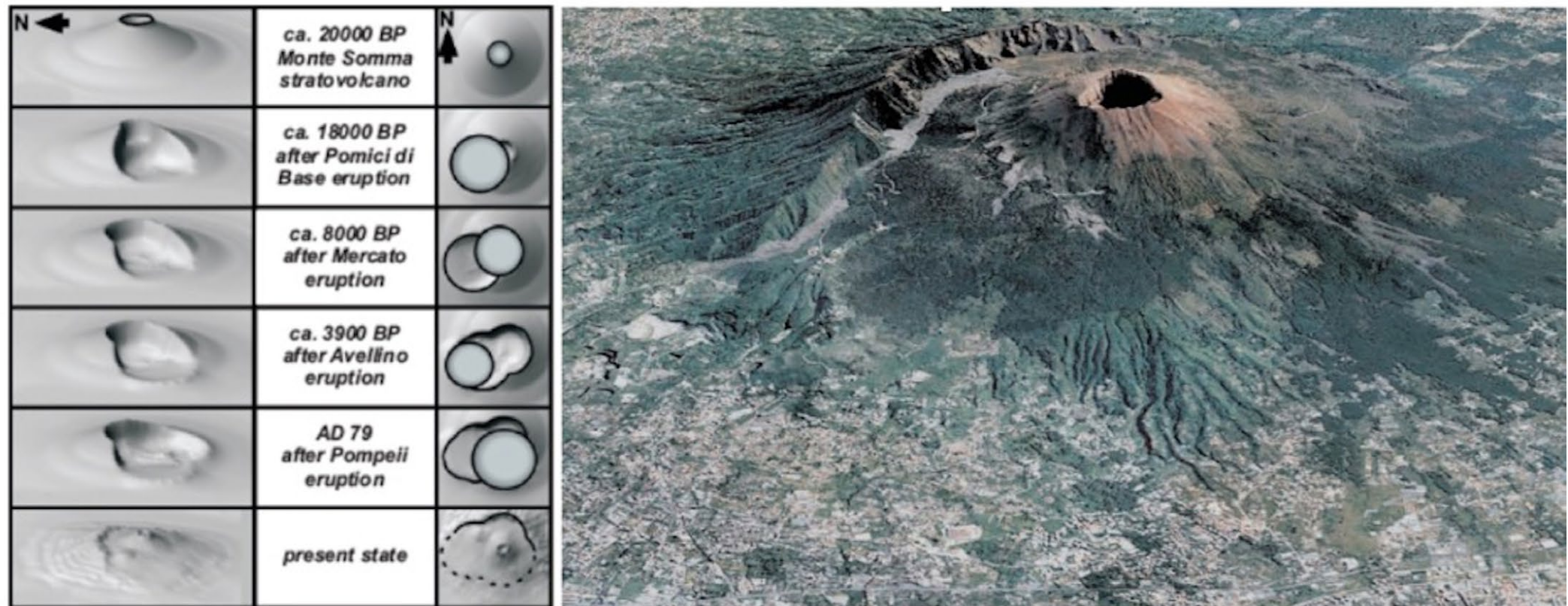


Fig. 31 - The Vesuvius cone and the Monte Somma caldera rim (Lab. Grafica e Immagini, INGV-Roma; modified from Cioni et al., 2008); on the left, scheme with the inferred evolution of the caldera (after Santacroce et al., 2003).

nonwelded pyroclastic deposits with a parasol-ribbing erosional pattern still exposed in the south. The present flat morphology of the Piano delle Ginestre records the filling of the old depression by historical lava flows that overflowed the seaward rim in 1694–1697 (Santacroce, 1987).

Although the general morphology of the volcano (Fig. 31) could be suggestive of the occurrence of lateral collapses of the seaward, western sector (Milia et al., 1998; Ventura et al., 1999; Rolandi et al., 2004), field evidence discards such a possibility at least for the last 20,000 years (Sulpizio et al., 2008a).

About 22 cal ky BP, the mainly effusive activity of Mt Somma changed into largely explosive (Fig. 33). At least four high-magnitude Plinian eruptions occurred, staggered with minor events covering a large range of magnitude and intensity.

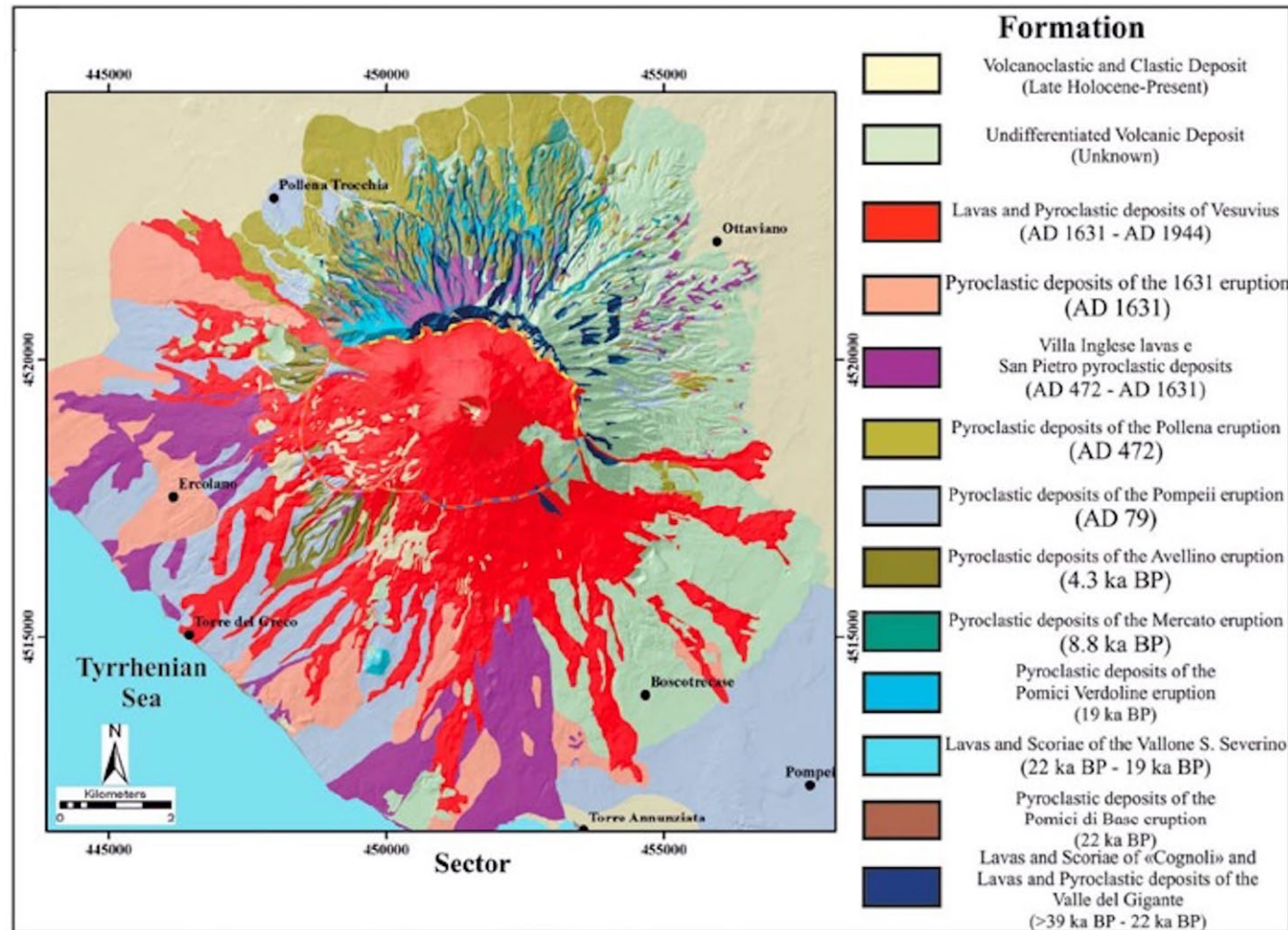


Fig. 32 - Schematic geologic map of Somma-Vesuvius (modified from Tadini et al., 2017).

High-intensity, explosive eruptions sporadically occurred, the two largest being the subplinian events of AD 472 (also known as Pollena eruption; Rosi & Santacroce, 1983; Sulpizio et al., 2005) and AD 1631 (Rosi et al., 1993; Bertagnini et al., 2006). The most recent period (1631-1944) was characterised by summit or lateral lava effusions and semi-persistent, mild explosive activity (small lava fountains, gases and vapour emission from the crater) interrupted by pauses lasting from months to a maximum of seven years (Santacroce, 1987; Arrighi et al., 2001).

The eruptive vents of the largest eruptions possibly occupied slightly

eccentric positions with respect to the old Somma cone, however insisting in a restricted area, as evidenced by the shape of the caldera and the dispersal of the products (Figs. 31 and 32). Vent position migrated irregularly in time inside the present caldera. Lateral activity was minor and, starting from the AD 79, the few eruptive fissures were confined to the western and southern sectors of the volcano (Cortini and Scandone, 1982; Santacroce, 1987; Acocella et al., 2006).

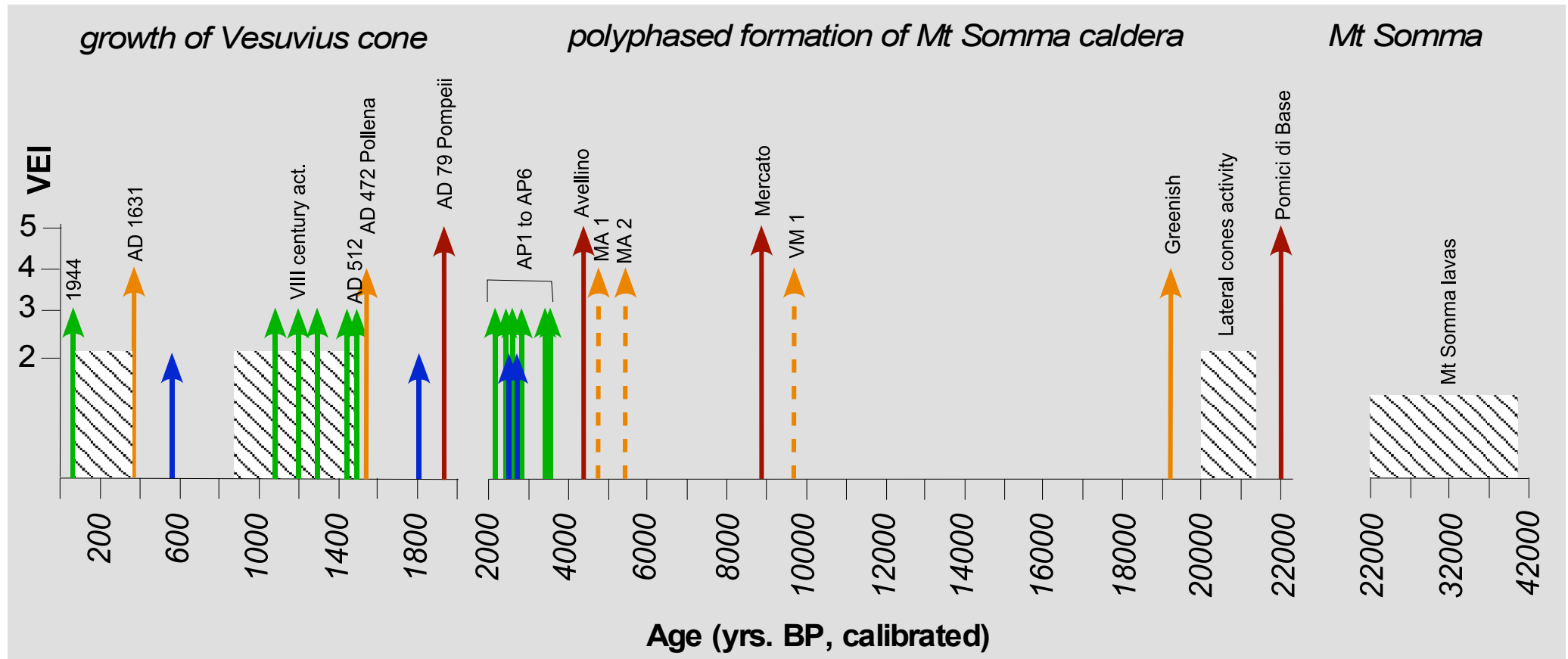


Fig. 33 - Chronogram of Somma-Vesuvius activity. Arrows refer to explosive eruptions, length and colour reflect the estimated VEI. Blue boxes show recorded or inferred periods of persistent mild Strombolian and effusive activity, punctuated by VEI 2-3 explosive eruptions. Orange-dashed arrows mark eruptions of uncertain source. Breaks in the chronogram mark changes of time-scale (modified from Cioni et al., 2008).

Stratigraphy and products

Borehole data show that the SV edifice lies on the Campanian Ignimbrite deposits (Brocchini et al., 2001; Santacroce and Sbrana, 2003; Di Renzo et al., 2007), being therefore younger than ca. 39 ka (De Vivo et al., 2001; Giaccio et al., 2017).

Explosive activity older than ca 22 ka (of uncertain source)

The products of the activity which formed the Somma stratovolcano are exposed in the inner wall of the caldera (Santacroce and Sbrana, 2003). They consist of a pile of lava flows spatter and scoria deposits reflecting dominantly effusive activity (Johnston Lavis, 1884; Santacroce, 1987). No large-scale pyroclastic deposits older than 22 ka have been recognized in proximal sectors. In medial and distal areas, several pyroclastic deposits occur between the CI (Campi Flegrei) and Pomici di Base (Somma- Vesuvius) deposits. Some of these have been correlated to the activity of Campi Flegrei, whereas the provenance of other three deposits is still a matter of debate.

Analyses of samples from pyroclastic deposits from a borehole located near Camaldoli della Torre lateral apparatus suggest the occurrence of important explosive activity in the Vesuvius area just after the deposition of the CI (CdTI layer in Di Renzo et al., 2007). The thickness of these deposits (ca. 60 m) may suggest a local source (Di Renzo et al., 2007). Di Vito et al. (2008) tentatively correlated these deposits to medial-distal pyroclastic fallout deposits of similar composition recognized on the mountains bordering the Campanian plain ("Schiava Pumice" of Sulpizio et al., 2003; Zanchetta et al., 2004) and previously considered as originated by Ischia volcanoes (Sulpizio et al., 2003).

Widely dispersed pyroclastic deposits correlated with the so-called "Codola eruption" (Alessio et al., 1974; Arnò et al., 1987; Giaccio et al., 2008) occur in many medial to distal marine and terrestrial successions (Brocchini et al., 2001; Sulpizio et al., 2003; Wulf et al., 2004; Sulpizio et al., 2010). The Codola deposits have an age of ca 33 cal ky BP (Giaccio et al., 2008).

Di Vito et al. (2008) suggested the occurrence of explosive activity from vents north-east of Somma-Vesuvius, possibly along the tectonic alignment of Palma Campania-Ottaviano in the period between 39 and 22 cal ky BP. Deposits that may represent this activity occur at the base of the Appennine Mountains, within a clear phase of aggradation of volcanoclastic alluvial fans related to reworking of pyroclastic fall deposits of the so-called "Taurano eruption" (Zanchetta et al., 2004).

Explosive activity from 22 ka

The stratigraphy of Somma-Vesuvius volcanic products postdating Mt. Somma was studied and reconstructed starting from the end of the XIXth century (Delibrias et al., 1979; Johnston Lavis, 1884; Santacroce, 1987; Cioni et al., 1999; Santacroce and Sbrana, 2003). The deposits of some 40 explosive eruptions are recognized, including some products related to Campi Flegrei activity (Cioni et al., 2008).

Four major Vesuvius Plinian eruptions are present in the volcanic succession of the circumvesuvian area: the "Pomici di Base", the "Mercato Pumice", the "Avellino Pumice", and the "Pompeii Pumice" (AD 79). These pyroclastic deposits represent clearly distinctive stratigraphic markers which define four distinct stratigraphic intervals: 1. B–M (between Pomici di Base and Mercato); 2. M–A (between Mercato and Avellino); 3. A–P (between Avellino and Pompeii); 4. P–XX (from the Pompeii Pumice to the last erupted products of the XXth century). Each stratigraphic interval includes the deposits of the oldest Plinian eruption and closes immediately below the following Plinian deposit. This subdivision is justified in the field by the presence of paleosols covered by the products of the Plinian eruptions (Santacroce et al., 2008). Fig. 34 summarizes the main features of deposits and the fallout dispersal of the explosive eruptions potentially useful for tephrostratigraphic studies in distal areas.

The Pomici di Base Plinian eruption and the B–M interval

The Pomici di Base eruption is the oldest and largest, caldera forming, explosive event which can be unequivocally assigned to the eruptive history of Vesuvius. Bertagnini et al. (1998) and Cioni et al. (1999), suggested a vent for the eruption located 1–2 km west of the summit of the ancestral Somma cone. The eruption progressed through three main phases: (1) opening, marked by the deposition of thin ash and pumice fall deposits; (2) Plinian, dominated by pumice and scoria fallout forming thick deposits dispersed in an E–NE direction; (3) phreato- magmatic, during which the emplacement of lithic-rich pyroclastic fall, surge and flow deposits accompanied the caldera collapse. The Plinian fall (Fig. 35), with an estimated volume of 4.4 km³, is by far the most significant deposit of Somma-Vesuvius activity. It consists of compositionally zoned products from a basal white, K-trachytic pumice bed to an upper black, K-latitic scoria.

Two ¹⁴C ages on charcoal (Siani et al., 2004; Santacroce et al., 2008) yield an average maximum age of 22,030 ± 175 cal yr BP, in agreement with a K/Ar determination on sanidine (22,520 ± 1000 cal yr BP; Santacroce et al., 2008).

After the Pomici di Base eruption, the activity resumed with the emission of K-latitic products through lateral vents in both the northern (lava flows and scoriae from Vallone San Severino and Vallone di Pollena) and southern (Camaldoli della Torre cinder cone; Joron et al., 1987) sectors of the volcano.

The second largest event of this interval was the subplinian "Greenish Pumice" eruption (Cioni et al., 2003), also called "Pomici Verdoline" (Delibrias et al., 1979; Santacroce and Sbrana, 2003) and "Seggiari-Novelle" (Ayuso et al., 1998). This large eruption was characterized by a complex alternation of pyroclastic fall and flow deposits

Eruption	Proximal deposits	Lithology	Isopach maps
AP1	<i>PFD</i> : two main lapilli beds separated by an accretionary lapilli-bearing, fine ash bed. Basal, light-grey pumice bed and dark green, thinly stratified, scoria lapilli bed. Accretionary lapilli-bearing ash bed at top. <i>PDC deposits</i> only present as stratified surge beds proximal to the vent area. These deposits are interbedded between the two main lapilli beds	<i>Light grey pumice</i> : highly vesicular, banded, subaphyric (san + cpx + amph + bt ± plag). Characteristics bt flakes. Glassy, lc-bearing groundmass. Phonolite <i>Dark green scoria</i> : moderately vesicular, porphyritic (plg+cpx+bt ± san). Glassy, lc-bearing groundmass. Tephri-phonolite <i>Lithic fragments</i> : lc-bearing lava, intrusive and skarn rocks; carbonate rocks (limestones and marbles). <i>Loose crystals</i> : bt	AP1
Mercato Pumice	<i>PFD</i> : three main well-sorted, light-coloured pumice lapilli beds, interlayered with pinkish-brown massive ash beds. The upper bed is lithic-rich. <i>PDC deposits</i> are mainly dispersed in the main valleys on the volcano slopes.	<i>White pumice</i> : highly to extremely vesicular, almost aphyric (san + cpx ± gt ± amph). Glassy, microlite-poor groundmass. Fine-sized, round vesicles and abundant tubular pumice. Phonolite <i>Lithic fragments</i> : lc-bearing lava, intrusive and skarn rocks; carbonate rocks (limestones and marbles). <i>Loose crystals</i> : rare	Mercato
Greenish Pumice	<i>PFD</i> : complex alternation of fine to coarse lapilli and ash layers. Different types of juvenile fragments mixed in the same stratigraphic level. Light-brown pumice and dark-green to brown scoria. Pumice lapilli only present in the basal lapilli bed. <i>PDC deposits</i> are scarce and are mainly present on northern slopes of Mount Somma	<i>Light-brown pumice</i> : highly vesicular, almost aphyric (san + amph + gt). Glassy, microlite-free groundmass. Trachyte <i>Dark-green to brown scoria</i> : highly to moderately vesicular, almost aphyric (san + amph + gt). Glass-bearing to completely crystalline groundmass (san + minor cpx + amph). Trachyte <i>Lithic fragments</i> : lc-bearing lava; marl; carbonate rocks (limestones and marbles). <i>Loose crystals</i> : rare	Greenish
Pomici di Base	<i>PFD</i> : white to grey pumice basal layer followed by a black scoriae upper layer. <i>PDC deposits</i> are poorly exposed and crop out mainly on northern slopes of Mount Somma	<i>White to grey pumice</i> : highly vesicular, almost aphyric (san + cpx + amph). Phenocrysts mainly assembled in glomerophyres. Glassy, microlite-free groundmass. Trachyte <i>Black scoria</i> : moderately vesicular, subaphyric (san + cpx). Microlite-rich, glass-poor to glass-free groundmass (san + plag + minor cpx). Latite to shoshonite. <i>Lithic fragments</i> : lc-bearing lava; rare carbonate rocks (limestones and marbles). <i>Loose crystals</i> : rare	Pomici di Base

Fig. 34 - Brief description of lithology and dispersal features for the most relevant eruptions of SV (from Cioni et al., 2008)

Eruption	Proximal deposits	Lithology	Isopach maps
AD 1631	<i>PFD</i> : Basal, few cm-thick layer of light grey scoria followed by an upper layer of dark grey scoria. Final fine ash of phreatomagmatic origin. <i>PDC deposits</i> abundant only on western and southern slopes of the volcano, at top of the main fallout beds.	<i>Light grey scoria</i> : highly to moderately vesicular, porphyritic (lc + cpx + san) Tephri-phonolite. Glassy groundmass <i>Dark grey scoria</i> : moderately to incipiently vesicular, highly porphyritic (lc + cpx + bt). Phono-tephrite. Microlite-rich groundmass. <i>Lithic fragments</i> : lc-bearing lava, intrusive and skarn rocks; rare carbonate rocks <i>Loose crystals</i> : abundant (lc + cpx)	AD 1631
AD 512 (AS1)	<i>PFD</i> : complex stratified sequence of scoria lapilli (from light brown, to dark brown to black) beds with minor ash interlayerings. <i>Minor PDC deposits</i> at the base of the sequence, only dispersed in very proximal sectors	<i>Brown scoria</i> : moderately to highly vesicular, crystal-poor (cpx + lc + bt), glassy scoria. Phono-tephrite. <i>Dark brown to black scoria</i> : moderately to poorly vesicular, crystal-poor (cpx + bt), hypocristalline groundmass (mainly lc-microlites). Phono-tephrite. <i>Lithic fragments</i> : lc-bearing lava <i>Loose crystals</i> : rare	
AD 472 (Pollena)	<i>PFD</i> : Complex stratified sequence. Basal layer of greenish-grey pumice followed by several layers of dark grey scoriae. Thin ash interbeds between the lapilli beds. Fine ash beds at top <i>PDC deposits</i> widely dispersed all around the volcano	<i>Greenish-grey pumice</i> : highly vesicular, porphyritic (lc + cpx + san + amph + gt), glassy groundmass. Tephri-phonolite to phonolite. <i>Dark grey scoria</i> : moderately to incipiently vesicular, highly porphyritic (lc + cpx + bt + dav). Leucititichthephrite phonolite. Cryptocrystalline groundmass. <i>Lithic fragments</i> : lc-bearing lava, intrusive and skarn rocks; rare carbonate rocks <i>Loose crystals</i> : abundant (lc + cpx + bt)	AD 472
AD 79 (Pompeii Pumice)	<i>PFD</i> : Compositionally zoned, two-fold pumice lapilli deposit. White pumice basal bed followed by a grey pumice upper bed. Four ash interlayers in the grey pumice. Thickly bedded fine ash at top of the sequence. <i>PDC deposits</i> interlayered in the grey pumice bed and at top of it, dispersed all around the volcano and in the plain nearby	<i>White pumice</i> : highly to extremely vesicular, porphyritic (san + cpx + gt + amph + bt); lc-bearing, microlite-rich groundmass. P Phonolite. <i>Grey pumice</i> : highly vesicular, porphyritic (san + cpx + bt); lc-bearing, microlite-rich groundmass. Tephri-phonolite. <i>Lithic fragments</i> : lc-bearing lava, tuffs, intrusive and skarn rocks; abundant carbonate rocks (limestones and marbles). <i>Loose crystals</i> : present (san + amph + cpx + gt + bt ± lc)	AD 79
AP6	<i>PFD</i> : stratified sequence of four alternate light-to dark-grey scoria lapilli and ash beds.	<i>Light grey scoria</i> : highly to moderately vesicular, subaphyric (lc + cpx ± bt). Microlite-rich groundmass (lc + cpx ± bt). Tephri-phonolite <i>Dark grey scoria</i> : moderately to poorly vesicular, subaphyric (lc + cpx ± bt). Microlite-rich groundmass <i>Lithic fragments</i> : lc-bearing lava <i>Loose crystals</i> : rare	
AP5	<i>PFD</i> : thinly stratified scoria lapilli bed, from dark brown to reddish at top. Violet coloured, lithic-rich, bt-bearing, coarse ash bed at top.	<i>Dark brown scoria</i> : poorly vesicular, subaphyric (cpx + bt ± plag). Glassy groundmass with leucite microphenocrysts (+ cpx + bt + san + plag). Tephri-phonolite. <i>Lithic fragments</i> : lc-bearing lava <i>Loose crystals</i> : abundant bt flakes in the ash beds	
AP4	<i>PFD</i> : complex sequence of three main beds. Stratified, ash and lapilli bed at the base, followed by a thinly stratified, coarse to fine scoria lapilli bed, topped by an accretionary lapilli-bearing, fine ash bed	<i>Dark brown scoria</i> : poorly vesicular, subaphyric (cpx + bt + plag ± san). Glassy groundmass with leucite microphenocrysts (+ cpx + bt + san + plag). Tephri-phonolite. <i>Lithic fragments</i> : lc-bearing lava, very minor carbonate rocks <i>Loose crystals</i> : rare	
AP3	<i>PFD</i> : main dark brown scoria, stratified, scoria lapilli bed sandwiched between two stratified, fine to coarse ash, accretionary lapilli beds.	<i>Dark brown scoria</i> : poorly vesicular, subaphyric (cpx + bt + plag ± san). Glassy groundmass with leucite microphenocrysts (+ cpx + bt + san + plag). Tephri-phonolite. <i>Lithic fragments</i> : lc-bearing lava, very minor carbonate rocks <i>Loose crystals</i> : rare	AP 3
AP2	<i>PFD</i> : two main lapilli beds separated by an accretionary lapilli-bearing fine ash bed. Basal, light-grey pumice bed and grey to dark green, lithic-rich, stratified scoria lapilli bed. Accretionary lapilli-bearing ash bed at top. <i>PDC deposits</i> only present as stratified surge beds proximal to the vent area. These deposits are interbedded between the two main lapilli beds	<i>Light grey pumice</i> : highly vesicular, subaphyric (plg + san + cpx + bt). Glassy, lc-bearing, poorly crystalline groundmass. Phonolite <i>Grey to dark green scoria</i> : poorly to highly vesicular, subaphyric (plg + cpx + bt). Glassy, lc-bearing (+ san + cpx + bt), microlite-rich groundmass. Tephri-phonolite <i>Lithic fragments</i> : lc-bearing lava, intrusive and skarn rocks; carbonate rocks (limestones and marbles). <i>Loose crystals</i> : rare	AP2

recording the transition from an initial phase of quasi-steady discharge (resulting in a convective column) to phases of more discontinuous, pulsating activity, with the formation of Vulcanian to Subplinian plumes (Cioni et al., 2003b). A paleosol locally occurs underneath the Greenish Pumice deposits. Two ^{14}C ages on charcoals yield an average maximum age of $19,265 \pm 105$ cal yr BP.



Four other pumice fallout layers occur between Greenish Pumice and Mercato deposits on the slopes of Mt. Somma. The thickest of these refers to the Campi Flegrei Plinian eruption of Agnano Pomici Principali (Agnano P.P.; Di Vito et al., 1999). The other three deposits crop out discontinuously and are less widely dispersed (two older and one younger than Agnano P.P.) and are also probably of Phlaegrean provenance. The oldest unit, the Lagno Amendolare Pumice, has long been considered as a Vesuvius deposit (Delibrias et al., 1979), but Andronico et al. (1995) and Andronico (1997) have attributed it to Campi Flegrei, basing on a reconstruction of the dispersal area.

The Mercato Plinian eruption and the M–A interval

The deposits of the Mercato eruption were first recognized by Johnston Lavis (1884) and named by Walker (1977). According to Cioni et al. (1999) the eruption occurred from a vent located close to the present Vesuvius cone, and again was characterized by three main phases (Mele et al., 2011). The Plinian fall deposits form about 90% of erupted material and consist of three ENE dispersed units separated by ash falls and strongly channelled, small-volume, pumice-rich PDC deposits. Two features of the Mercato deposits are peculiar with respect to the other Plinian eruptions of Somma-Vesuvius: i) the absence of compositional zoning (the whole deposit has a nearly homogeneous K-phonolitic composition), and ii) the absence of a phreatomagmatic phase (Mele et al., 2011). The three available ^{14}C ages on this eruption, obtained from soil organic fraction, give an average maximum age of 8890 ± 90 cal yr BP (Santacroce et al., 2008).

After the Mercato eruption, Vesuvius entered a long rest and no evidence has been so far found of significant activity before the following Avellino Plinian eruption. The Agnano Monte Spina pumice fall deposit from Campi Flegrei is the only widespread layer that occurs on the volcano slopes in the Mercato–Avellino interval. At some localities, it occurs between two other, discontinuous and partly pedogenized, trachytic

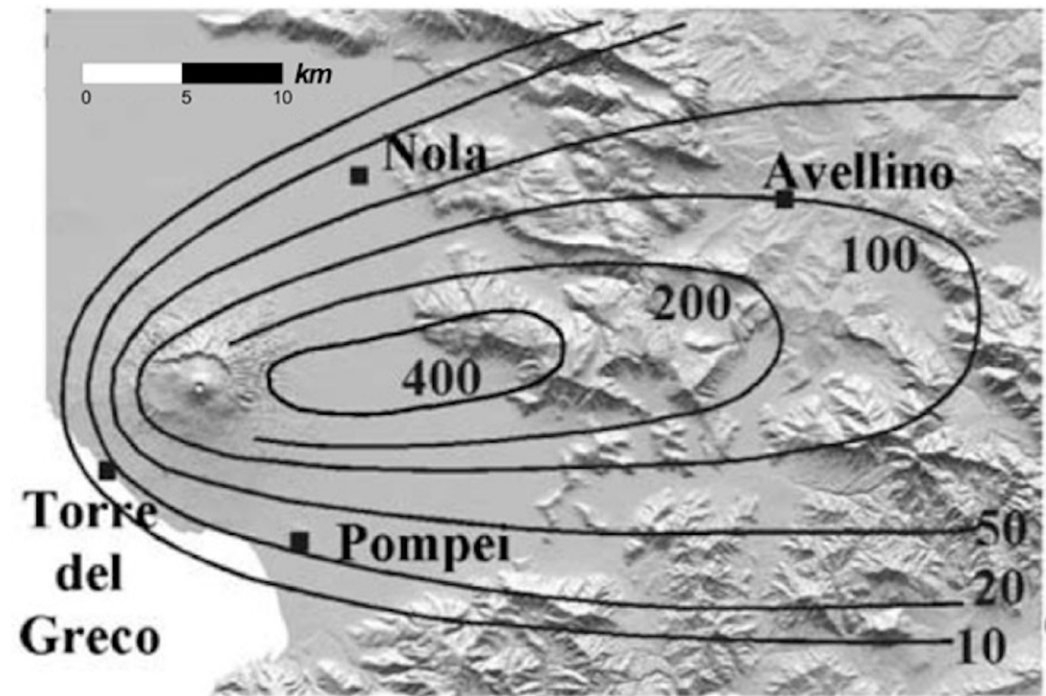


Fig. 35 - Total thickness isopach map (in cm) of the Pomici di Base Plinian fall deposit (modified from Cioni et al., 2003a).



fall deposits (MA1 and MA2), possibly related to Campi Flegrei activity (Andronico et al., 1997; Santacroce and Sbrana, 2003).

The Avellino Plinian eruption and the A-P interplinian interval

The pyroclastic deposits of the Avellino eruption (Lirer et al., 1973; Arnò et al., 1987; Rolandi et al., 1993a; Cioni et al., 2000; Sulpizio et al., 2010) have a bulk volume of ca. 1–2 km³ (Cioni et al., 2000; Sulpizio et al., 2010). The eruptive sequence is similar to that of the other Vesuvius Plinian events, with Opening, Plinian and Phreatomagmatic phases of activity distinguished on the basis of deposit characteristics. The areal

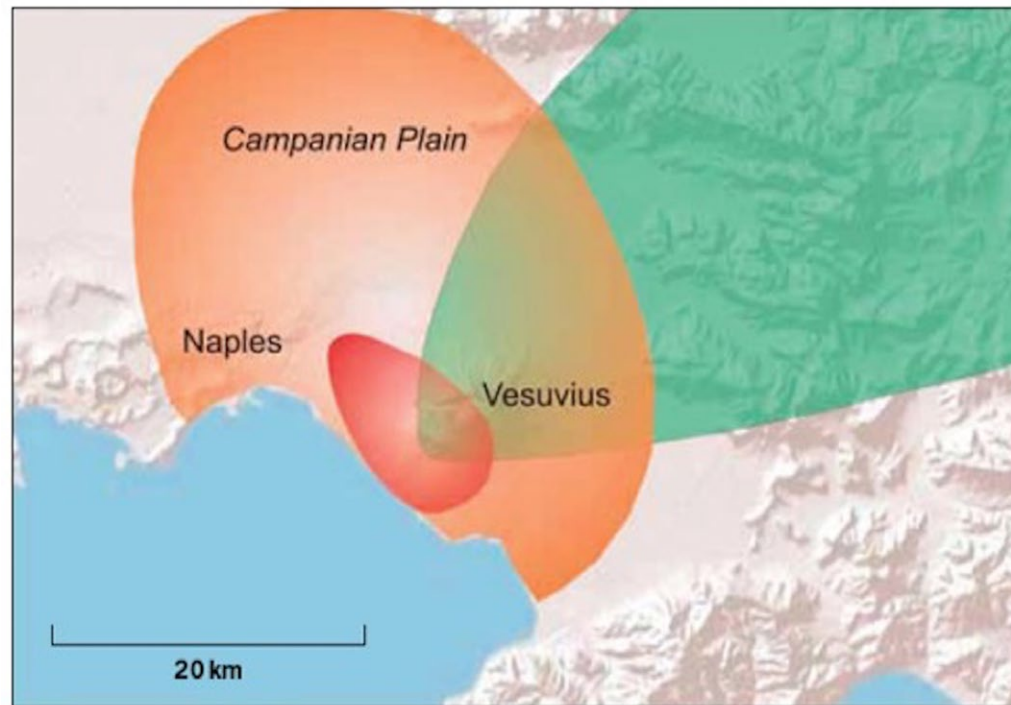


Fig. 36 - Main dispersal areas of the deposits of the Avellino Pumice eruption: in green, the area covered by more than 10 cm of fallout deposits; orange, area covered by more than 1 cm of PDC deposits and related ash fallout; red, area covered by a thickness of PDC deposits > 5 m.

distribution and the facies variations of the products indicate that the vent area was in a position coinciding with the Piano delle Ginestre, on the western slope of the volcano. The pyroclastic fall deposit shows a sharp change in colour from white in the lower half to grey at top, reflecting a change in the erupted magma from phonolitic to tephriphonolitic. The fall deposit is dispersed to the north-east, even if the grey pumice deposit exhibits a counter-clockwise rotation of 15–20° with respect to the underlying white pumice (Fig. 36; Cioni et al., 2000). A caldera collapse, enlarging the Pomici di Base caldera (Cioni et al., 1999), marked the transition from Plinian to Phreatomagmatic phase. During the latter, a pulsating column formed a giant tuff cone mantling the western rim of the caldera and generated mostly pyroclastic flows and surges, whose deposits, peculiar for their abundance (1.0 km³; Gurioli et al., 2010) and prevailing NW dispersion, reached a distance greater than 20 km from the vent (Sulpizio et al., 2008). The Avellino eruption has been dated by over 20 ¹⁴C age determinations on proximal areas. This

abundance arises from its importance in both the local and Mediterranean archaeological stratigraphy (Albore Livadie, 1999). Robust age determination indicates an average age of 3.9 cal ky BP (Sevink et al., 2011). An intense explosive activity repeatedly occurred between the eruptions of Avellino and Pompeii. By correlating more than 40 stratigraphic sections around the volcano, Andronico and Cioni (2002) identified six main eruptions (AP1–AP6, and few minor intervening events), whose deposits, in some cases, can be traced up to 20 km from the vent. AP deposits resulted from two main types of eruptions: (1) weak subplinian (AP1 and AP2, “Subplinian 2” in Cioni et al., 2008), consisting of pumice and scoria fall layers and minor fine-grained, vesiculated, accretionary lapilli-bearing ashes; and (2) mixed, Violent Strombolian to Continuous Ash Emission events (AP3–AP6), which deposited complex sequences of fallout, massive to thinly stratified, fine ash beds and minor scoria-bearing lapilli layers. The composition of the ejected material changes with time, and these changes are strongly correlated with vent position and eruption style. The maximum age for AP1 is 3500 ± 60 cal yr BP, which is not distinguishable from the available AP2 ages, despite a thin soil sandwiched between the two deposits. The age of the overlying AP3 deposits is 2830 ± 50 cal yr BP, which suggests a 5–7 centuries-long AP2–AP3 rest. The final products of this interval (AP6) were tentatively correlated by Andronico and Cioni (2002) to a (dubious) historic event reported by Stothers and Rampino (1983) on 217–216 BC.

The Pompeii Plinian eruption and the P–XX interval

Presently, a general consensus exists on the stratigraphy of the AD 79 eruption deposits (Sigurdsson et al., 1985; Cioni et al., 1992), which can be once more divided into three phases. The opening phase, comprising only a few centimetres of accretionary lapilli-bearing ash fall and very minor surge beds, was followed by the Plinian phase, mainly dispersed to SSW; Fig. 37), mostly consisting of tephra fallout ($2\text{--}4\text{ km}^3$, white and grey pumice layers, phonolitic to tephriphonolitic). This deposit is the product of a sustained Plinian column, which during the deposition of the grey pumice, collapsed at least four times, producing low concentration, turbulent PDC. According to Pliny the Younger’s letters to Tacitus and the chronology proposed by Sigurdsson et al. (1982, 1985), the Plinian phase of the eruption lasted no longer than 20 h. It was followed by a phreatomagmatic phase whose initial stages (formation of a short-lived sustained column concluded with the generation of a high-energy turbulent PDC) coincided with the onset of the caldera collapse that enlarged to the South the existing depression (Cioni et al., 1999). The AD 79 eruption closed with the emplacement of “wet” PDC and of a thick succession of accretionary lapilli-bearing ash beds.

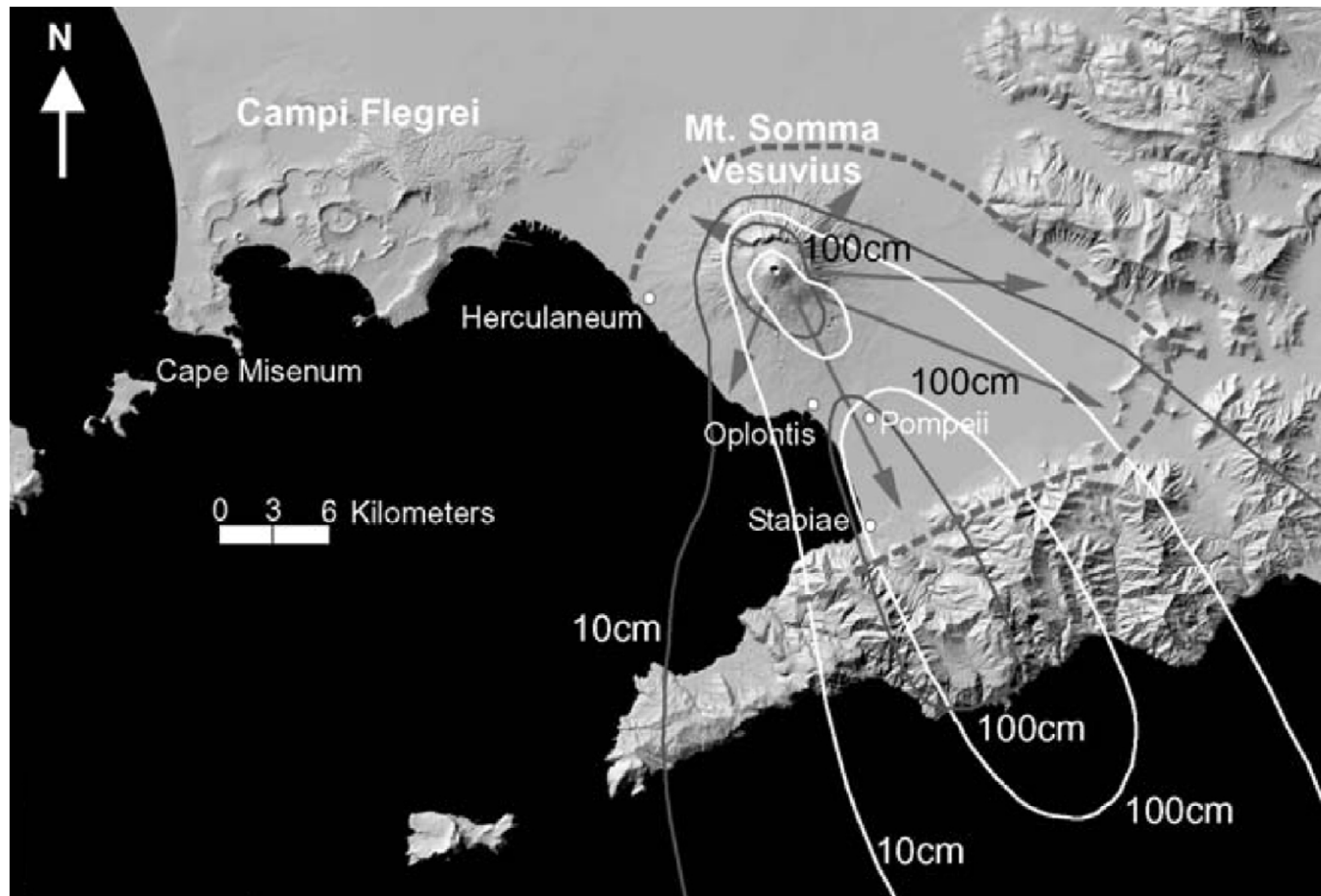


Fig. 37 - Dispersal of the fallout (white pumice, white lines; grey pumice, grey lines) and PDC (grey arrows) deposits of the AD 79 Pompeii eruption (redrawn from Gurioli et al., 2005).

compositional zoning from leucititic phonolite to leucititic tephriphonolite. Close to the Pollena eruption both in time and composition of erupted products, another subplinian event occurred in AD 512 (Cioni et al., 2011). During the Middle Age the Vesuvius cone grew discontinuously, alternating periods of open conduit, mild, persistent activity with lava effusions (from VIII to XII centuries, Principe et al., 2004), repose periods, and moderate size (Volcanic Explosivity Index VEI = 2–3) explosive eruptions. The pyroclastic deposits of at least four different major eruptions (AS2 to AS5; Cioni et al., 2008) have been recognized in this period.

On AD 1631, December 16, Vesuvius erupted suddenly (but precursors had been conspicuous; Rosi et al., 1993; Rolandi et al., 1993c; Bertagnini et al., 2006) after a quiescent period of uncertain length. The date of the last Vesuvius eruption prior the AD 1631 subplinian event is unclear. Historic estimates range from AD 1139 (preferred by Rolandi et al., 1998) to AD 1500 (Guidoboni and Boschi, 2006). After the onset of the eruption, a high eruptive column rapidly formed, causing lapilli fallout East of the volcano (8 h duration). A phase of repeated strong detonations and discontinuous block and ash fallout followed until the morning of December 17, when pyroclastic flows descended the flanks of the cone and devastated several villages (Fig. 38).

The AD 1631 eruption left the conduit open, and the volcano entered its period of modern activity, characterized by semi-persistent, mild activity (small lava fountains, gases and vapour emission from the crater), punctuated

by minor lava effusions from summit or lateral vents (Fig. 39) and short periods of repose (from months to a maximum of 7 years). Each of these rests was preceded by a more powerful, explosive-effusive, polyphased eruption ("Final Eruption"; Santacroce, 1987; Arrighi et al., 2001), whose largest examples occurred in 1944, 1906, 1822 and, possibly, 1794.



Fig. 38 - The 1631 eruption, as seen from Naples (engraving of G.B. Pagliari).

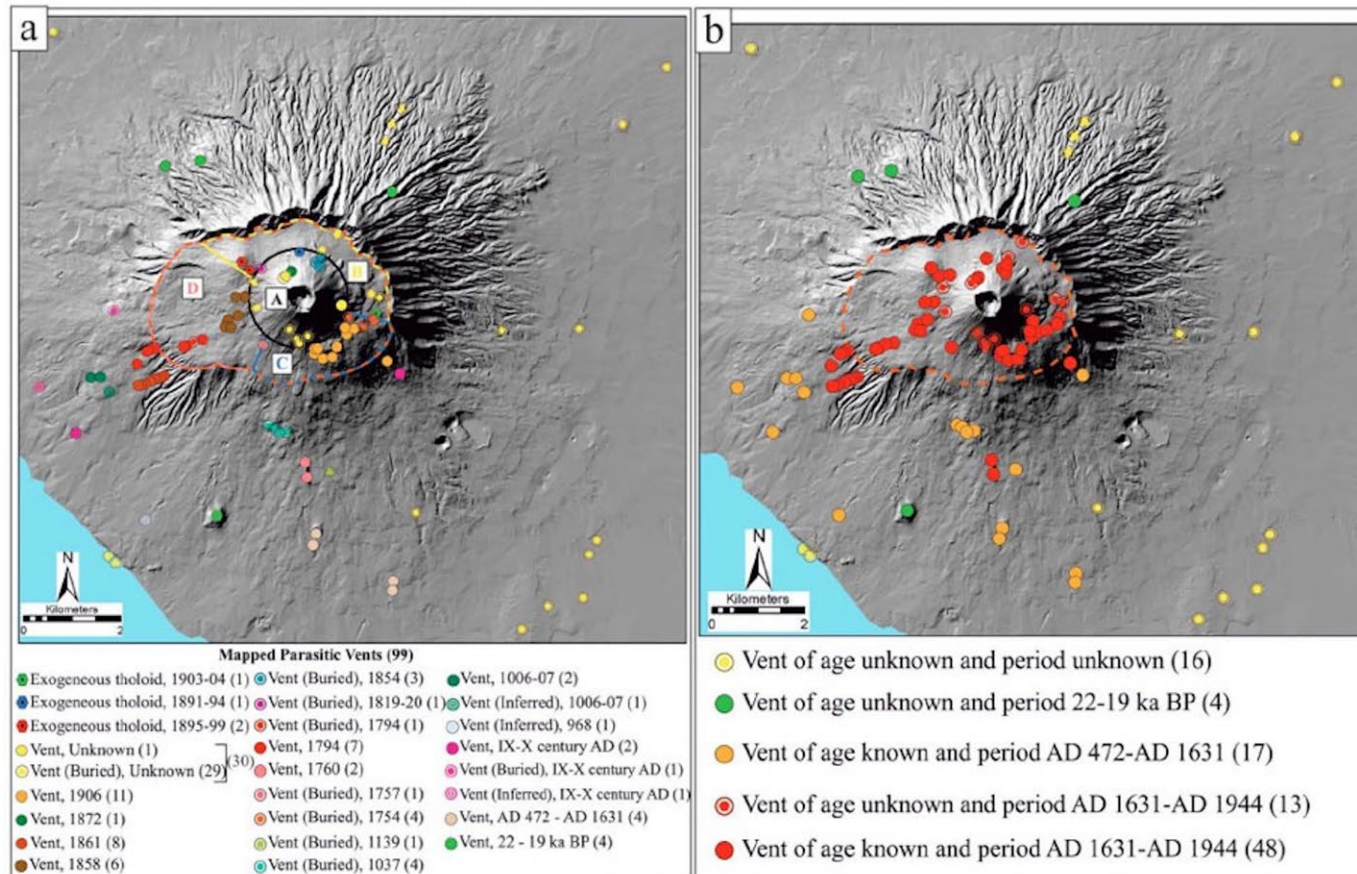


Fig. 39 - Parasitic vents of known (a) and unknown age (b). From Tadini et al., 2017.

The shift from Potassic magmas (represented by the trachytes and latites erupted in the period from the Pomici di Base to the Greenish Pumice) to K-rich compositions occurred before 8 ky ago. From 8 ka, products have been characterised by increasing alkalinity, and the products of the last 2 ka of activity (following the AD 79 Pompeii Pumice) show the most alkali-rich compositions and the lowest SiO₂ content of the whole set of erupted products.

Strongly silica - undersaturated magmas (pink field; Figs. 40 and 41)

This group comprises all the products erupted after the AD 79 Pompeii eruption. The most relevant common geochemical signatures of these rocks concern their lower silica and higher alkali

contents with respect to rocks with comparable evolution from the other two groups, as well as their very high Sr and Ba contents (Fig. 41). These features are consistent with evolutionary trends (mostly fractionation within a periodically supplied magma chamber) of K-tephritic liquids dominated by crystallization of leucite and mafic minerals, and characterized by minor role of plagioclase and the absence of K-feldspar fractionation.

Mildly silica - undersaturated magmas (green field; Figs. 40 and 41)

This group consists of the pyroclastic products of three Plinian eruptions (AD 79 "Pompeii", 3910 cal yr BP "Avellino" and 8,900 cal yr BP "Mercato") and at least six other explosive eruptions occurred between the

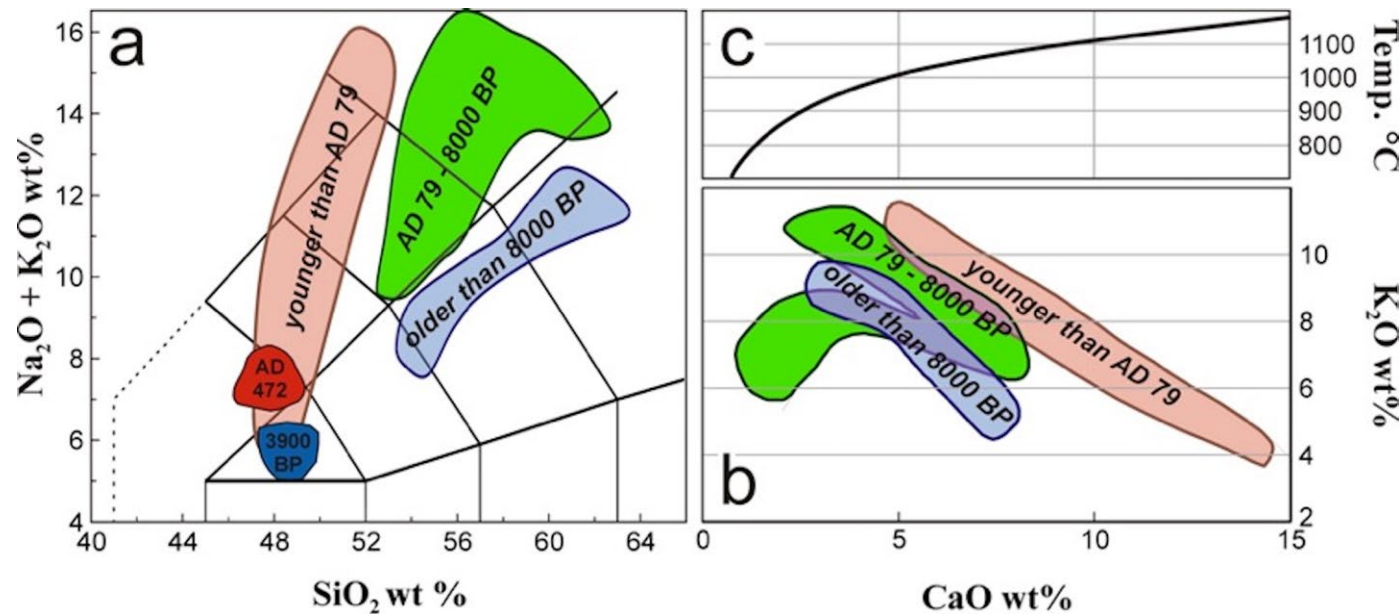


Fig. 40 - Total Alkalis vs. Silica (a) and K_2O vs. CaO (b) diagrams of Somma-Vesuvius products, showing the shift from potassic, slightly silica-undersaturated to highly-potassic, strongly undersaturated compositions (from Santacroce et al., 2008). The compositional range of melt inclusions in high-temperature phenocrysts from 3900 BP Avellino and AD 472 Pollena eruptions is reported in the fields 3900 BP and AD 472, respectively; c) empiric thermometer based on CaO content of melt inclusions in clinopyroxene phenocrysts proposed by Cioni et al. (1997). From Cioni et al., 2008.

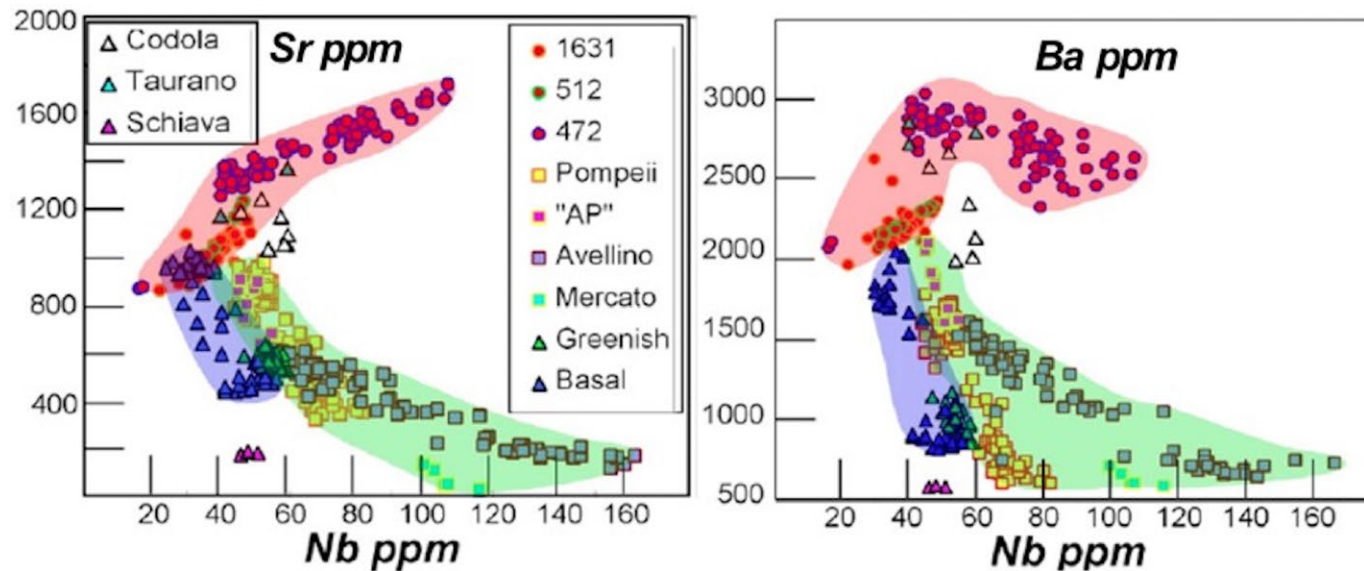


Fig. 41 - The variations of Nb, Sr and Ba of major explosive eruptions of SV discriminate the three groups of rocks, and are peculiar for most of single eruptions. Note the Pompeii trend in the Sr vs. Ba plot, completely out of the "mildly silica-undersaturated" field. (From Santacroce et al., 2008).

Avellino and Pompeii events (AP1 to AP6; Andronico and Cioni, 2002). Differently from the Mercato deposits, characterized by a strong compositional homogeneity all along the whole eruptive sequence, the products of the other eruptions of this group present important compositional variations, from the most evolved products at

the base to the least evolved toward the top. The Mercato and Avellino eruptions (first-erupted white pumice) are characterized by the emission of the most evolved products of Somma-Vesuvius ($\text{CaO} < 2.0\%$, $\text{Nb} > 100$ ppm; $\text{Zr} > 700$ ppm, Th up to 100 ppm).

Slightly silica - undersaturated (to saturated) magmas (blue field; Figs. 40 and 41)

Two large eruptions related to Somma-Vesuvius activity occurred in the period preceding the Mercato Eruption: the subplinian, 19,000 cal yr BP “Greenish Pumice” and the Plinian, 22,000 cal yr BP “Pomici di Base”. The most relevant common geochemical signature of the rocks of all these eruptions, related to their K-trachytic highly evolved composition, concerns the higher silica and lower alkali contents (with respect to rocks with comparable degree of evolution of the other two groups), as well as their moderate Sr and Ba contents (Fig. 41). As a whole the geochemical features of these rocks are coherent with evolutionary trends of K-basaltic liquids initially driven by crystallization of mafic phases and plagioclase and later involving K-feldspar fractionation.

The described large variability of Vesuvius magmas has been related to changes in the primary melts feeding the activity, and to the effect of shallow level crystallization under different thermodynamic conditions (Santacroce, 1987; Ayuso et al., 1993; Peccerillo, 2005; Di Renzo et al., 2007; Santacroce et al., 2008).

The presence of magma chambers at crustal levels at SV is strongly suggested by the occurrence, in many of the past plinian and subplinian eruptions, of thermometamorphic and skarn ejecta of carbonatic nature (Barberi and Leoni, 1980). Cioni et al. (1997) suggested that magma chambers associated with these eruptions had different volumes, ages and compositional layering, and were all located within the carbonate basement, at a pressure of about 150-200 MPa (Cioni et al., 1997; Cioni, 2000). These chambers were supplied by discrete, deep, mafic magma batches (possibly $5\text{-}10 \times 10^6 \text{ m}^3$ with a magma supply rate in the range $1\text{-}5 \times 10^6 \text{ m}^3 \text{ y}^{-1}$, Santacroce et al., 1994), whose compositional spectrum has been investigated through melt inclusions in high-T crystals (mostly olivine and diopside; Marianelli et al., 1995; Cioni et al., 1997). These have revealed the not truly primitive nature of the melts entering the magma chamber, as well as a change from K-basalt to K-tephrite which occurred during the period between the Avellino and the Pompeii Pumice eruptions. This change in the feeding magmas accompanies the important compositional change recorded by highly evolved magmas (K-phonolite to leucititic phonolite).

During the 1631-1944 period, characterized by a persistent activity under open conduit conditions, a shallow reservoir (< 3 km depth; Fulignati et al., 2004) was continuously tapped through effusive and mild to violent



strombolian activity. The periodic arrival in the shallow reservoir of mafic magma from a deeper region is recorded in the thermal and compositional history of high-T crystals (Cioni et al., 1997; Marianelli et al., 2005). Data from fluid and melt inclusions (Belkin et al., 1985; 1993; Marianelli et al., 1999; Fulignati et al., 2004; Marianelli et al., 2005) reveal the polybaric evolution of the erupted products, suggesting an 8-12 km deep provenance for tephrite to phonolitic tephrite magmas feeding the shallow reservoirs. Magma transfer to the shallow system resulted in eruptions whose dynamics episodically induced the nearly complete emptying of the reservoir. Activity resumed after short quiescent periods, possibly reflecting the time needed for the restoration of the shallow plumbing system. The present quiescence, lasting since 1944, departs from this pattern, and a generally accepted conclusion is that the 1944 eruption marked the transition to obstructed conduit conditions.

The present state of the volcano has been abundantly investigated through active seismic (Auger et al., 2001; Zollo et al., 1998; Del Pezzo et al., 2006), teleseismic (De Gori et al., 2001), magnetotelluric (Di Maio et al., 1998; Patella and Mauriello, 1999) and integrated (gravity, magnetic and self-potential data, Iuliano et al., 2002) tomographies. All these data evidenced a high velocity anomaly below the crater area, extended down to 5-6 km and interpreted as a rigid, high density residual left by the crystallization of magma filling the shallow plumbing system and “plugging the chimney” (Iuliano et al., 2002). However, the spatial resolution of all tomographic methods performed at Vesuvius does not exceed 300-500 m, being unable to reveal the presence of high aspect ratio, prolate (cigar-like) magma bodies with volume $< 0.1\text{-}0.2 \text{ km}^3$. All these data seem to rule out the presence of a large magma chamber at the same depth of those which characterised in the past the reawakening of the volcano. A possible zone of magma accumulation is suggested by seismic data at 8-10 km depth (Auger et al., 2001; 11-15 km according to De Natale et al., 2006), mainly constrained by reflected-converted seismic waves. This depth is roughly consistent with the pressure estimated for the mafic melts feeding shallow magma chambers during open periods (Marianelli et al., 1995; Marianelli et al., 2005) and with the experimental petrology results of Scaillet et al. (2008).

The record of the explosive activity

The pyroclastic products of Somma-Vesuvius have been widely studied in the past. More than 40 explosive events have been distinguished, recording a complex activity characterised by eruptions with a largely variable VEI as well as by very different eruption styles. The critical review of published data and of a large dataset of



unpublished stratigraphic and compositional data was used by Cioni et al. (2008) to address the problem of classification of the different types of eruption and to discuss the general behaviour of the volcano in terms of time frequency of the events, magnitude vs. intensity relationships, and intensity vs length of the repose time.

Eruption types

Retrospectively looking at the past explosive activity, the wide spectrum of eruption styles as recorded in the pyroclastic successions can be reconciled in a set of different eruption types each characterised by specific eruptive parameters:

- plinian eruptions
- subplinian eruptions (further subdivided in subplinian I and subplinian II)
- violent strombolian eruptions
- ash emission events
- prolonged mild strombolian activity

The distinction between the different types can be made both on the general features of their deposits and on the physical parameters estimated from the deposits themselves (see Fig. 42).

Frequency of the events

The general chronogram of Fig. 33 depicts a volcano characterised by important changes in eruption frequency, magnitude and intensity. These changes are also associated with the already described change in magma composition in terms of alkali and silica content (Fig. 40). No simple relationship exists between the age of the eruption and its type, even if most of the eruptions with $VEI \leq 3$ are present in the activity of the last 3.9 ka. The four Plinian events (and the related phases of caldera collapse) have occurred at time intervals decreasing with age, from the 13 ka separating the Pomici di Base and Mercato Pumice eruptions to the 2.5 ka interval between the Avellino and Pompeii Pumice eruptions (the intervals are derived from the calibrated ages of the eruptions, as given in Santacroce et al., 2008). In addition, following the Avellino Pumice eruption, an increase in the frequency of activity occurred, with several explosive eruptions of lower magnitude and intensity punctuating the interval between Avellino and Pompeii events. After AD 79 the activity was characterised by even more frequent eruptions, and the stratigraphic record testifies of periods of open-conduit activity alternated with pauses interrupted by explosive events. On the whole, the magnitude of the eruptions has been roughly decreasing with time while, since 3.9 cal ky BP, their frequency has been increasing.



Eruption type	Repose <i>years</i>	Volume <i>km³</i>	Peak MDR <i>kg s⁻¹</i>	Column height <i>km</i>	PDC	Composition	SiO ₂ <i>wt. %</i>	Alkalies <i>wt. %</i>
Plinian	10 ² - 10 ³	10 ⁰ - 10 ¹	10 ⁷ - 10 ⁸	>20	Yes	Trachyte Tephrite to Ph-Tephrite	54 - 61 54 - 62	8 - 12.5 11 - 16
Subplinian I	10 ²	10 ⁻¹ - 10 ⁰	10 ⁷	15 - 20	Yes	Te-Phonolite to Ph-Tephrite	48 - 52	8 - 16
Subplinian II	10 ²	10 ⁻² - 10 ⁻¹	10 ⁶ - 10 ⁷	10 - 15	Minor	Te-Phonolite to Ph-Tephrite	48 - 54	8 - 11
Violent Strombolian	10 ¹ - 10 ²	10 ⁻³ - 10 ⁻¹	10 ⁵ - 10 ⁶	5 - 10	Minor avalanching	Tephrite to Ph-Tephrite	48 - 52	6 - 12
Continuous ash emission	10 ¹ - 10 ²	up to 10 ⁻²	< 10 ⁵	< 5	No	Te-Phonolite to Ph-Tephrite	49 - 51	9 - 12
Mild Strombolian	10 ⁰ - 10 ¹	10 ⁻³			No	Tephrite to Ph-Tephrite	47 - 49	7 - 11

Fig. 42 - Main physical and compositional parameters associated with the different eruption types (From Cioni et al., 2008).

The difference in the number of events between the pre- and post-Avellino Pumice eruptions can pose some doubts about the reliability and completeness of the stratigraphic record. However, the reconstructed sequence of the products of the SV pyroclastic activity has to be considered a quite exhaustive picture of the explosive activity of the volcano, not suffering any major bias related to intrinsic incompleteness of the dataset, at least for VEI>3 explosive activity.

Magnitude vs. Intensity relationships

Magnitude and intensity data are now available for about 20 explosive eruptions. The peak Mass Discharge Rate (MDR, in kgs^{-1}) and the volume (V, in km^3) can be used as proxies for intensity and magnitude respectively, as suggested in Pyle (2000). When plotted in the diagram of Fig. 43, the two parameters exhibit a power law correlation, with an R coefficient of 0.55. With these data, however, a sigma-shaped fitting can also be tempted.



The main problem in establishing a good correlation is actually related to the gap existing for intermediate values of magnitude and intensity (V between 10^{-2} and 10^{-1} km³, MDR between 10^4 and 10^6 kgs⁻¹). On a general basis, it can be assumed that intensity increases with magnitude up to the category of Plinian eruptions. It is worth noting, however, that this correlation does not hold for the group of the four Plinian eruptions.

The V vs. MDR diagram of fig. 43 represents a first attempt to systematize the past 20 ka of activity of the volcano. Possible problems on the data can be related to:

- the plotted intensity values refer to the peak MDR, a value not representative of the whole eruption, especially for long-lasting, unsteady events;
- eruption rate is difficult to estimate for those phases of the eruptions characterised by important pyroclastic flow activity, where the flow rate could be higher than that estimated for the convective plinian column;
- Volume estimation especially suffers of problems related to the quantification of distal products, dispersed following different physics with respect to proximal and medial, easily recognizable and measurable deposits. This reflects in a different error distribution depending on the style of the eruption, being the error on high-intensity eruptions larger than that for low-intensity eruptions.

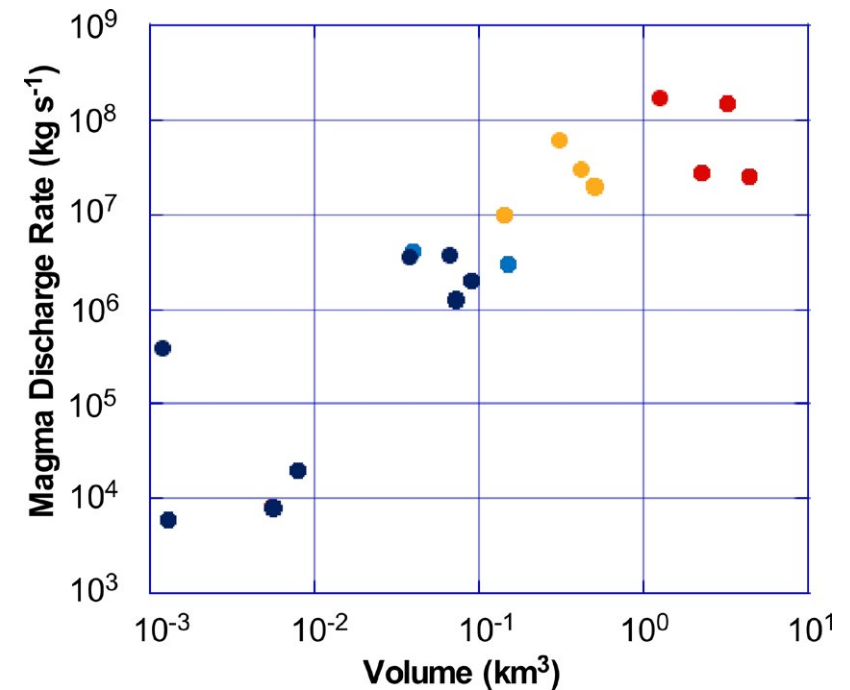


Fig. 43 - Log-log diagram showing Volume vs. Peak MDR (as proxies for magnitude and intensity respectively) of selected eruptions of Somma-Vesuvius. Colors as in Fig. 42

Magnitude vs. Repose time.

The systematic revision of the data on past activity provided also further information on the relationships between the size, in terms of magnitude, of past eruptions and the time elapsed between one eruption and the following, generally considered as the repose between two eruptions (Fig. 44).

The estimation of the length of repose is dependent on the methods used to define it. Looking at the stratigraphic succession of the products, the deposits of several eruptions have been unequivocally recognized, and the repose time before each eruption is represented by the difference in age between two overlapping deposits. In this case,

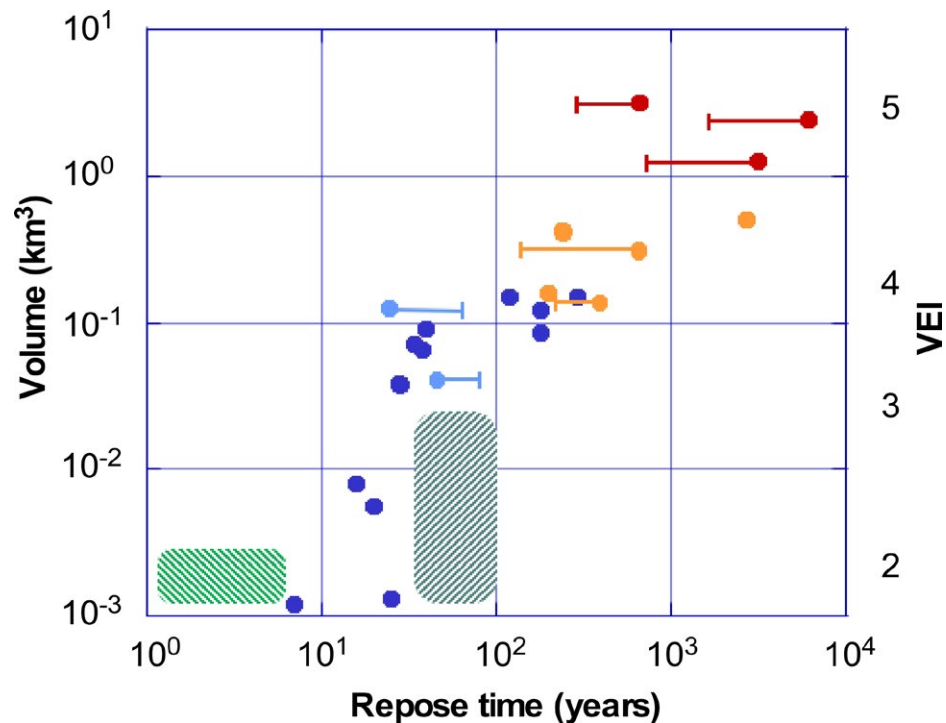


Fig. 44 - Apparent repose vs. magnitude of the eruption. The main physical parameters associated to each eruption type are shown in the inset. The red dashed window shows that a large variability in eruptive styles is associated to repose times of the order of 100 years, similar to the present one (From Cioni et al., 2008). Colors as in Fig. 42.

we should speak in terms of “apparent repose time”, as it is highly probable that in the case of an activity characterised by largely variable intensity of the eruptions, only some of these events, let say those with $VEI > 2$, are clearly recorded in the stratigraphic sequence. Conversely, when a set of historical data from direct observation is available, it is possible to deal with a “real” repose time. In the case of Somma-Vesuvius, this problem poses for the post AD 1631 period, during which the activity of the volcano was clearly dominated by open conduit conditions and characterised by decade-lasting eruptive periods with mild to low intensity effusive and explosive phases often culminated in larger, violent strombolian eruptions. To compare the length of repose time between eruptions occurred during these different periods we decided to consider in both cases an “Apparent repose time”, being the difference between the age of two consecutive eruptions whose deposits can be detected in the field. Using this methodology, the periods of open conduit conditions result as a sequence of few major events generally with a VEI not lower than 2.

A positive correlation between the length of repose and magnitude of the eruption is clearly evidenced by the data (Fig. 44). This was interpreted by Santacroce (1983) as an

evidence of a roughly constant deep magma feeding rate to a shallower magma storage system. As already discussed, a certain scatter exists between the size of an eruption and its intensity, so introducing a larger uncertainty when looking at the possible correlation between repose and eruption style. The length of the apparent repose is still well correlated with eruption size for the most intense eruptions (plinian and subplinian I), while the correlation is poorer for eruptions of intermediate size and intensity. In particular, a large variability in the magnitude and eruption style of the past eruptions is apparent for a window of repose time from dozens to hundreds of years.



Itinerary – Days 3 and 4

The 3rd and 4th days of the fieldtrip (Fig. 45) will be dedicated to visit several outcrops of ancient and recent deposits of SV activity, comparing and discussing the different eruptive styles (also in relation with time) and the possible impact of the different types of activity on the environment and human being. The fourth day will be mainly focussed on the famous AD 79 eruption, looking at the proximal deposits and the effects of the eruption as visible into archaeological sites.

Day 3

Stop 3.1: Caldera wall and Vesuvius Crater (40°49'22.68"N - 14°25'20.79"E)

Significance: The structure of Somma-Vesuvius. Inner portion of the caldera. The complex evolution of a volcanic crater. Syn-eruptive flank instabilities of a volcanic cone.

<https://doi.org/10.3301/GFT.2019.02>



Fig. 45 - Planned stops at Somma-Vesuvius.



Fig. 46 - Panoramic view of the Somma caldera from the Vesuvius cone. The grey area at the base of the caldera cliffs is the main 1944 lava flow, from Avanzinelli et al., 2017.

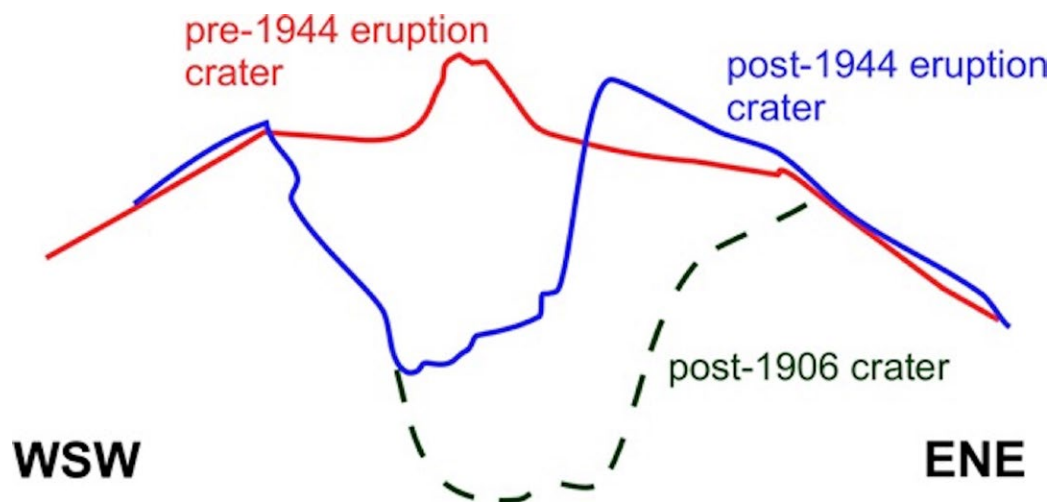


Fig. 47 - The evolution of Vesuvius crater from 1906 to the present one. Redrawn from Cole and Scarpati (2010).

The last part of the main road to the crater runs inside the Somma-Vesuvius caldera, a polyphased depression formed by repeated collapses following the main Plinian and subplinian eruptions (Fig. 1). The caldera walls are steep (Fig. 46) and intensely cut by dykes. The floor of the Valle dell'Inferno, the semicircular depression separating the caldera walls



from the Vesuvius cone, is partially invaded by the lava flow of the last eruptive event of Vesuvius, occurred on March 1944 eruption.

The crater formed as a consequence of a collapse which occurred in the last explosive phases of the 1944 eruption. The sequence of thin lava flows well visible on the steep walls of the crater were emitted during the period 1913-44, which followed the preceding large eruption of 1906. This left a much wider crater (part of the rim is still visible) which was slowly filled with lava until 1944, when a central conelet was approximately at the height of the north-west rim (Fig. 47). On top of the rim there is a thick lava flow (1944) covered by scoriae and lapilli of the last phase of the eruption. To the east an apparent fracture is visible. Actually, it is the contact between the lava flows of the 1913-44 crater and those of the 1872-1906 crater.

The slopes of the cone are characterized by several landslide scars, related to the formation of hot scoria avalanches during the eruption, probably triggered by the coupled action of rapid accumulation and syn-eruptive seismic shaking. The avalanching deposits are well visible at the foot of the cone (Fig. 48). The detachment surface of these landslides locally present welding structures and striae (Fig. 49).

Proceeding along the rim of the crater, one can observe the whole extent of the southern part of the volcano and, during days with good visibility, it is possible to see the entire gulf of Naples, from the Sorrento peninsula to Cape Miseno, Procida and Ischia.

Stop 3.2: The 1944 lava flow (40°49'49.27"N - 14°24'21.95"E)

Significance: The products of the most recent eruption of Vesuvius. Surface structures of a recent lava flow.

The stop is dedicated to observe the surface structures and lateral levees of the main *aa* lava flow of 1944 eruption.

The 1944 eruption

On March 13th, 1944 the summit conelet partially collapsed forming a depression of about 20 m depth. A slight explosive activity partially rebuilt the conelet on the 14th. This activity lasted intermittently till the 18th. At 16.30 (local time) of the 18th a lava flow was rapidly emitted from the remains of the conelet, overcame the crater wall. The eruption is classically divided into four phases (Ventura and Vilardo, 2008; Cole and Scarpati, 2010).



Fig. 48 - Left: Satellite image of the Vesuvius cone. The deposits of the hot scoria avalanches are well visible at the NW feet of the crater. A large landslide scar (and related deposits) is present in the NE side of the cone. Right: the deposits of the hot avalanches as seen from the summit of the cone.

Lava Flows

On the evening of 18th March several lava flows issued from Gran Cono (Fig. 50). The northern lava moved initially on the outer flank of the crater and bent to the west when it reached the caldera floor. At 22:30, the velocity of this lava flow was $\sim 10 \text{ m h}^{-1}$. On the evening of the 19th, at 11am, the northern flows reached the first houses. On March 21st the flow had reached the villages of S. Sebastiano (Fig. 50) and Massa di Somma. At the end of the eruption, the total length of this lava flow became 5.6 km. Because the northern lava flow emplaced in about 57 h, the average flow velocity was 98 m h^{-1} .



Lava Fountains

The first lava fountain started on March 21st at 17:15 and lasted for about 30 minutes causing an accumulation of scoriae on the flank of Gran Cono. Other 7 lava fountains occurred, the last, in the morning of March 22nd, lasted for about 5 hours.

Mixed explosions

The last lava fountain culminated with the formation of a sustained ash column which reached about 5 km above the crater rim. This phase and the following one were accompanied by the formation of small pyroclastic flows on the flank of the cone (Fig. 51).

Final phase

On March 27th and 28th the explosions were more rare and less violent, on March 29th, the eruption ended.

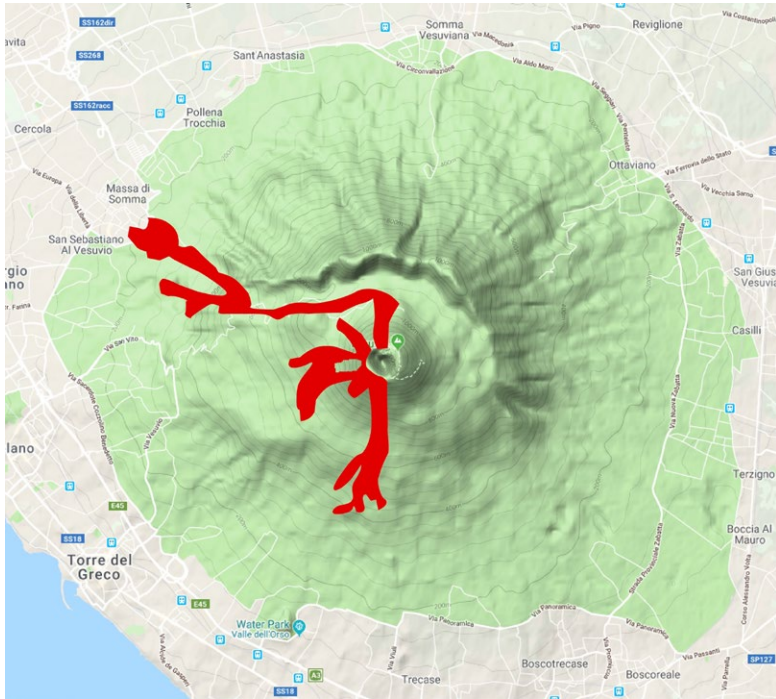
Stop 3.3: The Royal Observatory of Vesuvius

The Vesuvius Observatory is the oldest volcanological observatory in the world. It was founded in 1841 by the King of the Two Sicilies, Ferdinand II of Bourbons, in order to study the volcanic activity of Vesuvius, for the early warning of the population.

After the tragic experience of the 1631 sub-Plinian eruption of Vesuvius indeed, which caused more than 4,000 casualties, the need to alert the population at the first warning signs of intense phases of volcanic activity led the citizens living around the volcano to place numerous lookouts on bell towers and along the coast, to observe the volcano and the sea and detect any possible sign of renewed volcanic activity. With the coming of the Enlightenment, the approach to understanding eruptive phenomena changed completely, and the need arose to study the volcano systematically using scientific methods.



Fig. 49 - Close view of the detachment surface of the hot avalanches, presenting welding of the scoria and striae.



© 2002, SMU / MCSC

Fig. 50 - Left: The 1944 lava flows (modified from Ventura and Vilardo, 2008). Right: the lava front entering in the S. Sebastiano village

In this new rational and enlightened scientific climate, Ferdinand II of Bourbon, King of the Two Sicilies – in response to the requests of scientists from Italy and abroad – disposed the construction on the Hill of the Saviour, on the slopes of Vesuvius, of the world's very first volcanological observatory. On 3rd September 1841, the monarch approved the design of architect Gaetano Fazzini and agreed to finance the building of the Vesuvius Meteorological Observatory (Fig. A1). The building was officially opened on 28th September 1845 on occasion of the 7th Congress of Scientists in Naples, and handed over to its first director, the renowned physicist Macedonio Melloni, in March 1848.

"Gentlemen, in a century in which man is so successfully managing to tear from nature's bosom its deepest and

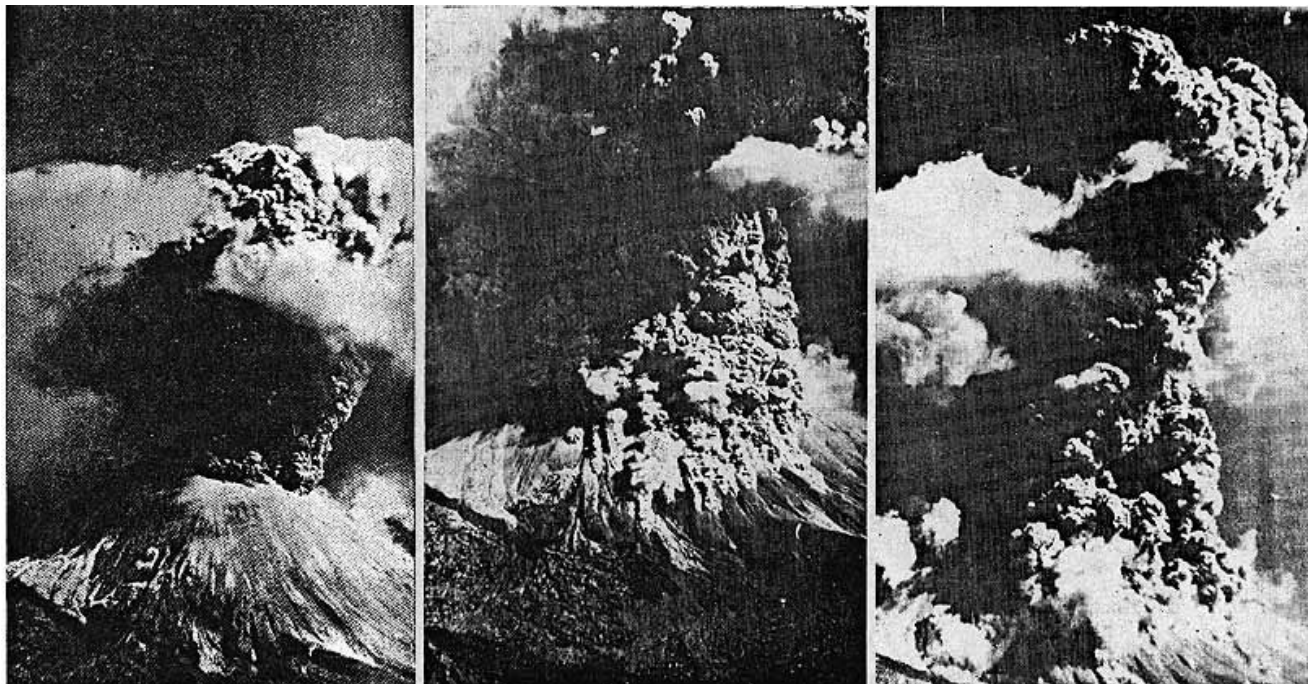


Fig. 51 - The mixed explosion activity of the 1944 eruption (from images of the time).



Fig. 52 - Anonymous: The works for the construction of the Vesuvius Observatory in 1844.

most intimate secrets, it had become a matter of great importance and urgency to build an observatory for the express purpose of the day-to-day, practical study of meteorology and terrestrial physics" (Macedonio Melloni. Speech at the inauguration of the Vesuvius Observatory, 1845).

For over 170 years the presence of the observatory has allowed detailed scrutiny of the eruptions of Vesuvius, the systematic sampling of volcanic emissions, and the design and testing of new scientific instruments – to the extent that Vesuvius is the best known and most thoroughly monitored volcano in the world.

The building that hosts the observatory was constructed in strict Neo-Doric style according to a design by the Court architect Gaetano Fazzini. Master builders were employed on the task from 1841 until the sixteenth of March 1848, when the headquarters was finally delivered to the director, Macedonio Melloni, complete with all its finishing.

The building has three stories. The façade looks southwards and involves two floors with separate

entrances, one above the other; that of the main piano nobile first floor is the monumental entrance, with a colonnaded porch reached by a staircase in lava stone with two side ramps. The first-floor façade is faced with blocks of piperno and lava which encase six arcades, with large windows framed in plastered bricks. The top-floor façade is also in plastered brick, with corners in lava blocks. On the main *façade* there are two sundials which indicate solar time and the months of the year. A stone slab in the centre bears an inscription recording the foundation of the Observatory at the behest of King Ferdinand II of Bourbon. Large terraces with panoramic views, designed to be used for external observations, are present on the first and second floors. The most prestigious room on the first floor is the elegant octagonal chamber, initially intended to house the marble



bust of Ferdinand II that had been carved for the occasion by Tito Angelini (1804-1878) but considered by Melloni to be more suitable for containing the magnetic instruments. On the second floor, there is the Great Hall, now the Palmieri Hall, embellished by the paintings of Gennaro Maldarelli (1795-1858), and ornamented with six 'shrines' framed by pilasters with capitals and decorated pediments featuring cornices and inscriptions in gypsum plaster. G. Maldarelli used the technique of oil on unprepared canvas. The subjects of the central paintings are: Minerva crowning the God of Science with various cherubs in attendance, Aeolus commanding the winds and the Forge of Vulcan. At the ends two atmospheric occurrences are portrayed: a Whirlwind and a Waterspout. The canvases offer representations of meteorological phenomena that refer to the four classic elements of air, water, earth and fire, the last of which is symbolized by Vulcan. The four elements, joined under the ellipse of a rainbow, serve to frame the central theme: the mythological scene in which Minerva, goddess of wisdom, crowns Prometheus, dispenser of the fire of knowledge.

The long history of the Royal Vesuvius Observatory is extensively documented in its collections.

This heritage – of great scientific and cultural value and unique for its abundance and variety – tells the story of the world's first observatory, closely linked to the activity of Vesuvius, and the commitment of many scientists who dedicated their lives to studying the volcano.

The Observatory owns and houses the following collections, unique in their combination of scientific, historical and artistic importance:

- Old books on Volcanological matters

The Observatory library treasures among its possessions numerous antique books of largely volcanological content including 9 sixteenth century volumes, 64 from the seventeenth century which deal mainly with questions regarding the 1631 eruption, while those of the 18th century are compendia of Vesuvian history by various famous writers like Serao, Sorrentino, Mecatti, De Bottis and Ascanio Filomarino. The most valuable book is undoubtedly that of the Jesuit Athanasius Kircher, *Mundus Subterraneus*, and dates to 1668.

- Vintage photographs and filmed sequences of eruptions

The collection contains a large number of photographs and films of eruptions made between 1865 and 1944. The oldest film in the archive is also the first film ever made of a volcano in eruption, shot by the Lumière Brothers in 1898, only two years after the invention of the cinematograph. The short film records the formation of Colle Umberto (1895-1899).



Another rarity is the film of the catastrophic 1906 eruption made by the Troncone Brothers.

The most recent film is of the 1944 eruption and was shot by the Allied Forces and donated to the director Giuseppe Imbò. The collection is completed by numerous photographic plates and negatives showing Vesuvius, Etna, Stromboli and Vulcano.

- Collection of Rocks, Minerals, volcanic ash and other materials from Historical-period eruptions of Vesuvius. Many of these samples were collected personally by Teodoro Monticelli, Arcangelo Scacchi, Vittorio Matteucci and Alessandro Malladra. They are samples of lava, ash, lapilli and bombs produced by eruptions since 1631.

- Recordings on smoked paper of Vesuvian Seismic activity from 1915 until 1970

These registrations are of notable scientific and historical value, since they are evidence of the volcano's seismic activity over a long-time period. The collection also includes apparatus for smoking the paper.

- Scientific Instruments

The instruments belonging to this collection illustrate the long journey made by seismology, the uncontested pioneers of which were Palmieri and Mercalli, both past directors of the Vesuvius Observatory.

Possessions include the oldest seismoscopes and Palmieri's famous electromagnetic seismograph (Fig. 2), all in excellent condition, as well as numerous pieces of meteorological, magnetic, geodetic and geochemical apparatus, used for the study and surveillance of Vesuvius since the birth of the Vesuvius Observatory. The Sensing Apparatus (left) is composed of two seismoscopes for vertical movements (B, C) and three for horizontal ones (A, C, D), of which only A and B are non-electrical and activated only by large earthquakes, whereas the others (C and D) are electrical and able to detect even small events. The Recording Apparatus (right) is formed of two clocks (1 and 2) and two electromagnets; of the latter, one is inserted into the circuit closed by the horizontal movement sensors and one in the vertical movements circuit.

- Geological and Geomorphological Maps and Models

The collection is privileged to include a geological map by Johnston Lavis (1888), one of the earliest volcanological maps of Vesuvius (Fig. 3). There are also surveys of the modifications undergone by the cone of Vesuvius following various eruptions, conducted by Matteucci, Mercalli and Malladra. The collection is completed by



numerous models of Vesuvius, Campi Flegrei, Santorini, Stromboli, Etna and Fogo (Cape Verde). The oldest dates from 1878 and represents Vesuvius on a zinc sheet electroplated with copper.

- Gouaches of Vesuvius

The collection consists of 15 gouaches of which three are by Odoardo Fischetti, one by Luigi Gentile and the others by unknown artists. They all share as their subject Vesuvius and its eruptions, and were painted between 1819 and 1834.

- Lava Medals

The collection consists of 95 pieces and bears witness to life around Vesuvius and the type of eruptive activity that occurred at the time of their production. The medals were made using small quantities of still molten lava taken as close as possible to the points of emission, and on them were inscribed images and writing using metal punches.

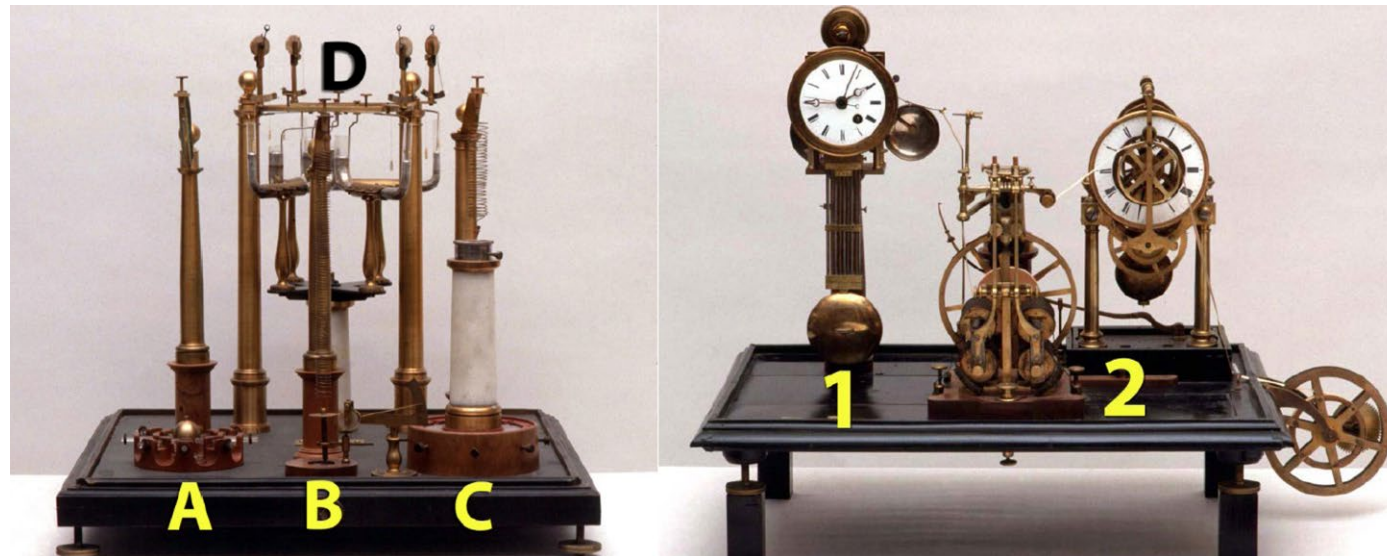


Fig. 53 - The Palmieri seismograph. Palmieri built several scientific instruments, essentially meteorological or seismological, of which the Palmieri Seismograph is undoubtedly the most famous. This instrument made it possible to record earthquakes on paper. The first model was built in 1856, provoking great interest in the international scientific community. For this invention, he received a prize of one thousand lire from the University of Boston and the gold medal of the Lisbon Academy.



Stop 3.4: San Vito Quarry (40°49'50.91"N - 14°22'54.84"E)

Significance: proximal deposits of a Plinian eruption; magmatic vs. phreatomagmatic activity; evidence of magma-rock interaction from lithic blocks

During the stop we will visit a large pozzolana quarry, used in the recent past as a public dump.

The main walls of the quarry expose a complex, proximal sequence of the deposits of the Bronze Age Avellino Pumice Plinian eruption.

The eruption sourced from a vent opened in the area of Piano delle Ginestre, on the western flank of the volcano, less than 1 km from the quarry. The general stratigraphy of the eruption (Fig. 54) is characterized by:

- the laterally variable (in aspect and thickness) deposits of the Opening Phase;
- a very thick, coarse fallout deposit with abundant lithic blocks, compositionally zoned from white phonolitic pumice at the base to grey tephriphonolitic pumice at top (Plinian Phase);
- several flow units of the Phreatomagmatic Phase.

A large number of the coarse lithic blocks scattered in the deposits represents cumulitic, metasomatic and skarn material from the magma-chamber-carbonatic basement interface.

Close to the entrance of the quarry, some PDC deposits of AD 79 Pompeii and AD 472 Pollena eruptions are visible inside a small paeovalley (Fig. 55).

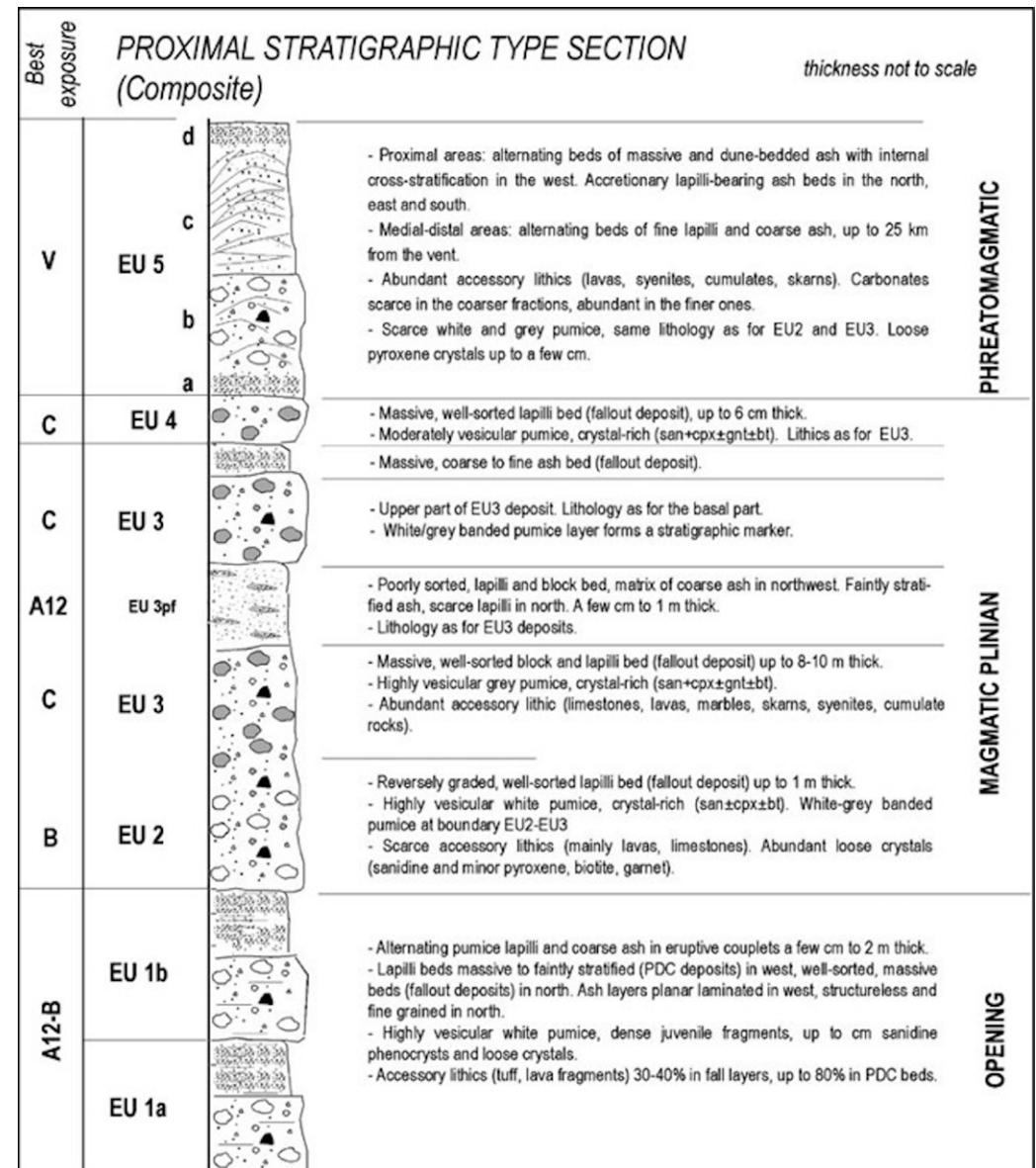


Fig. 54 - General stratigraphy for the deposits of the Avellino Pumice eruption (from Sulpizio et al., 2010).



Stop 3.5: Pollena Quarry (40°50'46.01"N - 14°23'24.09"E)

Significance: the general structure of the volcano; eccentric vents; the valley-ponded PDC deposits of the northern sector of the volcano, and the effects of the topographic barrier of Mt. Somma on PDC deposits

This is another large abandoned quarry in the northern slopes of the volcano, directly facing the Mt Somma rim. In the main cliffs, a nearly complete sequence of SV deposits is exposed, although now strongly covered by vegetation. Between the deposits of the Pomici di Base and Greenish eruptions, couple of cinder cones are exposed (Fig. 56). In one of these, thoroughly quarried, the feeder dyke and associated lava flow are well visible (Sparice et al., 2017).



Fig. 55 - Valley-filling deposits of AD 79 and AD 472 eruptions at S. Vito Quarry.



Fig. 56 - The core of the main cinder cone, with a lava flow on top.



The quarry develops along one of the main valleys draining from the outer Somma rim, interested by the accumulation of thick PDC sequences of the Avellino Pumice, Pompeii Pumice and AD 472 Pollena eruptions. The valleys are now deeply cut, showing an interesting sequence of deposits (Fig. 57).



Fig. 57 - The PDC deposits of the AD 79 Pompeii eruption (light color), followed by the dark-colored sequence of the PDC deposits of the AD 472 Pollena eruption (right flank of the valley, looking the volcano).



Day 4

Stop 4.1: Pozzelle Quarry (40°47'38.16"N - 14°28'09.70"E)

Significance: deposits of the whole SV sequence; the proximal deposits of the AD 79 Pompeii eruption; effects of local topography on the depositional features of PDC

This is the largest quarry in the area, now inactive. With its multiple cliffs, cut at with different orientations, the quarry is a highly didactic site where to discuss the effects of local topography on the lateral facies variations of pyroclastic deposits of different eruptions.

In the many cliffs at different elevations inside the quarry a complete sequence of the SV products is visible, from the Somma lava flows up to the XX century activity. At the base of the quarry, on top of the Mt Somma lavas, PDC deposits of the Pomici di Base Plinian eruption are visible, topped by the deposits of the Mercato Pumice.

In particular, the quarry represents one of the most complete sites for the AD 79 Pompeii eruption stratigraphy. Cioni et al. (1992; 1995) divided the deposits into eight eruption units (Figs. 58 and 59) and three phases: the opening phreatomagmatic phase (EU1), the Plinian magmatic phase (EU2 and EU3), and the final phreatomagmatic, caldera-collapse phase that was accompanied by progressively increasing involvement of external water (EU4 to EU8). Over the course of the eruption, first white, phonolitic pumice



Fig. 58 - The deposits of the AD 79 eruption are followed by thick, valley-filling, PDC deposits of the AD 472 Pollena subplinian eruption.



cm		Description	General distribution
100-200	EU8	Multiple light brown, pisolite bearing, fine ash beds. White pumice lapilli often occur at the bottom of these beds, together with rare lithic fragments.	The unit occurs with variable thickness over the whole southern sector. In the area north of Boscoreale thinly, cross or parallel laminated beds occur
0-30	EU7	Composite PDC unit, formed by a tripartite bedset with a basal coarse, grain supported lapilli bed, followed by cross-bedded coarse ash and by accretionary lapilli-bearing fine ash at top. The basal bed presents a peculiar enrichment in deep-seated lithic fragments (marbles, cumulitic and metasomatic rocks) and greenish, dense, px-bearing juvenile scoria	The unit is widely distributed over the whole southern sector
20-70			
3-7	EU6	Very thick, block-rich, matrix supported PDC deposit, with up to meter-sized lithic blocks (lavas, tuffites and cumulitic, thermometamorphic, metasomatic and subintrusive rocks) in a coarse ashy matrix with white and grey pumice lapilli. The deposit are generally confined in small paleovalleys. Block-enriched lenses occur in the medium portion of the bed. The PDC is often erosive on the substratum, cutting up to the basal white pumice fall layer.	Distributed in the area north of Boscoreale and Terzigno, this unit grades downvalley into lithic-enriched ash layers with a decreasing median grain size. It is very thickened at the outlet of some main paleovalleys.
0-1500			
0-350	EU5	Multiple ash flow units (at least two) formed by pumice and lithic lapilli in a coarse ashy matrix, massive or with thin parallel or cross-laminations. The massive units are strongly topographically-controlled. These PDCs have a strong erosive power in the more proximal areas.	This unit is only distributed north of Boscoreale, largely channelled in the main paleovalleys.
0-30			
20-400	EU4	Tripartite, fining-upward, bedset formed by a grain-supported basal layer with green pumice lapilli and lithic blocks of deep-seated rocks. This bed is normally graded and sometimes contains charred material at top. In proximal outcrops the layer grades upward in a coarse ash, thinly laminated bed followed by cross-laminated, dune-bedded coarse ash. This contains normally graded, white and grey, well rounded pumice swarms. The top of the unit is locally represented by an accretionary lapilli-bearing ash bed. The unit discordantly overlies the lower pumice flow deposit.	The unit is radially dispersed around the volcano, although with an evident lateral facies variation. The basal layer is only dispersed toward southeast. The topmost fine ash bed is rather discontinuous.
1-70			
5-500	EU3pf	Faintly to strongly laminated pumice flow sequence, with several interbeds and swarms of coarse ash and pumice lapilli. The sequence is generally normally graded for the lithic and reversely graded for the pumice fractions. Several flow units are present at some sections, with a general upward decrease of thickness and grain size of the units.	The thickness of this unit is locally strongly variable. Maximum accumulation is in the area north of Boscoreale and on the northern slopes of Mt Somma.
10-45	EU3	Fallout bed of grey pumice lapilli with lithic fragments of lavas, limestones and marbles. Pumice bombs and lithic blocks up to 30 cm in diameter. It is eroded by the following PDCs. In the area of Oplontis it shows several (at least 5) ash interbeds	The unit is distributed to SSE, reaching its maximum thickness in the area of Pompeii.
2-12	EU2/3pf	Coarse ash bed, white at bottom and grey at top. Faintly laminated, lenses of rounded pumice lapilli.	PDC deposit only present in the proximal sites of S and W sectors.
30-140	EU2	Massive, poorly sorted lapilli bed, with white, highly vesicular pumice and lithic fragments of lavas and rarer carbonate rocks.	The unit is distributed to SE, with its maximum thickness on the upper slopes of the volcano
1-5	EU1	Massive, accretionary lapilli-bearing, grey fine ash fallout bed	The unit is distributed to E.

(EU1 and EU2), then gray, tephri-phonolitic pumice (EU3–EU8), were erupted.

In the quarry (Fig. 58), on an agricultural soil, the fine ash bed of the opening phase of the eruption is well visible, followed by a m-thick deposit of the white pumice fallout (EU2), representing the first part of the Plinian phase. The grey pumice fallout (EU3) is locally strongly reduced in thickness by the erosional effect associated to PDC formation during the final collapse of the sustained column, here recorded by the EU3pf deposits. A grey to green, pumice fallout (EU4 base) very rich in deep xenoliths (marbles, cumulatic rocks, skarns) from the magma reservoir-host rock interface marks the onset of the caldera collapse and the beginning of the phreatomagmatic phase of the eruption, and it is followed by several PDC units with different lithologies (EU5 to EU8). A coarse, channel-filling, lithic-rich breccia (EU6) is here present, possibly related to a major phase of the caldera collapse.

Stop 4.2: Villa di Poppea archaeological excavations - Oplontis (40°45'27.29"N - 14°27'08.43"E)

Significance: dynamics of the AD 79 eruption column; Plinian fallout and deposits of partial column collapses; the phreatomagmatic phase of the eruption; the final lahar activity

The Villa di Poppea (the Emperor Nero's wife) was destroyed by the pumice plinian fallout of the AD 79 eruption (Fig. 60).

Fig. 59 - Stratigraphy of the AD 79 Pompeii eruption in the Pozzelle quarry From Cioni et al., 1992).



Fig. 60 - Panoramic view of the Villa di Poppea, Oplontis

Along the exterior of the Villa, it is well visible a nearly complete sequence of the fallout deposits of the eruption, and of the pyroclastic flows related to partial column collapses which repeatedly occurred during the plinian phase of the eruption. The top of the sequence is constituted by several lahar units (Fig. 29). In some places, the relationships between the deposits and related damages to the structure of the villa are well visible (Fig. 61), and will be discussed in detail.



Fig. 61 - Left: the deposits of the AD 79 eruption along the perimeter of the Villa di Poppea, at Oplontis. Right: a column of the outer colonnade of the villa knocked down and covered under the deposits of the white pumice fallout (EU2).



Oplontis archaeological excavations

The excavation sites of Oplontis are located in the middle of the modern town of Torre Annunziata. The only documentary evidence of the name Oplontis is in the Tabula Peutingeriana, a medieval copy of an ancient map of the roads existing in Italy at the time of the Roman Empire. The place name of Oplontis applies to a few buildings situated between Pompeii and Herculaneum. Hence, a series of archaeological finds have been ascribed to Oplontis which in fact relate to a suburban area of Pompeii. They consist of a residential villa, known as the villa of "Poppea"; a rustic villa thought to belong to L. Crassius Tertius in which a large quantity of gold and silver coins, along with a wealth of exquisite jewellery, were found lying next to numerous bodies of eruption victims; and thermal baths situated in the Oncino area, underneath the present Terme Nunziante Spa, which A. Maiuri has attributed to the consul M. Crassus Frugi. The main monument, which is the only site open to visitors and listed by UNESCO as a "World Heritage Site", is the villa of Poppea. This grand residential building, originally constructed in the mid-1st century BC, was extended during the Imperial Period and was undergoing renovation work at the time of the eruption. It is attributed to Emperor Nero's second wife, Poppaea Sabina, but belongs more generally to the imperial family's estates.

Source: <http://www.pompeisites.org/Sezione.jsp?titolo=Oplontis&idSezione=557>
Courtesy of "Parco Archeologico di Pompei"

Stop 4.3: Herculaneum archaeological excavations (40°48'21.51"N - 14°20'57.23"E)

Significance: the effects of PDC on a roman town

The city of Herculaneum, only 7 km west of the crater of Vesuvius, was buried under 20 m of pyroclastic deposits during the AD 79 eruption (Fig. 62). The deposits were mainly emplaced by PDC, as the town, although very close to the volcano, was outside the main dispersal fan of the fallout deposits.

According to the legend the city was founded by Hercules when he returned from Iberia. Herculaneum was a Greek city by origin, in fact it shows a horthogonal scheme of roads, NS and EW directed (respectively "cardo" and "decumanus") forming equal city blocks ("insulae"). In roman times the city was a prosperous and luxurious seaside resort. The city was situated on a hill or headland in front of the sea.

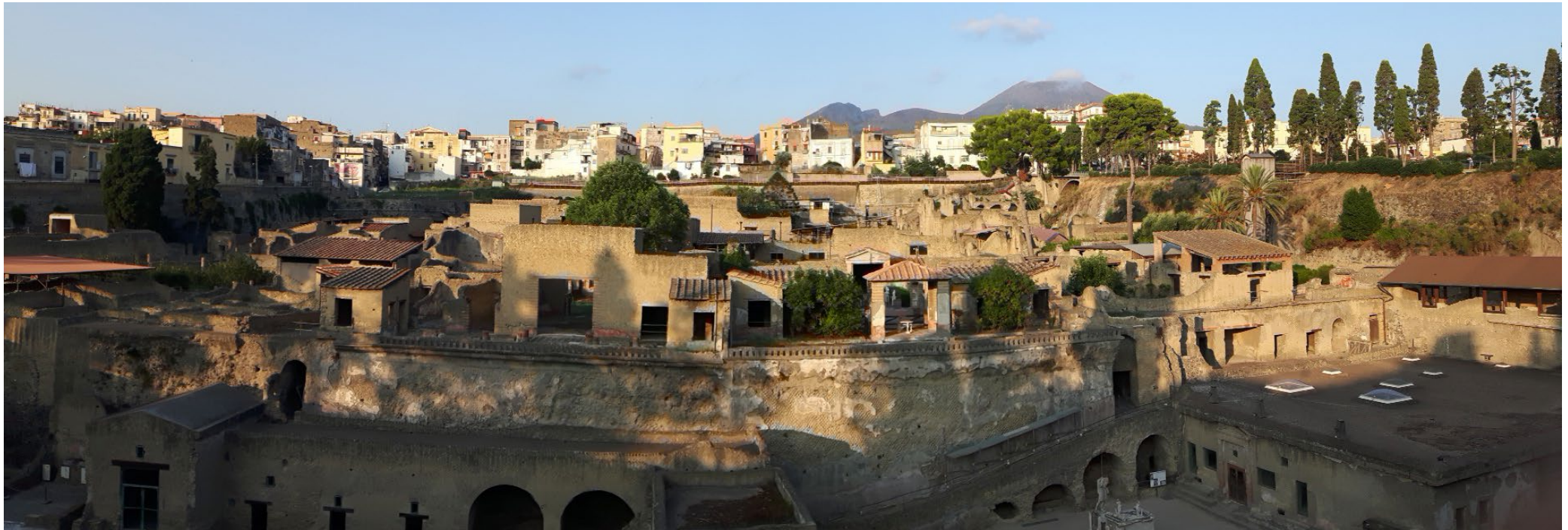


Fig. 62 - The Herculaneum excavations and, in the backside, the Vesuvius cone and the Somma rim., from Avanzinelli et al., 2017.

The deposits of the AD 79 Pompeii eruption are well visible along two main sections along the perimeter of the excavations, the Herculaneum beach, and the Palestra (Fig. 63).

Herculaneum Beach. - The cliff facing the sea (overlying the tunnel entrance) includes at least six units, and it is the most complete exposure of the AD 79 PDC deposits that buried Herculaneum. Along the waterfront a series of arches and related chambers form the base of the Sacred Area. The first deposit of the eruption is a 35 to 50 cm thick, unconsolidated, poorly sorted, massive grey layer (EU2/3pf) deposited by a dilute PDC which extends into the chambers. The arrival of this PDC marked the first, devastating event into the town. This unit is overlain by a lithified, sequence of pumice-rich flow deposits (EU3pf1; EU3pf2a; EU3pf2b), locally represented by fines-depleted, coarse grained beds with abundant building material. A fines-poor, discontinuous bed of pumice lapilli and lithic fragments (skarn, marbles and cumulitic rocks) represents the most important discontinuity

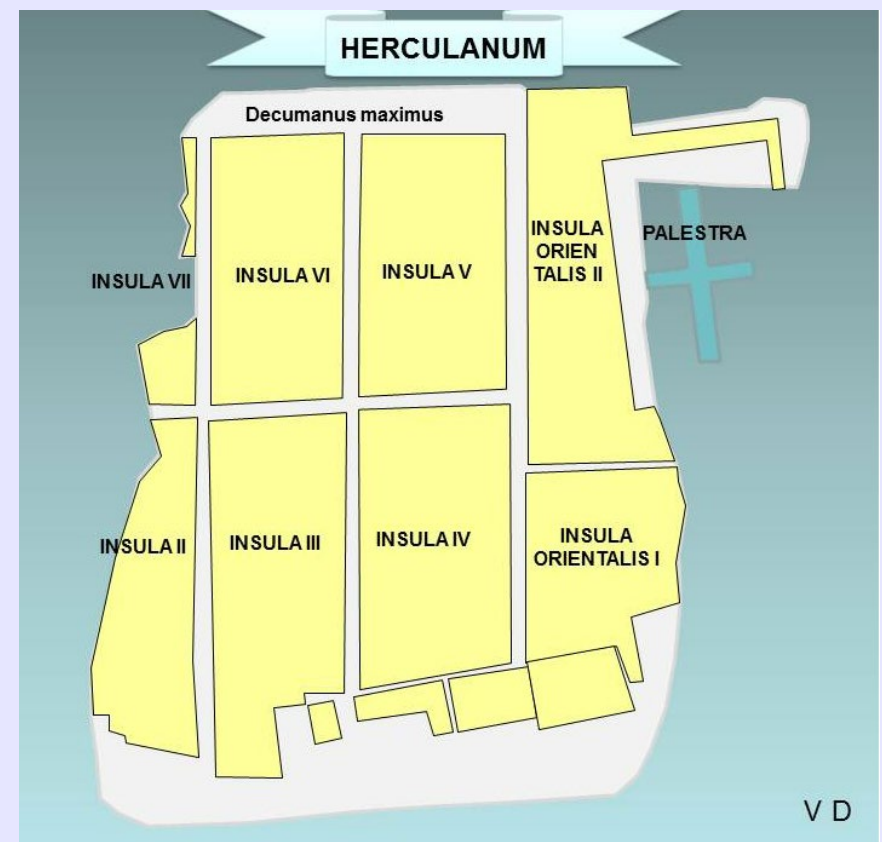


visible in this area. Its scalloped bottom is possibly related to the deformation effect of ballistic blocks. This bed marks the transition to the thick (up to 15 m) lithic rich flow deposits of the phreatomagmatic phase, possibly related to the basal layer of EU4 in the Pozzelle quarry (EU4). A massive, consolidated pyroclastic flow (s) deposit (yellow tuff), 8 m thick, follows. The last deposit (F4) is a massive, poorly lithified, lithic rich pyroclastic flow, up to 5 m thick.

Herculaneum Archaeological excavations

Ancient tradition connected Herculaneum with the name of the Greek hero Heracles (Hercules in Latin and consequently Roman Mythology), an indication that the city was of Greek origin. The first civilization on the site of Herculaneum seems to date back to the end of the 6th century BC. Soon after, the town came under Greek control and was used as a trading post because of its proximity to the Gulf of Naples. The Greeks named the city Ἡράκλειον, Heraklion. In the 4th century BC, Herculaneum again came under the domination of the Samnites. The city remained under Samnite control until it became a Roman municipium in BC 89, when, having participated in the Social War («War of The Allies» against Rome), it was defeated by Titus Didius, a legate of Sulla.

After the eruption of Mount Vesuvius in AD 79, the town of Herculaneum was buried under approximately 20 metres (50–60 feet) of ash. It lay hidden and largely intact until discoveries from wells and underground tunnels became gradually more widely known, and notably following the explorations in the early 18th century. Excavations continued sporadically up to the present although today over 75% of the town still remains buried. The inhabitants worshipped above all Hercules, who was believed to be the founder of both the town and Mount Vesuvius. Other important deities worshipped include Venus and Apollo, who are depicted in multiple statues in the city.



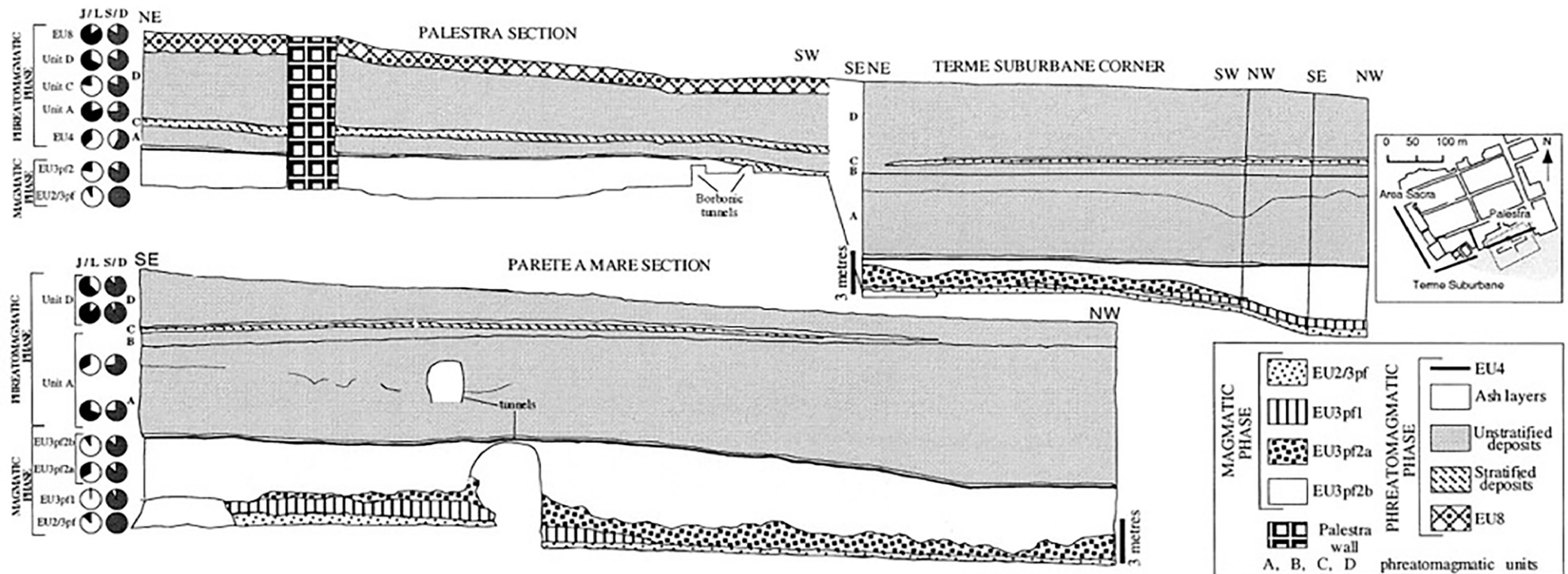


The buildings at the site are grouped in blocks (insulae), defined by the intersection of the east-west (cardi) and north-south (decumani) streets. To the east are two additional blocks: Orientalis I (oI) and Orientalis II (oII). To the south of Orientalis I (oI) lies one additional group of buildings known as the "Suburban District" (SD). Individual buildings having their own entrance number. For example, the House of the Deer is labelled (Ins IV, 3).

Source: <https://en.wikipedia.org/wiki/Herculaneum>

Palestra. The Palestra (the gym) is a rectangular park surrounded by porticos, and used for gymnastics, sports and games; in the centre of the park is a cross-shaped, 1.2 m deep swimming pool, buried under the EU3pf2 and EU4 deposits. EU2/3pf includes here a basal massive unit with a high amount of building materials. EU3pf2 is overlain by EU4, here marked by a clear unconformity with sparse blocks at the base and lithic rich pyroclastic deposits, 7 m thick.

Paleomagnetic thermoremanence data on lithic material and roof tiles embedded in the PDC deposits were carried out in the Herculaneum area by Cioni et al. (2004), giving a range of temperatures of the deposits between 300 and 360°C, on average higher of about 50°C respect to those generally measured on the deposits of the same eruption in the other sector of the volcano. A similar range of temperature, between 240 and 370°C, was measured by Caricchi et al. (2014) on the deposits of the close excavation of Villa dei Papiri by optical analysis in reflecting light on charred woods.



Sketch of the stratigraphic relations of the AD 79 deposits along the Palestra, Terme Suburbane corner and Parete a mare walls, inside the excavated area of Herculaneum. Location of the walls is indicated by the bold lines in the inset. The main units discussed in the text are indicated by different ornamentation (see legend at bottom right). Component data of the main flow units are shown on the left. J/L is the wt% ratio between juvenile (white) and wall rock lithic fragments (black). S/D is the wt% ratio between shallow-seated wall rock (lavas and tuffs; dark grey) and deep-seated wall rock components (cumulates, skarns and marbles; white).

Fig. 63 - The Palestra and Herculaneum Beach (Parete a mare) sections inside the Herculaneum excavations (from Gurioli et al., 2002).

References

- Acocella V. (2008) - Activating and reactivating pairs of nested collapses during caldera-forming eruptions: Campi Flegrei (Italy). *Geophysical Research Letters*, 35(17).
- Acocella V., Porreca M., Neri M., Massimi E., Mattei M. (2006) - Propagation of dikes at Vesuvio (Italy) and the effect of Mt. Somma. *Geophysical Research Letters* 33, L08301, doi:10.1029/2005GL025590.
- Albore Livadie C. (1999) - L'eruzione vesuviana delle 'Pomici di Avellino' e la facies di Palma Campania (Bronzo Antico). Edipuglia, Bari.
- Alessio M., Bella F., Improta S., Belluomini G., Calderoni G., Cortesi C., Turi B. (1974) - University of Rome carbon-14 dates XII. *Radiocarbon*, 16(3), 358-367.
- Amoruso A., Crescentini L., Sabetta I., De Martino P., Obrizzo F., Tammaro U. (2014) - Clues to the cause of the 2011–2013 Campi Flegrei caldera unrest, Italy, from continuous GPS data. *Geophysical Research Letters* 41, 3081-3088.
- Andronico D., Calderoni G., Cioni R., Sbrana A., Sulpizio R., Santacroce R. (1995) - Geological map of Somma-Vesuvius volcano. *Periodico di Mineralogia*, 64(1-2), 77-78.
- Andronico D. (1997) - La stratigrafia dei prodotti dell'eruzione di L'agno Amendolare (Campi Flegrei, Napoli). *Atti Soc. Toscana. Sci. Nat. Pisa Mem., Ser. A*, 104, 165-178.
- Andronico D., Cioni R. (2002) - Contrasting styles of Mount Vesuvius activity in the period between the Avellino and Pompeii Plinian eruptions, and some implications for assessment of future hazards. *Bull. Volcanol.*, 64, 372–391.
- Arienzo I., Mazzeo F. C., Moretti R., Cavallo A., D'Antonio M. (2016) - Open-system magma evolution and fluid transfer at Campi Flegrei caldera (Southern Italy) during the past 5ka as revealed by geochemical and isotopic data: The example of the Nisida eruption. *Chemical Geology*, 427, 109-124.
- Arienzo I., Moretti R., Civetta L., Orsi G., Papale P. (2010) - The feeding system of Agnano–Monte Spina eruption (Campi Flegrei, Italy): dragging the past into present activity and future scenarios. *Chemical Geology*, 270, 135-147.
- Armienti P., Barberi F., Bizogard H., Clocchiatti R., Innocenti F., Metrich N. (1983) - The Phlegraean Fields: magma evolution within a shallow chamber. *J. Volcanol. Geoth. Res.*, 17, 289-311.
- Arnò V., Principe C., Rosi M., Santacroce R., Sbrana A., Sheridan M. F. (1987) - Eruptive history. *Somma-Vesuvius*, 114, 53-103.
- Arrighi S., Principe C., Rosi M. (2001) - Violent strombolian and subplinian eruptions at Vesuvius during post-1631 activity. *Bull. Volcanol.*, 63, 126-150.
- Auger E., Gasparini P., Virieux J., Zollo A. (2001) - Seismic Evidence of an Extended Magmatic Sill Under Mt. Vesuvius. *Science*, 9918.
- Avanzinelli R., Cioni R., Conticelli S., Giodano G., Isaia R., Mattei M., Melluso L., Sulpizio R. (2017) - The Vesuvius and the other volcanoes of Central Italy. *Geological Field Trips*, Vol. 9 No. 1.1, 158 pp., 107 figs. (DOI 10.3301/GFT.2017.01).
- Ayuso R.A., De Vivo B., Rolandi G., Seal R.R. II, Paone A. (1998) - Geochemical and isotopic (Nd–Pb–Sr–O) variations bearing on the genesis of volcanic rocks from Vesuvius, Italy. *J. Volcanol. Geotherm. Res.*, 82, 53-78.

- Barberi F., Leoni L. (1980) - Metamorphic carbonate ejecta from Vesuvius plinian eruptions: evidence of the occurrence of shallow magma chambers. *Bull. Volcanol.*, 43, 107-120.
- Barberi F., Innocenti F., Lirer L., Munno R., Pescatore T., Santacroce R. (1978) - The Campanian Ignimbrite: a major prehistoric eruption in the Neapolitan area (Italy). *Bulletin Volcanologique*, 41(1), 10-31.
- Battaglia M., Troise C., Obrizzo F., Pingue F., De Natale G. (2006) - Evidence for fluid migration as the source of deformation at Campi Flegrei caldera (Italy). *Geophys. Res. Lett.*, 33, L01307-10.
- Bertagnini A., Landi P., Rosi M., Vigliargio A. (1998) - The Pomici di Base plinian eruption of Somma-Vesuvius. *J. Volcanol. Geotherm. Res.* 83 (3-4), 219-239.
- Bertagnini A., Cioni R., Guidoboni E., Rosi M., Neri A., Boschi E. (2006) - Eruption early warning at Vesuvius: The AD 1631 lesson. *Geophysical research letters*, 33(18).
- Bevilacqua A., Isaia R., Neri A., Vitale S., Aspinall W. P., Bisson M., Flandoli F., Baxter P.J., Bertagnini A., Esposti Ongaro T., Iannuzzi E. (2015) - Quantifying volcanic hazard at Campi Flegrei caldera (Italy) with uncertainty assessment: 1. Vent opening maps. *Journal of Geophysical Research: Solid Earth*, 120(4), 2309-2329.
- Bohrson W. A., Spera F. J., Fowler S. J., Belkin H. E., De Vivo B., Rolandi G. (2006) - Petrogenesis of the Campanian ignimbrite: implications for crystal-melt separation and open-system processes from major and trace elements and Th isotopic data. *Developments in Volcanology*, 9, 249-288.
- Brocchini D., Principe C., Castradori D., Laurenzi M.A., Gorla L. (2001) - Quaternary evolution of the southern sector of the Campanian Plain and early Somma Vesuvius activity: insights from the Trecase 1 well. *Mineral. Petrol.*, 73, 67-92.
- Cannatelli C. (2012) - Understanding magma evolution at Campi Flegrei (Campania, Italy) volcanic complex using melt inclusions and phase equilibria. *Mineralogy and Petrology*, 104, 29-42.
- Cannatelli C., Lima A., Bodnar R. J., De Vivo B., Webster J. D., Fedele L. (2007) - Geochemistry of melt inclusions from the Fondo Riccio and Minopoli 1 eruptions at Campi Flegrei (Italy). *Chemical Geology*, 237, 418-432.
- Cappelletti P., Cerri G., Colella A., de'Gennaro M., Langella A., Perrotta A., Scarpata C. (2003) - Post-eruptive processes in the Campanian Ignimbrite. *Mineralogy and Petrology*, 79(1-2), 79-97.
- Caricchi C., Vona A., Corrado S., Giordano G., Romano C. (2014) - 79 AD Vesuvius PDC deposits' temperatures inferred from optical analysis on woods charred in-situ in the Villa dei Papiri at Herculaneum (Italy). *Journal of Volcanology and Geothermal Research*, 289, 14-25.
- Carroll M. R., Blank J. G. (1997) - The solubility of H₂O in phonolitic melts. *American Mineralogist*, 82, 549-556.
- Chiodini G., Frondini F., Magro G., Marini L., Panichi C., Raco B., Russo M. (1997) - Chemical and isotopic variations of Bocca Grande fumarole (Solfatara volcano, Phlegrean Fields). *Acta Vulcanologica* 8, 228-232.
- Cioni R., Civetta L., Marianelli P., Métrich N., Santacroce R., Sbrana A., 1995. Compositional layering and syneruptive mixing of a periodically refilled shallow magma chamber: the AD 79 Plinian eruption of Vesuvius. *J. Petrol.* 36, 739-776.
- Cioni R., Santacroce R., Sbrana A. (1999) - Pyroclastic deposits as a guide for reconstructing the multi-stage evolution of the Somma-Vesuvius caldera. *Bull. Volcanol.*, 60, 207-222.

- Cioni R., Longo A., Macedonio G., Santacroce R., Sbrana A., Sulpizio R., Andronico D. (2003^o) - Assessing pyroclastic fall hazard through field data and numerical simulations: example from Vesuvius. *Journal of Geophysical Research: Solid Earth*, 108(B2), 2063, doi:10.1029/2001JB000642
- Cioni R., Sulpizio R., Garruccio N. (2003b) - Variability of the eruption dynamics during a Subplinian event: the Greenish Pumice eruption of Somma-Vesuvius (Italy). *J. Volcanol. Geotherm. Res.*, 124, 89-114.
- Cioni R. (2000) - Volatile content and degassing processes in the AD 79 magma chamber at Vesuvius (Italy). *Contrib. Mineral. Petrol.*, 140, 40-54.
- Cioni R., Marianelli P., Sbrana A. (1992) - Dynamics of the AD 79 eruption: stratigraphic, sedimentologic and geochemical data on the successions of the Somma-Vesuvius southern sector. *Acta Vulcanologica*, 2, 109-123.
- Cioni R., Marianelli P., Santacroce R. (1997) - Thermal and compositional evolution of the shallow magma chambers of Vesuvius: Evidence from pyroxene phenocrysts and melt inclusions. *J. Geophys. Res.*, 103, 18277-18294.
- Cioni R., Marianelli P., Santacroce R. (1999) - Temperature of Vesuvius magmas. *Geology*, 27, 443-446.
- Cioni R., Levi S., Sulpizio R. (2000) - Apulian Bronze Age pottery as a long-distance indicator of the Avellino Pumice eruption (Vesuvius, Italy). *Geological Society, London, Special Publications*, 171(1), 159-177.
- Cioni R., Bertagnini A., Santacroce R., Andronico D. (2008) - Explosive activity and eruption scenarios at Somma-Vesuvius (Italy): Towards a new classification scheme. *J. Volcanol. Geoth. Res.*, 178, 331-346
- Cioni R., D'Oriano C., Bertagnini A., Andronico D. (2013) - The 2nd to 4th century explosive activity of Vesuvius: new data on the timing of the upward migration of the post-AD 79 magma chamber. *Annals of Geophysics*.
- Cioni R., Bertagnini A., Andronico D., Cole P. D., Mundula F. (2011) - The 512 AD eruption of Vesuvius: complex dynamics of a small scale subplinian event. *Bulletin of Volcanology*, 73(7), 789-810.
- Civetta L., Orsi G., Pappalardo L., Fisher R., Heiken G., Ort M. (1997) - Geochemical zoning, mingling, eruptive dynamics and depositional processes - The Campanian Ignimbrite, Campi Flegrei caldera, Italy. *J. Volcanol. Geoth. Res.*, 75, 183-197.
- Civetta L., Santacroce R. (1992) - Steady-state magma supply in the last 3,400 years of Vesuvius, *Acta Vulcanol.* 2, 147-159.
- Civetta L., Galati R., Santacroce R. (1991a) - Magma mixing and convective compositional layering within the Vesuvius magma chamber. *Bull. Volcanol.*, 53, 287.
- Civetta L., Carluccio E., Innocenti F., Sbrana A., Taddeucci G. (1991b) - Magma chamber evolution under the Phlegrean fields during the last 10 ka: trace element and isotop data. *Europ. J. Mineral.*, 3, 415-428.
- Cole P. D., Scarpati C. (2010) - The 1944 eruption of Vesuvius, Italy: combining contemporary accounts and field studies for a new volcanological reconstruction. *Geological Magazine*, 147(3), 391-415.
- Cole P.D., Scarpati C. (1993) - A facies interpretation of the eruption and emplacement mechanisms of the upper part of the Neapolitan Yellow Tuff, Campi Flegrei, southern Italy. *Bull. Volcanol.*, 55, 311-326.
- Cortini M., Scandone R. (1982) - Feeding system of Vesuvius between 1754 and 1944. *J. Volcanol. Geotherm. Res.*, 12, 393-400.
- Costa A., Dell'Erba F., Di Vito M. A., Isaia R., Macedonio G., Orsi G., Pfeiffer T. (2009) - Tephra fallout hazard assessment at the Campi Flegrei caldera (Italy). *Bull. Volcanol.*, 71(3), 259.

- Costa A., Folch A., Macedonio G., Giaccio B., Isaia R., Smith V. (2012) - Quantifying volcanic ash dispersal and impact of the Campanian Ignimbrite super-eruption. *Geophys. Res. Lett.*, 39, L10310.
- D'Antonio M., Civetta L., Orsi G., Pappalardo L., Piochi M., Carandente A., De Vita S., Di Vito M.A., Isaia R. (1999) - The present state of the magmatic system of the Campi Flegrei caldera based on a reconstruction of its behaviour in the past 12 ka. *J. Volcanol. Geoth. Res.*, 91, 247-268.
- D'Antonio M., Tonarini S., Arienzo I., Civetta L., Di Renzo V. (2007) - Components and processes in the magma genesis of the Phlegrean Volcanic District, southern Italy. *Geological Society of America Special Papers*, 418, 203-220.
- D'Antonio M., Civetta L., Di Girolamo P. (1999) - Mantle source heterogeneity in the Campanian Region (South Italy) as inferred from geochemical and isotopic features of mafic volcanic rocks with shoshonitic affinity. *Mineral. Petrol.*, 67, 163-192.
- D'Orlando C., Poggianti E., Bertagnini A., Cioni R., Landi P., Polacci M., Rosi M. (2005) - Changes in eruptive style during the A.D. 1538 Monte Nuovo eruption (Phlegrean Fields, Italy): the role of syn-eruptive crystallization. *Bull. Volcanol.*, 67, 601-621.
- De Gori P., Cimini G. B., Chiarabba C., De Natale G., Troise C., Deschamps A. (2001) - Teleseismic tomography of the Campanian volcanic area and surrounding Apenninic belt. *Journal of Volcanology and Geothermal Research*, 109(1-3), 55-75.
- De Natale G., Troise C., Pingue F., Mastrolorenzo G., Pappalardo L. (2006) - The Somma-Vesuvius volcano (Southern Italy): structure, dynamics and hazard evaluation. *Earth-Science Reviews*, 74(1-2), 73-111.
- De Siena L., Del Pezzo E., Bianco F. (2010) - Seismic attenuation imaging of Campi Flegrei: Evidence of gas reservoirs, hydrothermal basins, and feeding systems. *Journal of Geophysical Research*, 115, B09312.
- De Vita S., Orsi G., Civetta L., Carandente A., D'Antonio M., Di Cesare T., Di Vito M., Fisher R.V., Isaia R., Marotta E., Ort M., Pappalardo L., Piochi M., Southon J. (1999) - The Agnano-Monte Spina eruption (4.1 ka) in the resurgent, nested Campi Flegrei caldera (Italy). *J. Volcanol. Geoth. Res.*, 91, 269-301.
- De Vivo, B., Rolandi, G., Gans, P.B., Calvert, A., Bohrsen, W.A., Spera, F.J., Belkin, H.E. (2001) - New constraints on the pyroclastic eruptive history of the Campanian volcanic Plain (Italy). *Mineral. Petrol.*, 73, 47-65.
- Deino A.L., Orsi G., De Vita S., Piochi M. (2004) - The age of the Neapolitan Yellow Tuff caldera-forming eruption (Campi Flegrei caldera, Italy) assessed by $^{40}\text{Ar}/^{39}\text{Ar}$ dating method. *J. Volcanol. Geother. Res.*, 133, 157-170.
- Del Gaudio C., Aquino I., Ricciardi G.P., Ricco C., Scandone R. (2010) - Unrest episodes at Campi Flegrei: a reconstruction of vertical ground movements during 1905-2009. *J. Volcanol. Geotherm. Res.*, 185, 48-56.
- Del Pezzo E., Bianco F., De Siena L., Zollo A. (2006) - Small scale shallow attenuation structure at Mt. Vesuvius, Italy. *Physics of the Earth and Planetary Interiors*, 157(3-4), 257-268.
- Dellino P., Isaia R., Orsi G. (2001) - Statistical analysis of textural data from complex pyroclastic sequences: implications for fragmentation processes of the Agnano-Monte Spina Tephra (4.1 ka), Phlegraean Fields, southern Italy. *Bulletin of Volcanology*, 63(7), 443-461.
- Dellino P., Isaia R., La Volpe L., Orsi G. (2004) - Interaction between particles transported by fallout and surge in the deposits of the Agnano-Monte Spina eruption (Campi Flegrei, Southern Italy). *Journal of Volcanology and Geothermal Research*, 133(1-4), 193-210.

- Di Girolamo P., Ghiara M.R., Lirer L., Munno R., Rolandi G., Stanzione D. (1984) - Vulcanologia e petrologia dei Campi Flegrei. *Boll. Soc. Geol. Ital.*, 103, 349-413.
- Di Maio R., Mauriello P., Patella D., Petrillo Z., Piscitelli S., Siniscalchi A. (1998) - Electric and electromagnetic outline of the Mount Somma-Vesuvius structural setting. *J. Volcanol. Geotherm. Res.*, 82, 219-238.
- Di Renzo V., Arienzo I., Civetta L., D'Antonio M., Tonarini S., Di Vito M.A., Orsi G. (2011) - The magmatic feeding system of the Campi Flegrei caldera: architecture and temporal evolution. *Chem. Geol.*, 281, 227-241.
- Di Renzo V., Di Vito M.A., Arienzo I., Carandente A., Civetta L., D'Antonio M., Giordano F., Orsi G., Tonarini S. (2007) - Magmatic history of Somma-Vesuvius on the basis of new geochemical and isotopic data from a deep borehole (Camaldoli della Torre). *J. Petrology*, 48, 4, 753-784.
- Di Vito M.A., Isaia R., Orsi G., Southon J., de Vita S., D'Antonio M., Pappalardo L., Piochi M. (1999) - Volcanism and deformation since 12000 years at the Campi Flegrei caldera (Italy). *J. Volcanol. Geoth. Res.*, 91, 221-246.
- Di Vito M. A., Acocella V., Aiello G., Barra D., Battaglia M., Carandente A., Del Gaudio C., de Vita S., Ricciardi G.P., Ricco C., Scandone R. (2016) - Magma transfer at Campi Flegrei caldera (Italy) before the 1538 AD eruption. *Scientific reports*, 6, 32245
- Di Vito M. A., Arienzo I., Braia G., Civetta L., D'Antonio M., Di Renzo V., Orsi G. (2011) - The Averno 2 fissure eruption: a recent small-size explosive event at the Campi Flegrei Caldera (Italy). *Bulletin of Volcanology*, 73(3), 295-320.
- Di Vito M., Lirer L., Mastrolorenzo G., Rolandi G. (1987) - The 1538 Monte Nuovo eruption (Campi Flegrei, Italy). *Bulletin of Volcanology*, 49(4), 608-615.
- Di Vito M. A., Sulpizio R., Zanchetta G., D'Orazio M. (2008) - The late Pleistocene pyroclastic deposits of the Campanian Plain: new insights into the explosive activity of Neapolitan volcanoes. *Journal of Volcanology and Geothermal Research*, 177(1), 19-48.
- Dvorak J. J., Gasparini P. (1991) - History of earthquakes and vertical ground movement in Campi Flegrei caldera, southern Italy: Comparison of precursory events to the AD 1538 eruption of Monte Nuovo and of activity since 1968. *Journal of Volcanology and Geothermal Research*, 48(1-2), 77-92.
- Faccenna C., Funiciello F., Civetta L., D'Antonio M., Moroni M., Piromallo C. (2007) - Slab disruption, mantle circulation, and the opening of the Tyrrhenian basins. *Geological Society of America Special Papers*, 418, 153-169.
- Fedele F.G., Giaccio B., Isaia R., Orsi G. (2003) - The Campanian Ignimbrite eruption, Heinrich event 4 and the Palaeolithic change in Europe: a high-resolution investigation. In A. Robock and C. Oppenheimer (eds.) "Volcanism and Earth's Atmosphere". Washington, USA, AGU Geophysical Monograph, 139, 301-325.
- Fedele L., Scarpati C., Lanphere M., Melluso L., Morra V., Perrotta A., Ricci G. (2008) - Breccia Museo formation, Campi Flegrei, southern Italy: geochronology, chemostratigraphy and relationship with the Campanian Ignimbrite eruption. *Bull. Volcanol.*, 70, 1189-1219.
- Fisher R.V., Orsi G., Ort M., Heiken G. (1993) - Mobility of a large-volume pyroclastic flow-emplacement of the Campanian ignimbrite, Italy. *J. Volcanol. Geoth. Res.*, 56, 205-220.

- Forni F., Petricca E., Bachmann O., Mollo S., De Astis G., Piochi M. (2018) - The role of magma mixing/mingling and cumulate melting in the Neapolitan Yellow Tuff caldera-forming eruption (Campi Flegrei, Southern Italy). *Contributions to Mineralogy and Petrology*, 173, 45.
- Fourmentraux C., Métrich N., Bertagnini A., Rosi M. (2012) - Crystal fractionation, magma step ascent, and syn-eruptive mingling: the Averno 2 eruption (Phlegraean Fields, Italy). *Contributions to Mineralogy and Petrology*, 163, 1121-1137.
- Fowler S. J., Spera F. J., Bohrsen W. A., Belkin H. E., De Vivo B. (2007) - Phase equilibria constraints on the chemical and physical evolution of the Campanian Ignimbrite. *Journal of Petrology*, 48, 459-493.
- Fulignati P., Marianelli P., Santacroce R., Sbrana A. (2004) - Probing the Vesuvius magma chamber-host rock interface through xenoliths. *Geol. Mag.*, 141, 417-428.
- Fulignati P., Panichi C., Sbrana A., Caliro S., Gioncada A., Del Moro A. (2005) - Skarn formation at the walls of the 79AD magma chamber of Vesuvius (Italy): Mineralogical and isotopic constraints. *N. Jahrb. Mineralogie-Abhandlungen*, 181, 53-66.
- Giaccio B., Isaia R., Fedele F., Di Canzio E., Hoffecker J., Ronchitelli A., Sinitsyn A., Anikovich M., Lisitsyn S., Popov V. (2008) - The Campanian Ignimbrite and Codola tephra layers: two temporal/stratigraphic markers for the Early Upper Palaeolithic in southern Italy and eastern Europe. *J. Volcanol. Geoth. Res.*, 177, 208-226.
- Giaccio B., Hajdas I., Isaia R., Deino A., Nomade S. (2017) - High-precision ^{14}C and $^{40}\text{Ar}/^{39}\text{Ar}$ dating of the Campanian Ignimbrite (Y-5) reconciles the time-scales of climatic-cultural processes at 40 ka. *Scientific reports*, 7, 45940.
- Giaccio B., Marra F., Hajdas I., Karner D.B., Renne P.R., Sposato A. (2009) - $^{40}\text{Ar}/^{39}\text{Ar}$ and ^{14}C geochronology of the Albano maar deposits: Implications for defining the age and eruptive style of the most recent explosive activity at Colli Albani Volcanic District, Central Italy. *J. Volcanol. Geotherm. Res.*, 185, 203-213.
- Giardini D., Velonà M. (1991) - The deep seismicity of the Tyrrhenian Sea. *Terra Nova*, 3(1), 57-64.
- Giudicepietro F., D'Auria L. (2013) - Storia del dibattito scientifico sul Serapeo di Pozzuoli. *Miscellanea INGV*, 20, 1-15.
- Gualda G. A. R., Ghiorso M. S., Lemons R. V., Carley T. L. (2012) - Rhyolite-MELTS: a modified calibration of MELTS optimized for silica-rich, fluid-bearing magmatic systems. *Journal of Petrology*, 53, 875-890.
- Guidoboni E., Ciuccarelli C. (2011) - The Campi Flegrei caldera: historical revision and new data on seismic crises, bradyseisms, the Monte Nuovo eruption and ensuing earthquakes (twelfth century 1582 ad). *Bull. Volcanol.*, 73, 655-677.
- Guidoboni E., Boschi E. (2006) - Vesuvius before the 1631 eruption. *Eos, Transactions American Geophysical Union*, 87(40), 417-423.
- Gurioli L., Cioni R., Sbrana A., Zanella E. (2002) - Transport and deposition of pyroclastic flows over an inhabited area: the deposits of the AD 79 eruption of Vesuvius at Herculaneum (Italy). *Sedimentology*, 49, 929-953.
- Gurioli L., Houghton B. F., Cashman K. V., Cioni R. (2005) - Complex changes in eruption dynamics during the 79 AD eruption of Vesuvius. *Bull. Volcanol.*, 67, 144-159.
- Gurioli L., Sulpizio R., Cioni R., Sbrana A., Santacroce R., Luperini W., Andronico D. (2010) - Pyroclastic flow hazard assessment at Somma-Vesuvius based on the geological record. *Bulletin of Volcanology*, 72(9), 1021-1038.

- Isaia R., Marianelli P., Sbrana A. (2009) - Caldera unrest prior to intense volcanism in Campi Flegrei (Italy) at 4.0 ka B.P.: implications for caldera dynamics and future eruptive scenarios. *Geophys Res Lett*, 36, L21303. doi:10.1029/2009GL040513.
- Isaia R., D'Antonio M., Dell'Erba F., Di Vito M., Orsi G. (2004) - The Astroni volcano: the only example of closely spaced eruptions in the same vent area during the recent history of the Campi Flegrei caldera (Italy). *J. Volcanol. Geother. Res.* 133, 171–192.
- Isaia R., Smith V.C. (2013) - Tefrostratigrafia del vulcanismo ai Campi Flegrei negli ultimi 15 ka. In M. Di Vito and S. de Vita (eds.) "L'impatto delle Eruzioni Vulcaniche sul Paesaggio, sull'Ambiente e sugli Insediamenti Umani - Approcci Multidisciplinari di tipo Geologico, Archeologico E Biologico". *Miscellanea INGV, Scuola Estiva AIQUA 2013, Napoli*, 22–26.
- Isaia R., Vitale S., Di Giuseppe M. G., Iannuzzi E., D'Assisi Tramparulo F., Troiano A. (2015) - Stratigraphy, structure, and volcano-tectonic evolution of Solfatara maar-diatreme (Campi Flegrei, Italy). *Geol. Soc. Am. Bulletin*, 127(9–10), 1485–1504.
- Iuliano T., Mauriello P., Patella D. (2002) - Looking inside Mount Vesuvius by potential fields integrated probability tomographies. *Journal of Volcanology and Geothermal Research*, 113(3–4), 363–378.
- Johnston Lavis H.J. (1884) - The Geology of the Mt. Somma and Vesuvius: being a study of Volcanology. *Q. J. Geol. Soc. Lond.*, 40, 35–149.
- Joron J.L., Metrich N., Rosi M., Santacroce R., Sbrana A. (1987) - Chemistry and petrography. In: "Somma-Vesuvius" R. Santacroce ed., *CNR Quaderni Ricerca Sci.* 114.
- Lirer L., Luongo G., Scandone R. (1987) - On the volcanological evolution of Campi Flegrei. *EOS*, 68, 226–234.
- Lirer L., Pescatore T., Booth B., Walker G.P.L. (1973) - Two Plinian pumice-fall deposits from Somma-Vesuvius, Italy. *Geol. Soc. Am. Bull.*, 84, 759–772.
- Mangiacapra A., Moretti R., Rutherford M., Civetta L., Orsi G., Papale P. (2008) - The deep magmatic system of the Campi Flegrei caldera (Italy). *Geophysical Research Letters*, 35, L21304.
- Marianelli P., Métrich N., Santacroce R., Sbrana A. (1995) - Mafic magma batches at Vesuvius: a glass inclusion approach to the modalities of feeding stratovolcanoes. *Contrib. Mineral. Petrol.*, 120, 159–169.
- Marianelli P., Sbrana A., Métrich N., Cecchetti A. (2005) - The deep feeding system of Vesuvius involved in recent violent Strombolian eruptions. *Geophys. Res. Lett.*, 32, L02306, doi:10.1029/2004GL021667.
- Marianelli P., Sbrana A., Proto M. (2006) - Magma chamber of Campi Flegrei supervolcano at the time of eruption of the Campanian Ignimbrite. *Geology*, 34, 937–940.
- Marianelli P., Métrich N., Sbrana A. (1999) - Shallow and deep reservoir involved in magma supply of the 1944 eruption of Vesuvius. *Bull. Volcanol.*, 61 (1–2), 48–63.
- Mele D., Sulpizio R., Dellino P., La Volpe L. (2011) - Stratigraphy and eruptive dynamics of a pulsating Plinian eruption of Somma-Vesuvius: the Pomici di Mercato (8900 years BP). *Bulletin of Volcanology*, 73(3), 257–278.
- Mele D., Dioguardi F., Dellino P., Isaia R., Sulpizio R., Braia G. (2015) - Hazard of pyroclastic density currents at the Campi Flegrei Caldera (Southern Italy) as deduced from the combined use of facies architecture, physical modeling and statistics of the impact parameters. *Journal of Volcanology and Geothermal Research*, 299, 35–53.

- Melluso L., Morra V., Perrotta A., Scarpato C., Adabbo M. (1995) - The eruption of Breccia Museo (Campi Flegrei, Italy): Fractional crystallization processes in a shallow, zoned magma chamber and implications for the eruptive dynamics. *J. Volcanol. Geotherm. Res.*, 68, 325-339.
- Middlemost E. A. (1975) - The basalt clan. *Earth-Science Reviews*, 11(4), 337-364.
- Milia A., Mirabile L., Torrente M. M., Dvorak J. J. (1998) - Volcanism offshore of Vesuvius volcano in Naples Bay. *Bulletin of Volcanology*, 59(6), 404-413.
- Morhange C., Marriner N., Laborel J., Todesco M., Oberlin C. (2006) - Rapid sea-level movements and noneruptive crustal deformation in the Phlegrean Fields caldera, Italy. *Geology*, 34, 93-96.
- Nazzaro A. (1997) - Vesuvio: storia eruttiva e teorie vulcanologiche. Liguori ed., Napoli, 380 pp.
- Orsi G., Civetta L., D'Antonio M., Di Girolamo P., Piochi M. (1995) - Step-filling and development of a three-layers magma chamber: the Neapolitan Yellow Tuff case history. *J. Volcanol. Geotherm. Res.*, 67, 291-312.
- Orsi G., Civetta L., Del Gaudio C., De Vita S., Di Vito M.A., Isaia R., Petrazzuoli S., Ricciardi G.P., Ricco C. (1999) - Short-term ground deformations and seismicity in the nested Campi Flegrei caldera (Italy). *J. Volcanol. Geotherm. Res.*, 91, 415-451.
- Orsi G., D'Antonio M., de Vita S., Gallo G. (1992) - The Neapolitan Yellow Tuff, a large-magnitude trachytic phreatoplinian eruption: eruptive dynamics, magma withdrawal and caldera collapse. *J. Volcanol. Geotherm. Res.*, 53, 275-287.
- Orsi G., Di Vito M., de Vita S. (1996) - The restless, resurgent Campi Flegrei Nested Caldera (Italy): constraints on its evolution and configuration. *J. Volcanol. Geoth. Res.*, 74, 179-214.
- Orsi G., Di Vito M.A., Isaia R. (2004) - Volcanic hazard assessment at restless Campi Flegrei caldera. *Bull. Volcanol.*, 66, 514-530.
- Orsi G., Di Vito M. A., Selva J., Marzocchi W. (2009) - Long-term forecast of eruption style and size at Campi Flegrei caldera (Italy). *Earth and Planetary Science Letters*, 287(1-2), 265-276.
- Ort M.H., Rosi M., Anderson C.H. (1999) - Correlation of deposits and vent locations of the proximal Campanian Ignimbrite deposits, Campi Flegrei, Italy, based on natural remanent magnetization and anisotropy of magnetic susceptibility characteristics. *J. Volcanol. Geoth. Res.*, 91, 167-178.
- Pabst S., Wörner G., Civetta L., Tesoro R. (2008) - Magma chamber evolution prior to the Campanian ignimbrite and Neapolitan Yellow Tuff eruptions (Campi Flegrei, Italy). *Bulletin of Volcanology*, 70, 961-976.
- Pappalardo L., Civetta L., D'Antonio M., Deino A., Di Vito M., Orsi G., Carandente A., de Vita S., Isaia R., Piochi M. (1999) - Chemical and Sr-isotopical evolution of the Phlegraean magmatic system before the Campanian Ignimbrite and the Neapolitan Yellow Tuff eruptions. *J. Volcanol. Geoth. Res.*, 91, 141-166.
- Pappalardo L., Civetta L., de Vita S., Di Vito M., Orsi G., Carandente A., Fisher R.V. (2002a) - Timing of magma extraction during the Campanian Ignimbrite eruption (Campi Flegrei caldera). *J. Volcanol. Geotherm. Res.*, 114, 479-497.
- Pappalardo L., Piochi M., D'Antonio M., Civetta L., Petrini R. (2002b) - Evidence for multi-stage magmatic evolution during the past 60 kyr at Campi Flegrei (Italy) deduced from Sr, Nd and Pb isotope data. *Journal of Petrology*, 43, 1415-1434.
- Patacca E., Scandone P. (1989) - Post-Tortonian mountain building in the Apennines. The role of the passive sinking of a relic lithospheric slab. *Atti dei Convegni Lincei*, 80, 157-176.

- Patella D., Mauriello P. (1999) - The geophysical contribution to the safeguard of historical sites in active volcanic areas. The Vesuvius case-history. *J. Appl. Geophys.*, 41, 241-258.
- Peccerillo A. (2005) - Plio-quaternary volcanism in Italy (Vol. 365). Springer-Verlag Berlin Heidelberg.
- Piochi M., Bruno P.P., De Astis G. (2005) - Relative roles of rifting tectonics and magma uprising processes: inferences from geophysical, structural and geochemical data of the Neapolitan volcanic region (southern Italy). *GCubed*, 2005.
- Pistolesi M., Bertagnini A., Di Roberto A., Isaia R., Vona A., Cioni R., Giordano G. (2017) - The Baia-Fondi di Baia eruption at Campi Flegrei: stratigraphy and dynamics of a multi-stage caldera reactivation event. *Bulletin of Volcanology*, 79(9), 67.
- Pistolesi M., Isaia R., Marianelli P., Bertagnini A., Fourmentaux C., Albert P. G., Tomlinson E.L., Menzies M.A., Rosi M., Sbrana A. (2016) - Simultaneous eruptions from multiple vents at Campi Flegrei (Italy) highlight new eruption processes at calderas. *Geology*, 44(6), 487-490.
- Principe C., Tanguy J. C., Arrighi S., Paiotti A., Le Goff M., Zoppi U. (2004) - Chronology of Vesuvius' activity from AD 79 to 1631 based on archeomagnetism of lavas and historical sources. *Bulletin of Volcanology*, 66(8), 703-724.
- Pyle D. M., Ricketts G. D., Margari V., van Andel T. H., Sinitsyn A. A., Praslov N. D., Lisitsyn S. (2006) - Wide dispersal and deposition of distal tephra during the Pleistocene 'Campanian Ignimbrite/Y5' eruption, Italy. *Quaternary Science Reviews*, 25 (21-22), 2713-2728.
- Reubi O., Blundy J., Varley N. R. (2013) - Volatiles contents, degassing and crystallisation of intermediate magmas at Volcan de Colima, Mexico, inferred from melt inclusions. *Contributions to Mineralogy and Petrology*, 165, 1087-1106.
- Rolandi G., Munno R., Postiglione I. (2004) - The A.D. 472 eruption of the Somma volcano. *J. Volcanol. Geotherm. Res.*, 129, 291-319.
- Rolandi G., Bellucci F., Heizler M.T., Belkin H.E., De Vivo B. (2003) - Tectonic controls on the genesis of ignimbrites from the Campanian Volcanic Zone, souther Italy. *Mineral. Petrol.*, 79, 3-31.
- Rolandi G., Maraffi S., Petrosino P., Lirer L. (1993a) - The Ottaviano eruption of Somma-Vesuvio (8000 y. B.P.): a magmatic alternating fall and flow-forming eruption. *J. Volcanol. Geotherm. Res.*, 58 (1-4), 43-65.
- Rolandi G., Mastrolorenzo G., Barrella A.M., Borrelli A. (1993b) - The Avellino plinian eruption of Somma-Vesuvius (3760 y. B.P.): the progressive evolution from magmatic to hydromagmatic style. *J. Volcanol. Geotherm. Res.*, 58, 67-88.
- Rolandi G., Barrella A. M., Borrelli A. (1993c) - The 1631 eruption of Vesuvius. *Journal of Volcanology and Geothermal Research*, 58(1-4), 183-201.
- Rolandi G., Petrosino P., Mc Geehin J. (1998) - The interplinian activity at Somma-Vesuvius in the last 3500 years. *Journal of Volcanology and Geothermal Research*, 82(1), 19-52.
- Rosi M., Santacroce R. (1983) - The AD 472 "Pollena" eruption: volcanological and petrological data for this poorly-known, Plinian-type event at Vesuvius. *Journal of Volcanology and Geothermal Research*, 17(1-4), 249-271.
- Rosi M., Sbrana A. (1987) - The Phlegraean Fields. *CNR, Quaderni de 'La ricerca Scientifica'* 114, Rome.
- Rosi M., Vezzoli L., Aleotti P., De Censi M. (1996) - Interaction between caldera collapse and eruptive dynamics during the Campanian Ignimbrite eruption, Phlegraean Fields, Italy. *Bull. Volcanol.*, 57, 541-554.

- Rosi M., Vezzoli L., Castelmennano A., Grieco G. (1999) - Plinian pumice fall deposit of the Campanian Ignimbrite eruption (Phlegraean Fields, Italy). *J. Volcanol. Geotherm. Res.*, 91, 179-198.
- Rosi M., Principe C., Vecchi R. (1993) - The 1631 Vesuvius eruption. A reconstruction based on historical and stratigraphical data. *Journal of Volcanology and Geothermal Research*, 58(1-4), 151-182.
- Santacroce R., Cioni R., Marianelli P., Sbrana A., Sulpizio R., Zanchetta G., Donahue D.J., Joron J.L. (2008) - Age and whole rock-glass compositions of proximal pyroclastics from the major explosive eruptions of Somma-Vesuvius: a review as a tool for distal tephrostratigraphy. *J. Volcanol. Geotherm. Res.*, 177, 1-18.
- Santacroce R. (1983) - A general model for the behavior of the Somma-Vesuvius volcanic complex. *J. Volcanol. Geotherm. Res.*, 17, 237-248.
- Santacroce R. (1987) - Somma Vesuvius. CNR, Quaderni de 'La ricerca Scientifica' 114, Rome, pp. 251.
- Santacroce R., Cioni R., Civetta L., Marianelli P., Métrich N., Sbrana A. (1994) - How Vesuvius works. In "Large Explosive Eruptions", *Atti Conv. Acc. Naz. Lincei*, 112, 185-196.
- Santacroce R., Sbrana A. (Eds.) (2003) - The Vesuvius geological map, CARG Project, Servizio Geologico d'Italia, Naples.
- Scaillet B., Pichavant M., Cioni R. (2008) - Upward migration of Vesuvius magma chamber over the past 20,000 years. *Nature*, 455, 216-219.
- Scandone R., Bellucci F., Lirer L., Rolandi G. (1991) - The structure of the Campanian Plain and the activity of the Neapolitan volcanoes Italy. *J. Volcanol. Geotherm. Res.*, 48, 1-31.
- Scarpato C., Cole P., Perrotta A. (1993) - The Neapolitan Yellow Tuff - A large volume multiphase eruption from Campi Flegrei, southern Italy. *Bull. Volcanol.*, 55, 343-356.
- Scarpato C., Perrotta A. (2012) - Erosional characteristics and behavior of large pyroclastic density currents. *Geology*, 40, 1035-1038.
- Scarpato C., Perrotta A., Lepore S., Calvert A. (2012) - Eruptive history of Neapolitan volcanoes: constraints from ^{40}Ar - ^{39}Ar dating. *Geol. Mag.*, 150, 412-425.
- Sevink J., van Bergen M. J., Van Der Plicht J., Feiken H., Anastasia C., Huizinga A. (2011) - Robust date for the Bronze Age Avellino eruption (Somma-Vesuvius): 3945 ± 10 calBP (1995 ± 10 calBC). *Quaternary Science Reviews*, 30(9-10), 1035-1046.
- Siani G., Sulpizio R., Paterne M., Sbrana A. (2004) - Tephrostratigraphy study for the last 18,000 14 C years in a deep-sea sediment sequence for the South Adriatic. *Quaternary Science Reviews*, 23(23), 2485-2500.
- Signorelli S., Vaggelli G., Francalanci L., Rosi, M. (1999) - Origin of magmas feeding the Plinian phase of the Campanian Ignimbrite eruption, Phlegraean Fields (Italy): constraints based on matrix-glass and glass-inclusion compositions. *J. Volcanol. Geotherm. Res.*, 91, 199-220.
- Sigurdsson H., Carey S., Cornell W., Pescatore T. (1985) - The eruption of Vesuvius in A.D. 79. *Nat. Geogr. Res.*, 1, 332-387.
- Sigurdsson H., Cashdollar S., Sparks R. S. J. (1982) - The eruption of Vesuvius in AD 79: reconstruction from historical and volcanological evidence. *American Journal of Archaeology*, 39-51.
- Smith V.C., Isaia R., Pearce N.J.G. (2011) - Tephrostratigraphy and glass compositions of post-15 kyr Campi Flegrei eruptions: implications for eruption history and chronostratigraphic markers. *Quaternary Sci. Rev.*, 30, 3638-3660.

- Smith V. C., Isaia R., Engwell S. L., Albert P. G. (2016) - Tephra dispersal during the Campanian Ignimbrite (Italy) eruption: implications for ultra-distal ash transport during the large caldera-forming eruption. *Bulletin of Volcanology*, 78(6), 45.
- Sparice D., Scarpati C., Perrotta A., Mazzeo F. C., Calvert A. T., Lanphere M. A. (2017) - New insights on lithofacies architecture, sedimentological characteristics and volcanological evolution of pre-caldera (> 22 ka), multi-phase, scoria-and spatter-cones at Somma-Vesuvius. *Journal of Volcanology and Geothermal Research*, 347, 165-184.
- Stock M. J., Humphreys M. C. S., Smith V. C., Isaia R., Pyle D. M. (2016) - Late-stage volatile saturation as a potential trigger for explosive volcanic eruptions. *Nature Geoscience*, 9, 249-254.
- Stock M., Humphreys M., Smith V.C., Isaia R., Brooker R.A., Pyle D.M. (2018) - Tracking volatile behaviour in sub-volcanic plumbing systems using apatite and glass: insights into pre-eruptive processes at Campi Flegrei, Italy. *Journal of Petrology*, epy020, 1-29.
- Stothers R. B., Rampino M. R. (1983) - Volcanic eruptions in the Mediterranean before AD 630 from written and archaeological sources. *Journal of Geophysical Research: Solid Earth*, 88(B8), 6357-6371.
- Sulpizio R., Bonasia R., Dellino P., Di Vito M. A., La Volpe L., Mele D., Zanchetta G., Sadori L. (2008) - Discriminating the long-distance dispersal of fine ash from sustained columns or near ground ash clouds: the example of the Pomici di Avellino eruption (Somma-Vesuvius, Italy). *Journal of Volcanology and Geothermal Research*, 177(1), 263-276.
- Sulpizio R., Cioni R., Di Vito M. A., Mele D., Bonasia R., Dellino P. (2010) - The Pomici di Avellino eruption of Somma-Vesuvius (3.9 ka BP). Part I: stratigraphy, compositional variability and eruptive dynamics. *Bulletin of Volcanology*, 72(5), 539-558.
- Sulpizio R., Cioni R., Di Vito M. A., Santacroce R., Sbrana A., Zanchetta G. (2008) - Comment on: "The dark nature of Somma-Vesuvius volcano: Evidence from the ~ 3.5 ka BP Avellino eruption" by Milia A., Raspini A., Torrente MM. *Quaternary International*, 192(1), 102-109.
- Sulpizio R., Mele D., Dellino P., La Volpe L. (2005) - A complex, Subplinian-type eruption from low-viscosity, phonolitic to tephri-phonolitic magma: the AD 472 (Pollena) eruption of Somma-Vesuvius, Italy. *Bulletin of Volcanology*, 67(8), 743-767.
- Sulpizio R., Zanchetta G., Paterne M., Siani G. (2003) - A review of tephrostratigraphy in central and southern Italy during the last 65 ka. *Il Quaternario*, 16, 91-108.
- Tadini A., Bisson M., Neri A., Cioni R., Bevilacqua A., Aspinall W. P. (2017) - Assessing future vent opening locations at the Somma-Vesuvio volcanic complex: 1. A new information geodatabase with uncertainty characterizations. *Journal of Geophysical Research: Solid Earth*, 122(6), 4336-4356.
- Tomlinson E. L., Arienzo I., Civetta L., Wulf S., Smith V. C., Hardiman M., Lane C. S., Carandente A., Orsi G., Rosi M., Müller W., Menzies M. A. (2012) - Geochemistry of the Phlegraean Fields (Italy) proximal sources for major Mediterranean tephras: Implications for the dispersal of Plinian and co-ignimbritic components of explosive eruptions. *Geochimica et Cosmochimica Acta*, 93, 102-128.
- +Tonarini S., D'Antonio M., Di Vito M.A., Orsi G., Carandente A. (2009) - Geochemical and B-Sr-Nd isotopic evidence for mingling and mixing processes in the magmatic system that fed the Astroni volcano (4.1–3.8 ka) within the Campi Flegrei caldera (southern Italy). *Lithos*, 107, 135-151.

- Tonarini S., Leeman W. P., Civetta L., D'antonio M., Ferrara G., Necco A. (2004) - B/Nb and $\delta^{11}\text{B}$ systematics in the Phlegrean Volcanic District, Italy. *Journal of Volcanology and Geothermal Research*, 133, 123-139.
- Ventura G., Vilardo G. (2008) - Emplacement mechanism of gravity flows inferred from high resolution Lidar data: The 1944 Somma-Vesuvius lava flow (Italy). *Geomorphology*, 95(3-4), 223-235.
- Ventura G., Vilardo G., Bruno P. P. (1999) - The role of flank failure in modifying the shallow plumbing system of volcanoes: an example from Somma-Vesuvius, Italy. *Geophys. Res. Lett.*, 26, 3681-3684
- Vilardo G., Isaia R., Ventura G., De Martino P., Terranova C. (2010) - InSAR Permanent Scatterer analysis reveals fault reactivation during inflation and deflation episodes at Campi Flegrei caldera. *Remote Sensing of Environment*, 114, 2373-2383.
- Vitale S., Isaia R. (2014) - Fractures and faults in volcanic rocks (Campi Flegrei, southern Italy): Insight into volcano-tectonic processes. *Inter. J. Earth Sci.*, 103, 801-819.
- Walker G.P.L. (1977) - Metodi geologici per la valutazione del rischio vulcanico. *Atti Conv I vulcani attivi dell'area napoletana. Regione Campania, Napoli*, 53-60
- Webster J. D., Raia F., Tappen C., De Vivo B. (2003) - Pre-eruptive geochemistry of the ignimbrite-forming magmas of the Campanian Volcanic Zone, Southern Italy, determined from silicate melt inclusions. *Mineralogy and Petrology*, 79(1-2), 99-125.
- Webster J. D., Goldoff B., Sintoni M. F., Shimizu N., De Vivo B. (2014) - C-O-H-Cl-S-F volatile solubilities, partitioning, and mixing in phonolitic-trachytic melts and aqueous-carbonic vapor \pm saline liquid at 200 MPa. *Journal of Petrology*, 55, 2217-2248.
- Wohletz K., Orsi G., de Vita S. (1996) - Eruptive mechanisms of the Neapolitan Yellow Tuff interpreted from stratigraphie, chemical, and granulometric data. *J. Volcanol. Geother. Res.*, 67, 263-290.
- Woo J. Y. L., Kilburn C. R. J. (2010) - Intrusion and deformation at Campi Flegrei, southern Italy: Sills, dikes, and regional extension. *Journal of Geophysical Research*, 115, B12210.
- Wulf S., Kraml M., Brauer A., Keller J., Negendank J. F. (2004) - Tephrochronology of the 100 ka lacustrine sediment record of Lago Grande di Monticchio (southern Italy). *Quaternary International*, 122(1), 7-30.
- Zanchetta G., Sulpizio R., Di Vito M. A. (2004) - The role of volcanic activity and climate in alluvial fan growth at volcanic areas: an example from southern Campania (Italy). *Sedimentary Geology*, 168(3-4), 249-280.
- Zollo A., Maercklin N., Vassallo M., Dello Iacono D., Virieux J., Gasparini P. (2008) - Seismic reflections reveal a massive melt layer feeding Campi Flegrei caldera. *Geophysical Research Letters*, 35, L12306.
- Zollo A., Gasparini P., Virieux J., Biella G., Boschi E., Capuano P., de Franco R., Dell'Aversana P., de Matteis R., De Natale G., Iannaccone G., Guerra I., Le Meur H., Mirabile L. (1998) - An image of Mt. Vesuvius obtained by 2D seismic tomography. *J. Volcanol. Geotherm., Res.* 82, 161-173.